Université de Montréal

Développement de systèmes polymère-(poly)peptide en vue de l'immobilisation de vésicules lipidiques

par

Aline Percot

Département de Chimie
Faculté des Arts et des Sciences

Thèse présentée à la faculté des études supérieures
en vue de l'obtention du grade de
Philosophiae Doctor (Ph.D.)
En Chimie

Février 2000

Université de Montréal
Faculté des études supérieures

Cette thèse intitulée:

Développement de systèmes polymère-(poly)peptide en vue de l'immobilisation de vésicules lipidiques

présentée par:
Aline Percot

a été évaluée par un jury composé des personnes suivantes:

...Professeur Thomas Ellis, Président-rapporteur.....

...Professeur Julian Zhu, Directeur de recherche.....

...Professeur Michel Lafleur, Codirecteur.....

...Professeur Antonella Badia, Membre du jury.....

...Professeur Françoise Winnik, Examinateur externe.....

Thèse acceptée le: .....

SOMMAIRE

Le but de ce travail est de développer un support solide permettant d'immobiliser des vésicules lipidiques. Un tel système possède de nombreuses applications dans des domaines aussi divers que la libération contrôlée de médicaments, le développement de supports chromatographiques, l'encapsulation d'enzymes membranaires...

Au cours de ce travail, nous avons mis au point deux systèmes à base de polymère, en utilisant une ancre de nature peptidique comme intermédiaire entre le support solide et la vésicule lipidique.

Un premier système sera constitué d'un peptide amphiphile greffé sur une résine polymère. La première partie du travail a consisté à concevoir un peptide amphiphile le plus simple possible, soluble dans l'eau et capable d'interagir spontanément et fortement avec une vésicule sans la perturber. Quatre peptides différents ont été synthétisés et étudiés. Afin d'optimiser le design du peptide qui sera greffé sur le support solide, on a fait varier des paramètres tels que la longueur du segment hydrophobe, la présence de charges positives à une extrémité ou aux deux extrémités du peptide, ainsi que son sens. Les peptides synthétisés ont une structure primaire amphiphile et sont constitués d'un segment hydrophobe à base d'alanines et de leucines, ainsi que de segments hydrophiles à base de lysines. Un tryptophane a été inséré à l'interface hydrophile-hydrophobe comme sonde fluorescente dans un but analytique. On a ainsi pu déterminer que la longueur désirable pour le segment hydrophobe est de 24 acides aminés. En effet un peptide avec un segment hydrophobe de 12 acides aminés est trop court pour adopter une conformation stable et pour établir des interactions hydrophobes avec des vésicules neutres. La présence de charges négatives aux deux extrémités du peptide empêche la translocation du peptide à travers la membrane lipidique. Le peptide le plus performant a ainsi pu être déterminé. Sa structure primaire est la suivante: Ala-Ala-Leu-Leu-Leu-Ala-Ala-Ala-Ala-Ala-Ala-Ala-Ala-Ala-Ala-Ala-Ala-Ala-Ala-Ala-Ala-Ala-Ala-Ala-Ala-Trp-Lys-Lys-Lys-Lys-Lys-Lys ($A_2L_3A_{19}WK_6$). Malgré la présence du segment hydrophobe, on a pu déterminer que les interactions peptide-lipide sont majoritairement de nature électrostatique. Ce peptide a ensuite été synthétisé en phase solide sur des billes de polystyrène. L'affinité de vésicules lipidiques pour ce système polymère-peptide a été

mesurée pour différentes populations de vésicules, en faisant varier la proportion de lipides chargés négativement dans la composition des vésicules. En neutralisant les charges du peptide dans un cas et en utilisant des lipides chargés négativement, on a pu montrer que la nature de l'interaction entre les vésicules et les billes de polymères recouvertes de peptides est majoritairement électrostatique. On a pu immobiliser jusqu'à 200 μmol de lipides par gramme de résine sèche. Ce système a ensuite été utilisé pour immobiliser une enzyme membranaire modèle, la γ-glutamyltranspeptidase. L'enzyme a été reconstituée dans des vésicules qui ont été subséquemment immobilisées sur le système polymère-peptide. Cette approche a permis d'obtenir un réacteur dont la mise en œuvre est simple et rapide et qui maintient l'activité de l'enzyme pour plusieurs cycles. En effet, après 8 cycles, l'enzyme conserve 50% de son activité.

Le deuxième système est constitué d'un copolymère thermosensible, le poly(*N*-isopropylacrylamide-co-*N*-acryloxysuccinimide) réticulé par de la polylysine. Il en résulte un hydrogel transparent présentant lui aussi des propriétés de thermosensibilité. A la température critique de transition, l'hydrogel se retracte tout en expulsant de l'eau. La mesure de cette température de transition, ainsi que la compréhension du phénomène restent problématiques dans le cas de polymères réticulés. Nous avons mis au point une méthode de spectroscopie infrarouge simple permettant de mesurer cette température avec plus de précision que les méthodes classiques et permettant d'obtenir des informations quant aux groupements impliqués dans la transition. Les principales conclusions ressortant de cette étude sont que les chaînes principales et latérales sont impliquées dans la transition et que la transition est de même nature pour les polymères linéaires et les hydrogels qui en dérivent.

Dans une deuxième partie, nous avons synthétisé plusieurs hydrogels, avec des polylysines de différentes longueurs et avec plus ou moins de points d'attache sur le polymère. Les propriétés de ces différents gels, incluant l'affinité des vésicules pour ces hydrogels ont été déterminées. On a pu constater que la longueur de la polylysine a une influence sur le gonflement du gel, ainsi que sur l'immobilisation des vésicules. L'hydrogel le plus performant est constitué de poly(*N*-isopropylacrylamide-co-*N*-acryloxysuccinimide) (94-6 mol.) réticulé par de la polylysine longue avec un degré de polymérisation de 288. Ce gel est capable d'immobiliser jusqu'à 1000±100 μmol de

lipides par gramme de gel sec sans que perméabilité des vésicules soit perturbée. Comme application, nous montrons que ce système peut relarguer le contenu de vésicules immobilisées par simple augmentation de la température au-dessus de la température de transition de l'hydrogel.

Mots clés

Peptide amphiphile, perméabilité, interactions peptide-lipide, polymère, immobilisation, vésicule lipidique, enzyme membranaire, poly(*N*-isopropylacrylamide), hydrogel, thermosensibilité, FTIR, LCST, polylysine, libération contrôlée

TABLE DES MATIÈRES

LISTE DES TABLEAUX

LISTE DES FIGURES

LISTE DES ABRÉVIATIONS

AA:	Acide acrylique
Ala:	Alanine
BSA:	Albumine de sérum bovin (bovine serum albumin)
DMPC:	Dimyristoylphosphocholine
DP:	Degré de polymérisation
FTIR:	Infrarouge à transformée de Fourier (Fourier transform infrared)
γ-GT:	γ-Glutamyl transpeptidase
HPLC:	Chromatographie liquide à haute pression (high pressure liquid chromatography)
IAM:	Membrane artificielle immobilisée (immobilized artificial membrane)
LCST:	Température critique de solution (lower critical solution temperature)
LUV:	Grosse vésicule unilamellaire (large unilamellar vesicle)
Lys:	Lysine
MBA:	*N,N'*-Méthylènebisacrylamide
NAS:	*N*-Acryloxysuccinimide
NHS:	*N*-Hydroxysuccinimide
PC:	Phosphatidylcholine
PL:	Polylysine
PNIPAAm:	Poly(*N*-isopropylacrylamide)
PNIPAS:	Poly(*N*-isopropylacrylamide-*co*-*N*-acryloxysuccinimide)
POPC:	Palmitoyloléoylphosphocholine
POPG:	Palmitoyloléoylphosphoglycérol
PS:	Polystyrène
Q:	Efficacité de l'extinction de la fluorescence (quenching)
Ri:	Rapport molaire d'incubation lipide/peptide
RMN:	Résonance magnétique nucléaire

SRB:	Sulforhodamine B
SSV:	Vésicule sphérique supportée (spherical supported vesicles)
SUV:	Petite vésicule unilamellaire (small unilamellar vesicle)
Trp:	Tryptophane

REMERCIEMENTS

Je tiens à témoigner ici ma profonde reconnaissance à mes deux directeurs de thèse, les professeurs Julian Zhu et Michel Lafleur. Je remercie Julian de m'avoir acceptée dans son groupe de recherche et d'avoir suivi ce travail avec un enthousiasme communicatif. J'ai apprécié sa disponibilité, même à distance, ainsi que la grande liberté qu'il m'a laissée tout au long de ce travail, le constant intérêt et la confiance qu'il m'a accordés tout au long de ma recherche. Je remercie Michel d'avoir accepté de m'accompagner tout au long de ce travail. J'ai tout particulièrement apprécié sa rigueur scientifique ainsi que ses qualités humaines. Je le remercie pour sa grande disponibilité, les discussions quotidiennes et stimulantes, et finalement pour son soutien quotidien tant moral que scientifique.

Je remercie le Dr Michel Belletête pour le support technique apporté lors des expériences de fluorescence, ainsi que le professeur Gilles Durocher pour le prêt des appareils.

Je remercie toute l'équipe de l'atelier mécanique et d'électronique, ainsi que Clément Chayer et Sylvie Marceau pour leur aide.

Je remercie Jean Lefebvre de l'Institut de Recherches en Biotechnologie, responsable de la synthèse des peptides, pour sa patience et ses réponses à mes nombreuses questions.

Je remercie tous mes collègues d'en haut et d'en bas: Alexandra, Damien, David, Eric, Iren, Lucie, Marcella, Mohand, Rachida, Sébastien, Sumitra, Sung Jong, Vera, Wilms ... et en particulier Chantal et Laurent qui m'ont accompagnée durant toutes ces années. Je remercie Nancy pour son soutien quotidien, son amitié et sa bonne humeur.

Je remercie finalement mes parents pour leur soutien tout au long de mes études et pour bien d'autres choses encore.

CHAPITRE 1

INTRODUCTION

1.1 Intérêt de la recherche et applications possibles

L'immobilisation de vésicules lipidiques ou de cellules sur des supports solides fait l'objet de nombreuses recherches dans le domaine de la chimie. Les membranes biologiques et modèles sont capables d'interagir plus ou moins fortement avec une grande variété de biomolécules, incluant les médicaments, les sucres, les acides aminés, les acides nucléiques et les protéines. Cette propriété fait des membranes lipidiques des entités de choix dans la mise au point de nouvelles phases stationnaires pour l'analyse chromatographique de biomolécules. Par extension, d'autres applications peuvent être envisagées, telles que la mise au point de réacteurs enzymatiques ou l'immobilisation de cellules entières. Au cours de cette thèse, nous allons donc présenter le design et le développement de nouveaux supports polymères permettant d'immobiliser de façon stable et rapide des vésicules lipidiques intactes. L'aspect innovateur de ces supports est qu'ils sont constitués de polymères auxquels sont couplés des (poly)peptides qui servent de sites d'ancrage aux membranes. Leur polyvalence sera illustrée à l'aide des exemples de libération contrôlée et de création d'un réacteur enzymatique.

La chromatographie est une technique analytique permettant de séparer, d'isoler et d'identifier les composés d'un mélange. La chromatographie liquide à haute pression (HPLC) en phase inverse est de plus en plus populaire notamment pour la séparation des peptides. Dans ce cas, la phase stationnaire utilisée est hydrophobe. Selon leur hydrophobicité, les peptides interagiront plus ou moins avec la phase stationnaire et seront retenus en conséquence par la colonne. Cette technique d'HPLC en phase inverse

est déjà utilisée comme modèle physico-chimique de systèmes biologiques[1], cependant, ce modèle reste éloigné de la membrane biologique.

Aujourd'hui, de nouveaux systèmes chromatographiques sont développés: des membranes lipidiques sont immobilisées sur la phase solide constituant la phase stationnaire[2-4]. Les analytes, en fonction de leur affinité pour les lipides interagiront plus ou moins avec la phase stationnaire. De tels supports solides permettent d'étudier les interactions entre les biomolécules et les membranes, de calculer des constantes d'équilibre ainsi que l'énergie impliquée dans le phénomène d'adsorption. Ces phases stationnaires peuvent aussi être utilisées pour la purification de protéines membranaires[3,5-7]. Dans certains cas, des récepteurs peuvent être reconstitués dans les membranes lipidiques immobilisées de la phase stationnaire et permettre d'étudier l'interaction de ces récepteurs avec différentes protéines[8].

Le même type de support peut être utilisé en biotechnologie pour la mise en œuvre de nouveaux réacteurs enzymatiques. En effet, l'immobilisation d'enzyme est un secteur de la biotechnologie en développement car elle présente de nombreux avantages tels que: une réutilisation possible de la biomasse, la possibilité d'arrêter la réaction enzymatique rapidement en enlevant l'enzyme du milieu réactionnel, la stabilisation de l'enzyme, un milieu réactionnel non contaminé par l'enzyme (important dans l'industrie alimentaire, la médecine et le pharmaceutique), ainsi que le développement de nouvelles méthodes analytiques (biosenseurs, électrodes)[9]. Il existe une vaste littérature portant sur l'immobilisation d'enzymes. Plusieurs stratégies peuvent être utilisées, telles que la réticulation de l'enzyme avec le support solide ou à sa surface, l'attachement covalent au support solide, l'adsorption à la surface ou à l'intérieur du support solide[10]. Cependant, plusieurs enzymes fonctionnent de façon optimale lorsqu'elles sont solubilisées dans des structures organisées. La reconstitution de l'enzyme dans une membrane permet d'optimiser les performances de l'enzyme tout en la stabilisant. Afin de combiner les avantages de l'immobilisation d'enzymes sur un support solide à ceux de la reconstitution de l'enzyme dans une membrane biologique, il est intéressant d'immobiliser l'enzyme reconstituée dans une membrane liée à un support solide.

La membrane biologique étant principalement constituée de lipides, des supports solides d'immobilisation de membranes peuvent aussi être utilisés pour immobiliser des

cellules vivantes. Les cellules ainsi immobilisées, capables de maintenir leur activité métabolique pendant une longue période peuvent présenter des applications intéressantes dans des domaines tels que la médecine (développement d'organes artificiels[11]), l'environnement (immobilisation de bactéries[12]) ou la biologie (étude de la prolifération des cellules[13]).

1.2 Systèmes déjà existants

Dans la littérature, il existe de nombreux exemples de systèmes permettant d'immobiliser des lipides. On peut séparer tous les systèmes mis au point en fonction de la stratégie utilisée pour immobiliser les lipides. Ils peuvent être divisés en deux grandes familles: les méthodes mettant en jeu une interaction non covalente entre le support solide et les lipides et les méthodes impliquant un lien covalent. Dans chacun des cas, nous analyserons les avantages et les inconvénients de chacune des méthodes et nous détaillerons certaines des applications développées.

1.2.1 Immobilisation non covalente des lipides:

1.2.1.1 Piégeage dans une matrice polymère:

Lors du piégeage des liposomes dans un réseau de chaînes de polymère enchevêtrées, aucune interaction spécifique n'est impliquée entre les lipides et le support solide (Fig. 1.1). Les objectifs visés sont d'immobiliser les lipides de façon à avoir la plus grande surface lipidique possible et à maximiser les interactions analyte-phase stationnaire. Plusieurs méthodes sont utilisées afin de piéger les liposomes, telles que la dialyse, des cycles successifs gel-dégel, la lyophilisation suivie d'une réhydratation et l'évaporation en phase inverse. Chacune de ces méthodes possède ses avantages et ses inconvénients. Un des principaux inconvénients communs à ces méthodes est la faible stabilité de l'immobilisation. Sous l'effet de gradients d'élution, de la pression ou du

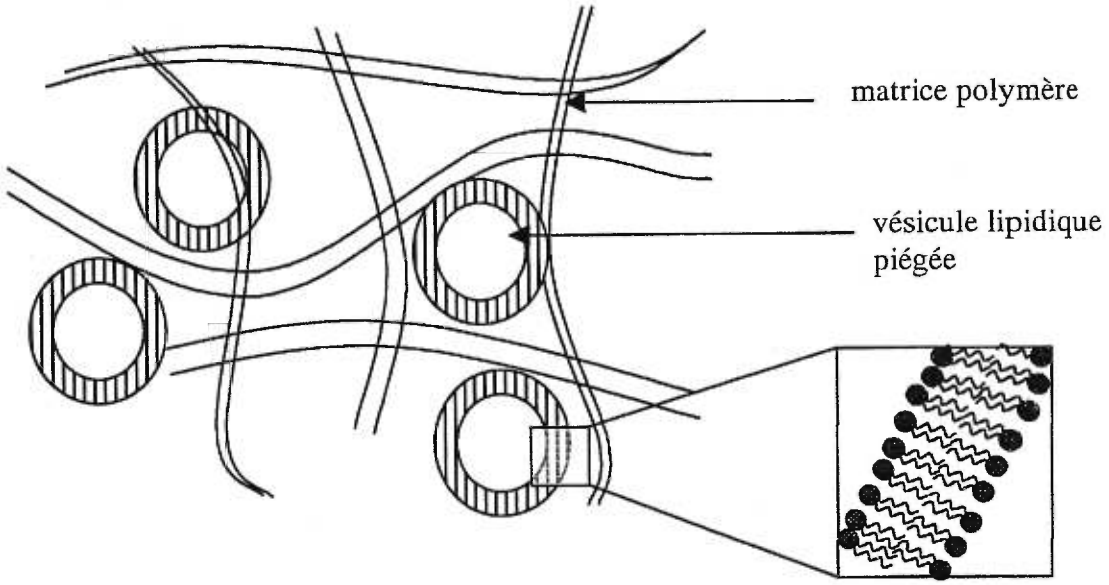

Figure 1.1 Représentation schématique d'un gel poreux contenant des liposomes piégés dans les mailles du réseau polymère.

stockage, on observe une diffusion des liposomes vers l'extérieur de la matrice polymère. De plus, avec les méthodes décrites ci-dessus, il est impossible d'encapsuler des molécules à l'intérieur des vésicules. La dialyse présente en plus l'inconvénient d'être un procédé lent, impliquant l'utilisation de détergents. Ces méthodes peuvent aussi mener à l'obtention de vésicules multilamellaires, ce qui peut être problématique pour certaines applications. Cependant, aucune modification préalable des lipides ou du support n'est nécessaire et la nature des lipides immobilisés peut être facilement modifiée.

De tels biomatériaux ont été mis au point par Lundahl et al et sont utilisés comme supports chromatographiques. Les formes monomères et dimères de l'albumine de sérum bovin (BSA) ont pu être ainsi séparées par chromatographie sur une colonne de Sépharose 6B dans laquelle ont été piégées des vésicules constituées de stéarylamine/lécithine d'œuf (20/80). Les protéines sont alors adsorbées à la surface des liposomes et séparées en fonction de leur charge et de leur taille[14]. Des vésicules de phosphatidylsérine/phosphatidylcholine (PC) ont aussi été piégées dans des billes de gel d'agarose et utilisées pour séparer des protéines telles que le lysosyme, la ribonuclease A et le cytochrome C[15]. Le potentiel de cette approche est grand puisque de multiples supports peuvent être mis au point en variant la composition des vésicules immobilisées.

La γ-glutamyl transpeptidase (γ-GT), une enzyme membranaire modèle, a pu être immobilisée dans des billes de gels par piégeage des liposomes[16,17]. Le bioréacteur obtenu présente tous les avantages liés à l'immobilisation des enzymes. La γ-GT ainsi immobilisée et reconstituée dans une membrane lipidique est activée et stabilisée. En vue d'applications reliées aux enzymes, le mode d'immobilisation des liposomes est un paramètre très important car certains traitements peuvent dénaturer l'enzyme et affecter son activité (présence de détergent lors de la dialyse qui peut s'avérer dénaturante, tampons utilisés)[16,17].

Des cellules entières peuvent aussi être piégées dans les pores d'un support polymère. Des cellules de foie ont ainsi pu être piégées dans les pores d'un support microporeux à base de cellulose recouverts de collagène. Un tel bioréacteur peut être utilisé comme foie artificiel[11] (Fig. 1.2).

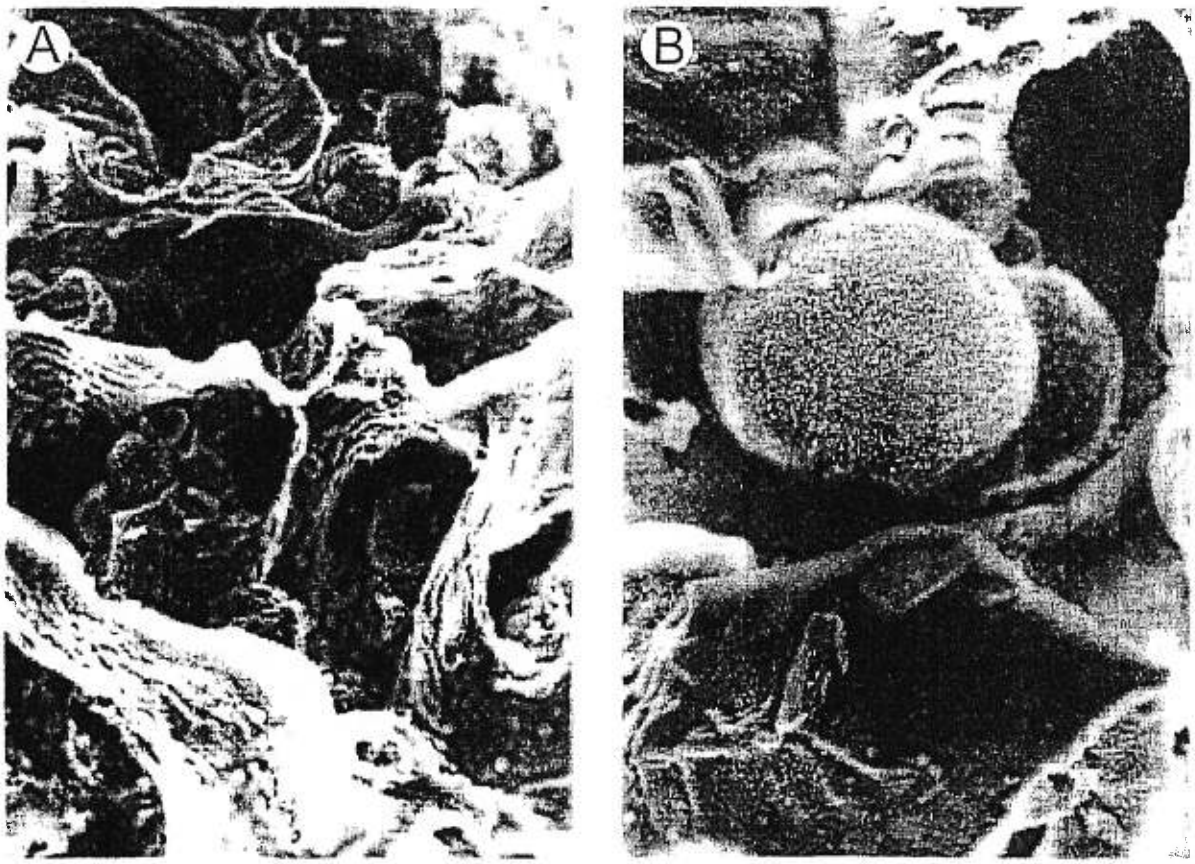

Figure 1.2 Micrographies à balayage électronique d'hépatocytes immobilisés sur un support microporeux (agrandissement: A, × 700; B, × 2000)[11].

1.2.1.2 Immobilisation par adsorption: Vésicules sphériques supportées (SSV)

Une bicouche de lipide peut être adsorbée à la surface de billes de silice. Le support est alors recouvert d'une bicouche lipidique séparée de la surface du support par une mince couche d'eau (Fig. 1.3). Ces supports ont tout d'abord été développés afin de combler le manque de systèmes modèles unilamellaires, avec une forme bien définie, préférablement sphérique, ajustable, avec une étroite distribution de taille. De tels modèles permettent d'obtenir des informations fondamentales sur la structure et la dynamique des membranes biologiques. Ces systèmes modèles ont été développés par Bayerl et al[18] et sont appelés vésicules sphériques supportées ou SSV pour "spherical supported vesicles". Dans ce cas, des vésicules intactes ou des cellules ne peuvent être immobilisées sur le support.

Une bicouche de dimyristoylphosphocholine (DMPC) a été adsorbée sur une bille de verre[18]. Les propriétés physiques de la membrane ont pu être étudiées par résonance magnétique nucléaire (RMN) du ^2H. Des paramètres tels que la taille des billes ainsi que la nature des lipides sont facilement modifiables. De plus, les bicouches immobilisées présentent la même température de transition, ainsi que les mêmes propriétés dynamiques qu'une bicouche sans support.

La méthode de SSV peut être utilisée pour recouvrir la surface de gel de silice utilisés en chromatographie. Certaines protéines possèdent une affinité différente pour la bicouche lipidique selon qu'elle est en phase gel ou en phase fluide. Cette propriété a été utilisée pour isoler la 'bindine', une protéine extraite du sperme de l'oursin, qu'on adsorbe lorsque les SSV sont en phase gel et qu'on désorbe lorsque la température de la colonne est augmentée au-dessus de la température de transition des SSV[5]. Un tel système a aussi permis de séparer des protéines avec différents points isoélectriques dans des conditions douces (sans nécessiter de changement de force ionique), par simple chauffage[2].

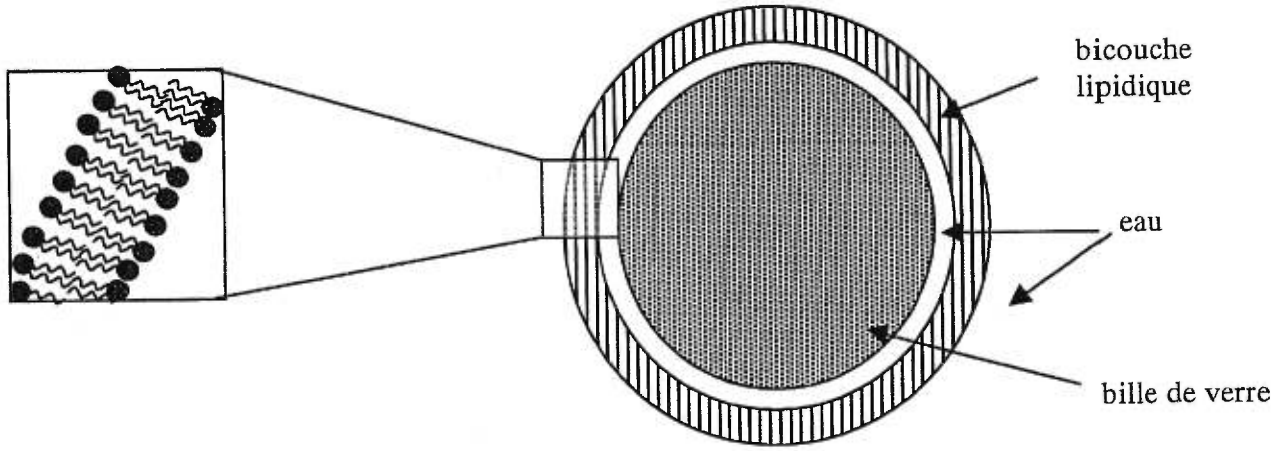

Figure 1.3 Représentation schématique d'une SSV[18].

1.2.1.3 Adsorption avec interaction hydrophobe:

Les vésicules peuvent être adsorbées sur des surfaces et dans ce cas, des dérivés hydrophobes du support solide doivent être préparés (Fig. 1.4). Les groupements hydrophobes interagissent alors avec le segment hydrophobe des lipides. Le groupement hydrophobe sert alors d'ancre entre le support solide et les lipides. Cette méthode est utilisée pour immobiliser des bicouches lipidiques planes[19-22] ainsi que des vésicules intactes[6,23] sur différents types de surfaces. La nature des lipides, les conditions thermodynamiques d'immobilisation, ainsi que la nature et la densité des ligands hydrophobes sur le support déterminent l'organisation des lipides immobilisés. Dans certaines conditions, on peut même induire la fusion des vésicules et utiliser ce phénomène pour étaler les bicouches lipidiques sur le support. Dans la suite de ce travail, nous nous interesserons principalement à l'immobilisation de liposomes. Pour des applications en chromatographie, l'existence d'interactions parasites entre les ancres hydrophobes et les analytes doit être prise en compte. De courtes chaînes alkyles (de 4 à 12 carbones) ou des groupements aryles sont souvent utilisés pour recouvrir le support solide. Un tel système peut être utilisé pour concentrer des vésicules, pour étudier les interactions lipide/surface hydrophobe, la perméabilité des membranes, les interactions membrane/médicaments ou pour immobiliser des enzymes membranaires.

Des billes d'agarose fonctionnalisées par des groupements octyls ont été utilisées pour immobiliser des liposomes à base de lécithine d'œuf. Ces billes ont été utilisées comme phase stationnaire afin de séparer des solutés capables de pénétrer dans le liposome de ceux qui ne le peuvent pas[6]. Une protéine transmembranaire responsable du transport du D-glucose à travers la membrane a été reconstituée dans la bicouche lipidique et a permis de séparer l'énantiomère bioactif, le D-glucose de la forme inactive L-glucose[4]. Le même type de support a été utilisé afin de prédire la diffusion de médicaments à travers la membrane[23].

La même stratégie a été utilisée pour immobiliser des cellules sur un substrat fonctionnalisé par des lipides[24].

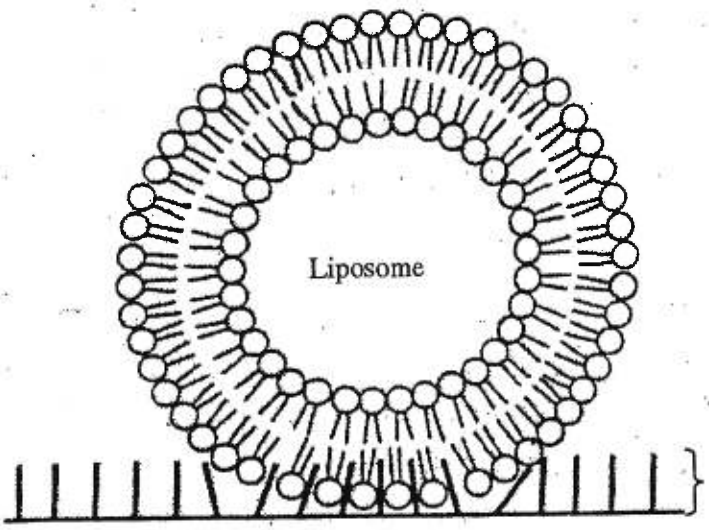

Figure 1.4 Représentation schématique d'une vésicule lipidique immobilisée par des interactions hydrophobes entre les lipides et les ligands alkyles recouvrant la surface du support solide[23].

1.2.1.4 Interactions spécifiques: avidine-biotine

L'interaction avidine-biotine peut aussi être utilisée pour immobiliser des vésicules lipidiques sur un support solide. Certaines applications chromatographiques ont été mises au point par Lundahl et al[25]. Les billes de gel dérivées par de l'avidine ou de la streptavidine permettent d'immobiliser des liposomes unilamellaires de taille variable contenant une certaine proportion de lipides biotinylés. Cette technique permet d'immobiliser de petites vésicules unilamellaires (SUV) ainsi que de grosses vésicules unilamellaires (LUV) intègres avec une grande stabilité. Un tel support est utilisé en chromatographie, comme phase stationnaire[25] ou en électrophorèse capillaire pour recouvrir les parois du capillaire[26], afin d'étudier les interactions médicaments/membrane (Fig. 1.5A et 1.5B).

1.2.2 Immobilisation covalente des lipides: Membranes artificielles immobilisées (IAM)

Les membranes artificielles immobilisées (ou IAM pour "immobilized artificial membranes") ont été développées dans le but de mettre au point des supports chromatographiques mimant les membranes biologiques[3]. Dans ce cas, la surface du support doit être modifiée chimiquement afin de pouvoir se coupler avec un lipide (Fig. 1.6). Cette méthode permet d'obtenir une densité de recouvrement de la surface proche de la densité des membranes biologiques. Cependant, les lipides ainsi immobilisés ne possèdent pas de mobilité latérale et une seule et unique couche de lipide recouvre ainsi la surface du support solide. Ces propriétés font des supports IAM des supports très stables, pouvant être utilisés en milieu organique ou aqueux, pouvant supporter de fortes pressions. Cependant, de tels supports ne sont pas optimaux pour reconstituer des protéines membranaires car une seule couche de lipides recouvre la surface. Changer la composition lipidique implique de recommencer une nouvelle synthèse et immobiliser deux lipides différents sur une même surface nécessite une chimie particulière. Comme dans le cas des SSV, il s'agit du recouvrement d'une surface et non pas de l'immobilisation de vésicules intègres ou de cellules entières.

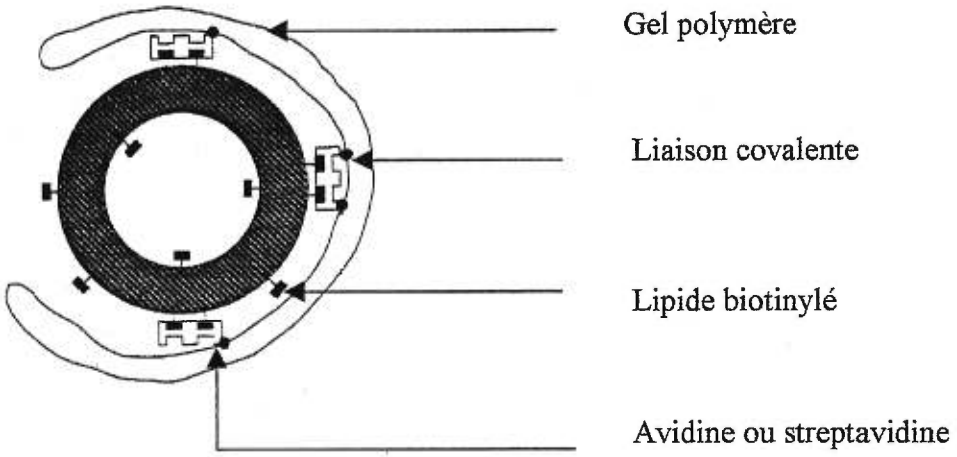

(A)

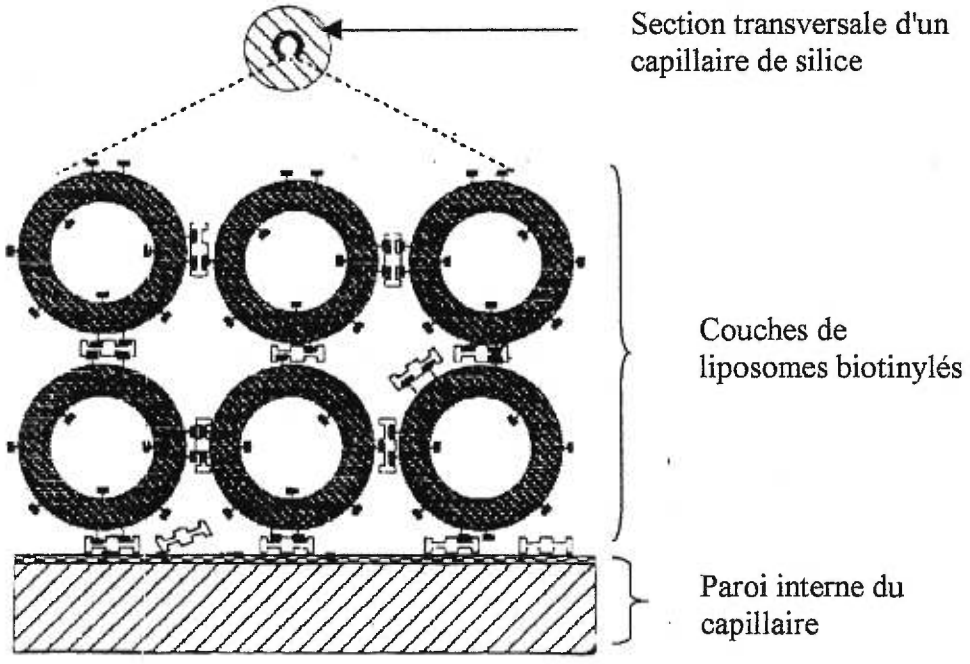

(B)

Figure 1.5 Représentation schématique d'un liposome biotinylé immobilisé par des liaisons (strept)avidine-biotine dans un gel poreux (A)[25] et à la surface d'un capillaire (B)[26].

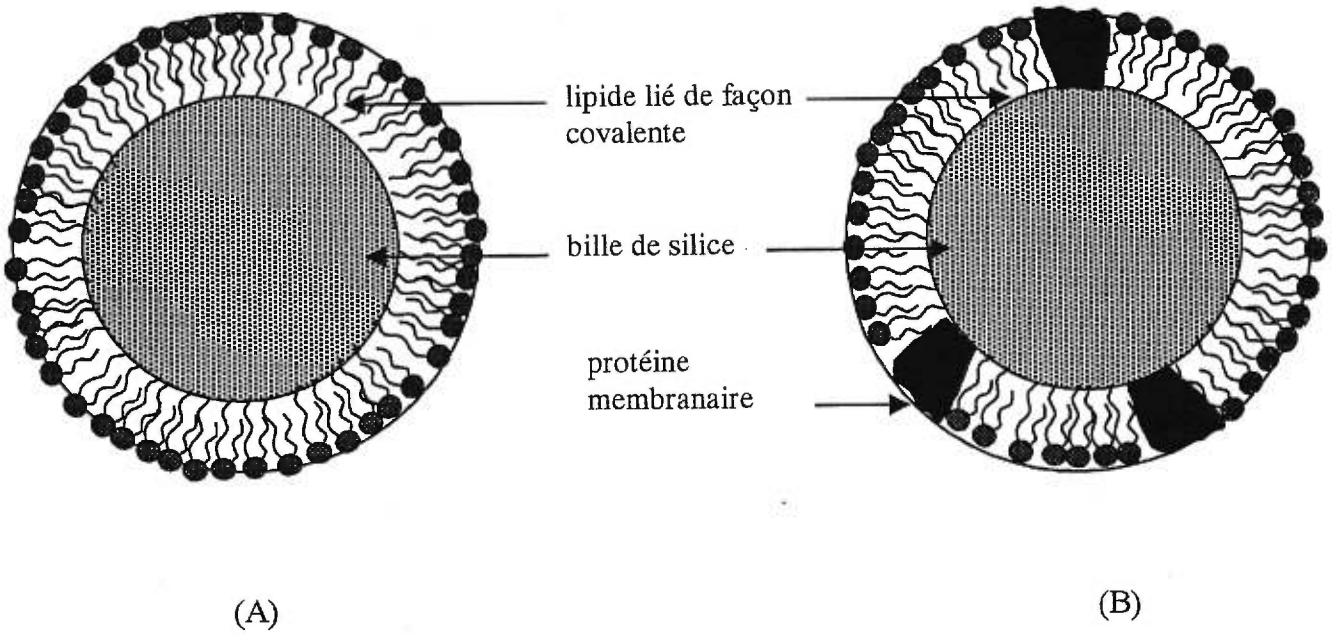

Figure 1.6 Représentation schématique de membranes artificielles immobilisées (IAM): lipides liés de façon covalente au support solide (A) avec des protéines reconstituées dans la membrane (B)[3].

Ces supports ont été utilisés pour caractériser au niveau moléculaire les interactions solutés/IAM par RMN du ^{31}P et étudier comment la structure et les propriétés des lipides immobilisés sont perturbés par l'adsorption du soluté[27].

Ces supports fonctionnalisés sont aussi utilisés en chromatographie de manière à caractériser le rôle de certains acides aminés lors de l'interaction protéine/membrane. Par exemple, il a été montré que la cystéine stabilise les interactions entre le peptide et les têtes phosphocholine des lipides de la membrane[3].

Certaines phases stationnaires IAM ont aussi été mises au point afin de prédire le transport de médicaments ou de biomolécules à travers la membrane biologique[8,27]. De très bons résultats ont été obtenus avec les stéroïdes, les alcools, les médicaments, les acides aminés et les sels biliaires. Des constantes de liaisons, ainsi que des énergies d'adsorption sont ainsi calculées.

L'IAM a aussi été utilisée pour immobiliser des enzymes[28]. La trypsine et l'α-chymotrypsine ont été piégées dans les cavités hydrophobes du support IAM. L'activité des enzymes ainsi immobilisées a été déterminée et des informations sur les interactions enzyme/substrat et enzyme/inhibiteur ont été obtenues.

1.3 Notre approche

Au cours de cette étude, nous allons développer de nouveaux supports solides permettant d'immobiliser des vésicules lipidiques *via* des (poly)peptides. Comme détaillé précédemment, il existe déjà de nombreux systèmes fonctionnels dans la littérature. La plupart de ces systèmes nécessitent au préalable une modification chimique des lipides ou du support solide, conduisent à une immobilisation peu stable ou sont longs à mettre en œuvre. Au cours de ce travail, on a donc voulu mettre au point des supports polymères présentant certaines caractéristiques. On a tout d'abord voulu développer des méthodes permettant une immobilisation rapide et simple des liposomes. De plus, on souhaite que la perméabilité des liposomes ne soit pas perturbée lors de l'interaction avec le support solide, afin que l'on puisse immobiliser des liposomes

intacts, avec un volume encapsulé à l'intérieur. Ceci pourrait être avantageux pour des applications futures. L'immobilisation doit aussi être la plus stable possible pour pouvoir résister à l'élution par de grandes quantités de tampon (applications chromatographiques) ou à des étapes de centrifugation. Le support ne doit pas être soluble dans des solvants des lipides tels que l'éthanol afin que l'on puisse le laver et le réutiliser pour immobiliser de nouveaux liposomes. Les systèmes mis au point seront suffisamment polyvalents pour permettre l'immobilisation de plusieurs types de lipides, l'interaction entre le support solide et les lipides impliquant soit des interactions électrostatiques avec la tête polaire des lipides ou des interactions hydrophobes avec les chaînes acyles des lipides. Les supports utilisés doivent aussi être biocompatibles, non dénaturants pour les protéines afin d'être utilisables en enzymologie. Pour certaines applications spécifiques, le support doit être résistant à la pression. Au cours de ce travail, nous allons donc développer des supports solides ayant pour point commun d'impliquer une ancre peptidique entre le support et les vésicules. Nous utiliserons deux types de peptides faisant intervenir des interactions différentes entre les lipides et le peptide. Ces peptides seront couplés de façon covalente à des supports polymères de nature différente.

Dans la suite de ce travail, nous utiliserons des vésicules lipidiques constituées de palmitoyloléoylphosphocholine (POPC) et de palmitoyloléoylphosphoglycérol (POPG), deux phospholipides qu'on retrouve en grande quantité dans les membranes cellulaires animales et bactériennes[29]. De plus, ces lipides sont en phase fluide à température ambiante puisque leur température de transition de phase gel-cristal liquide est de -2°C pour la POPC et de 1°C pour le POPG[30]. La charge de la membrane sera modulée en variant la proportion de POPC (globalement neutre) et de POPG (chargé négativement).

1.3.1 Développement d'un système polymère-peptide amphiphile

Lors de ce projet, nous avons choisi d'utiliser un peptide amphiphile pour jouer le rôle d'ancre entre le support solide et la vésicule lipidique. Dans ce cas-ci, l'interaction entre le support et la vésicule devrait impliquer des interactions électrostatiques et hydrophobes. La première étape dans ce travail consistera à mettre au point un peptide amphiphile le plus simple possible, capable d'interagir spontanément et fortement avec

les vésicules, sans perturber leur perméabilité. Afin que le peptide perturbe le moins possible les membranes et que l'insertion soit la plus stable possible, nous avons choisi la séquence d'acide aminés afin d'avoir un peptide hélicoïdal et transmembranaire. Nous nous sommes inspirés de peptides existant déjà dans la nature et possédant ces caractéristiques pour le choix des acides aminés[31]. Nous avons choisi une séquence primaire amphiphile, et nous avons ainsi conçu quatre peptides avec des modifications systématiques de la séquence (Fig. 1.7, Table I). Dans tous les cas, les peptides choisis possèdent un segment hydrophile constitué par des lysines (Lys) et un segment hydrophobe constitué par des alanines (Ala). La longueur du segment hydrophobe a été choisie en fonction de l'épaisseur hydrophobe d'une bicouche lipidique classique (26 Å pour une bicouche à base de POPC[32]), en supposant que le segment hydrophobe adopte une conformation en hélice α. Un peptide plus court sera aussi synthétisé: $A_{12}WK_6$. Son segment hydrophobe a une longueur à peu près équivalente à l'épaisseur hydrophobe d'une couche de lipide (Fig. 1.8 B). Pour $K_6WA_{19}L_3A_2K_2$ et $K_2A_2L_3A_{19}WK_6$, le segment hydrophobe est terminé à chaque extrémité par un segment hydrophile dans le but de stabiliser l'insertion au cas où le peptide s'insérerait dans la bicouche perpendiculairement au plan de la membrane (Fig. 1.8 A). Ces deux peptides possèdent la même séquence d'acide aminés avec inversion des extrémités COOH et NH_2 afin que l'on puisse déterminer l'influence du sens du peptide sur ses caractéristiques, paramètre important lors de l'immobilisation du peptide sur un support solide par une des extrémités. Les structures secondaires, ainsi que l'affinité pour des vésicules lipidiques de ces quatre peptides sont déterminées. Leur influence sur la perméabilité des membranes est aussi estimée. Le peptide présentant les propriétés les plus appropriées comme ancre de vésicules est ainsi identifié. Ce peptide est alors synthétisé en phase solide sur une résine de synthèse peptidique classique, à base de polystyrène (PS) réticulé par du divinylbenzène. Le système polymère/peptide obtenu (Fig. 1.9) est alors utilisé pour immobiliser des vésicules lipidiques. L'affinité du système pour des vésicules, ainsi que l'influence de l'immobilisation sur leur perméabilité est déterminée. Le système polymère/peptide amphiphile obtenu est un support facilement synthétisable en phase solide. Les billes de polymères à base de PS possèdent les qualités de stabilité requises. Il en est de même pour le lien amide entre le peptide et le support solide.

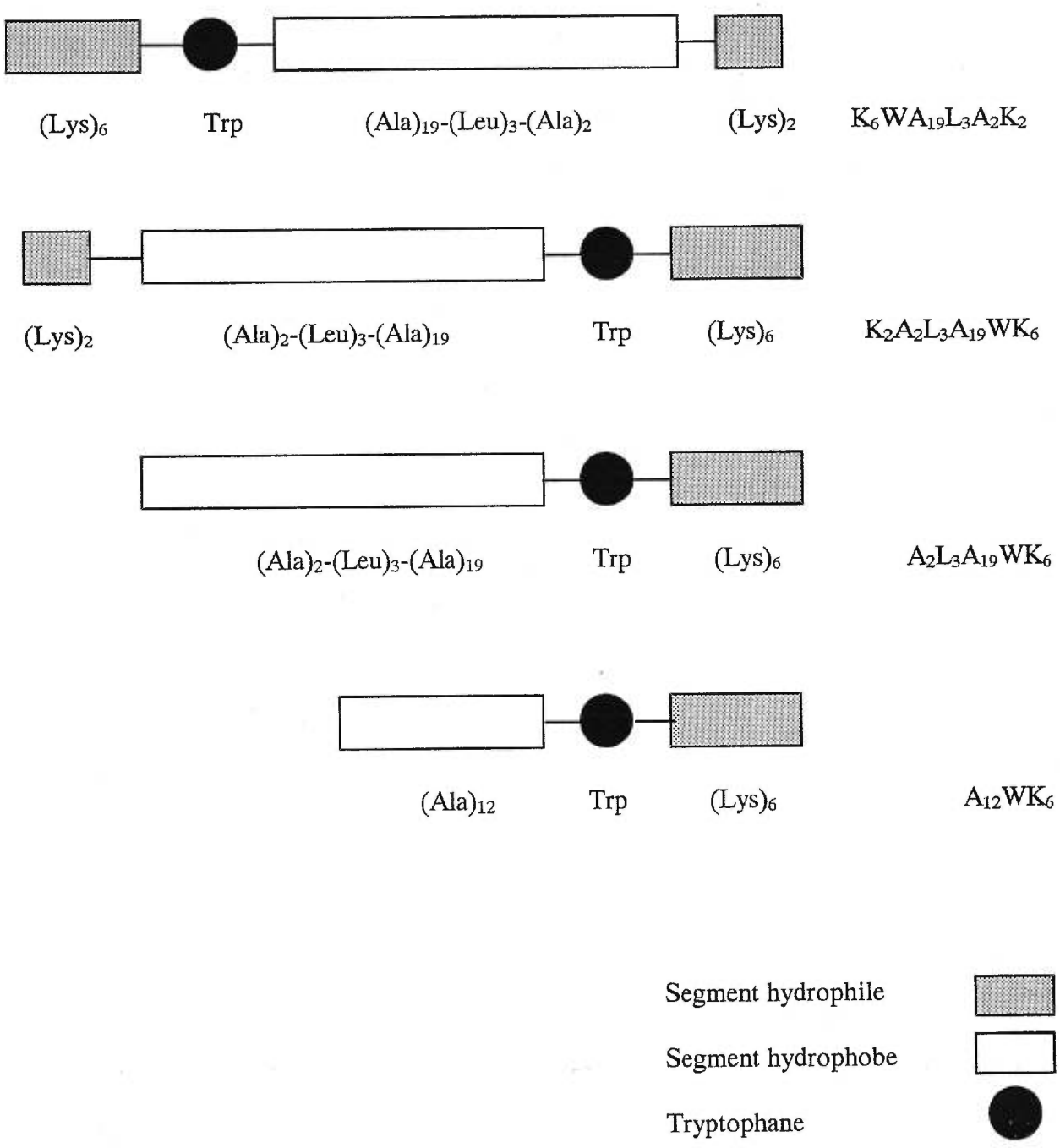

Figure 1.7 Représentation schématique des structures primaires des peptides synthétisés.

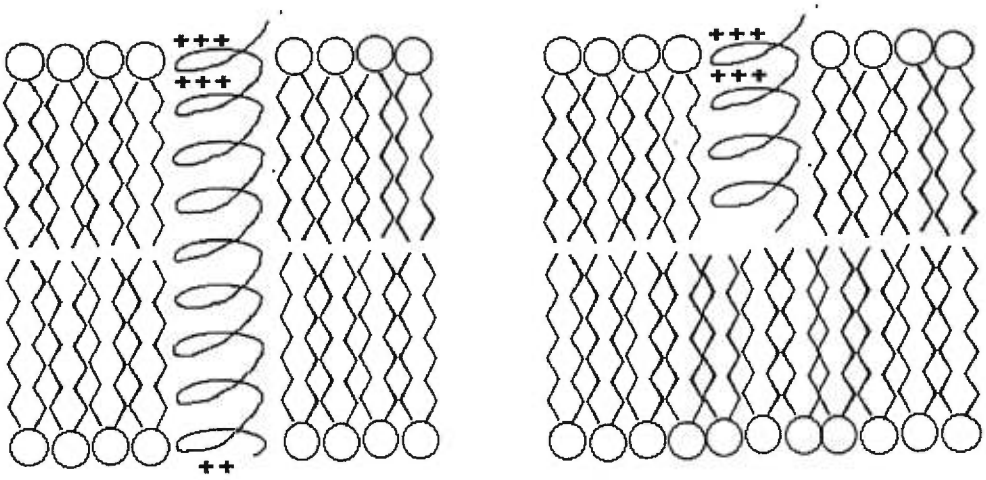

Figure 1.8 Représentation schématique d'un peptide amphiphile transmembranaire inséré dans une bicouche lipidique perpendiculairement au plan de la membrane. Insertion de $K_6WA_{19}L_3A_2K_2$ ou de $K_2A_2L_3A_{19}WK_6$ (A) et de $A_{12}WK_6$ (B).

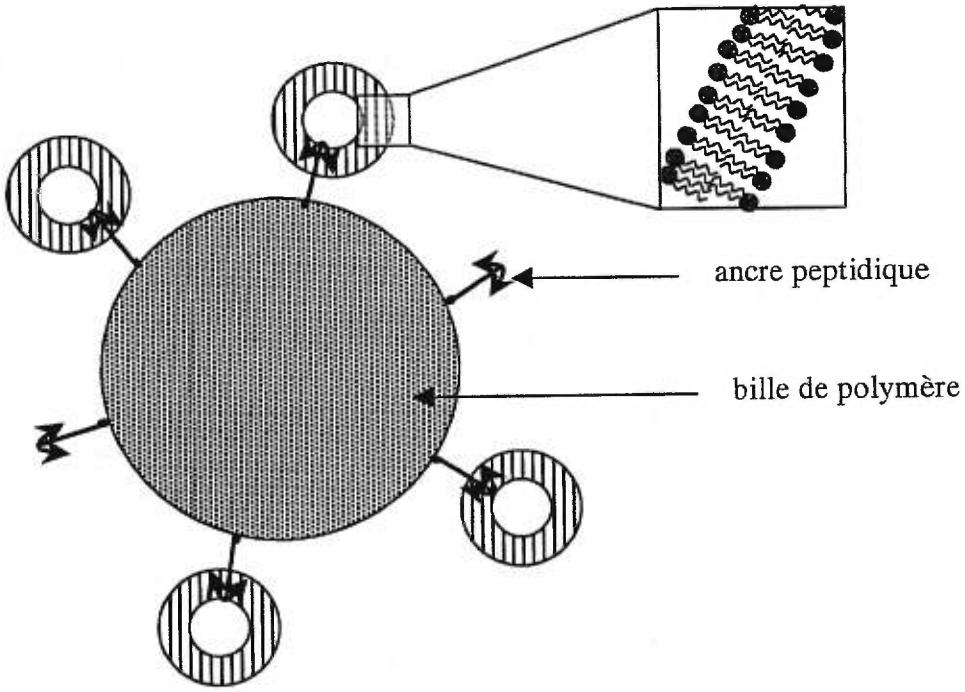

Figure 1.9 Représentation schématique de liposomes immobilisés à la surface d'une bille de polymère par l'intermédiaire d'ancres peptidiques.

L'étape d'immobilisation est rapide et triviale à mettre en œuvre et ne nécessite aucune modification préalable des lipides. Les vésicules immobilisées sont intactes. Le système mis au point possède les caractéristiques souhaitées lors du design et peut être utilisable pour de nombreuses applications.

1.3.2 Développement d'un hydrogel chargé positivement

Dans ce système, les interactions entre les liposomes et le support solide sont majoritairement électrostatiques. La polylysine, un polypeptide cationique est utilisé comme ancre, ainsi que comme réticulant. Contrairement au système précédant où les vésicules sont principalement immobilisées à la surface des billes de polymère, dans ce cas, on a voulu mettre au point un hydrogel permettant de piéger des vésicules en surface mais aussi à l'intérieur des mailles du réseau. L'hydrogel développé est constitué de poly-*N*-isopropylacrylamide (PNIPAAm), un polymère thermosensible compatible avec de nombreuses biomolécules, déjà couramment utilisé pour des applications biomédicales, réticulé par de la polylysine. Les groupements amine de la polylysine servent de points d'attache pour les chaînes de PNIPAAm ainsi que d'ancres chargées positivement pour l'immobilisation des vésicules. Ces segments chargés sont aussi bien en surface qu'à l'intérieur du gel. En plus d'assurer ce rôle d'ancres, ces charges positives augmentent le degré d'hydrophilie de l'hydrogel ainsi que son taux de gonflement. Différents hydrogels ont été synthétisés en utilisant des polylysines plus ou moins longues et en variant le nombre de points d'attache par chaîne de PNIPAAm. Ces hydrogels sont utilisés pour immobiliser des vésicules lipidiques (Fig. 1.10). L'influence de l'immobilisation sur la perméabilité des vésicules est aussi estimée. Le système développé permet d'immobiliser des vésicules sans perturber leur perméabilité. De plus, les propriétés thermosensibles du PNIPAAm permettent d'envisager des applications spécifiques reliées à la libération contrôlée.

1.3.3 Applications

Les deux systèmes mis au point au cours de cette thèse permettent d'immobiliser

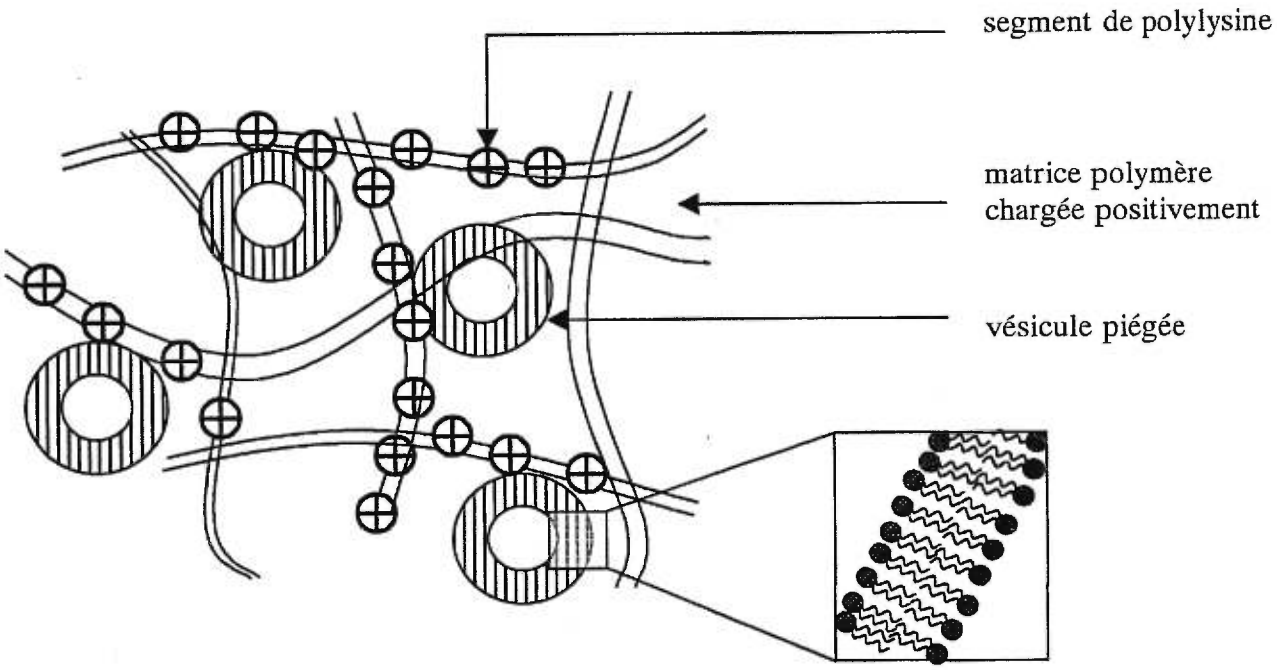

Figure 1.10 Représentation schématique de liposomes immobilisés dans une matrice polymère chargée positivement par l'intermédiaire d'interactions électrostatiques.

des vésicules intactes de façon stable. De nombreuses applications peuvent donc être envisagées pour ces deux systèmes. Au cours de ce travail, nous développerons une application pour chaque système.

Le système polymère-peptide amphiphile est utilisé pour immobiliser des liposomes dans lesquels sont reconstitués une enzyme membranaire. La γ-GT est utilisée comme enzyme membranaire modèle. L'enzyme est alors reconstituée dans la membrane lipidique par simple gel-dégel. Le mélange enzyme libre-enzyme reconstituée est alors mis en contact avec le système polymère-peptide. Un simple lavage permet d'éliminer l'enzyme non immobilisée. L'activité de l'enzyme ainsi immobilisée est alors mesurée. Un des principaux avantages d'un tel système est que l'immobilisation des vésicules contenant l'enzyme est très simple et très rapide à mettre en œuvre. De plus, l'immobilisation est suffisamment stable pour permettre un lavage et une réutilisation de la biomasse. Le bioréacteur enzymatique développé est utilisable pour plusieurs cycles, l'activité de l'enzyme étant conservée.

Dans le cas du système polymère-polylysine, le polymère choisi comme base pour la synthèse de l'hydrogel est un polymère thermosensible qui présente la propriété d'être solubilisé en bas de la température de solution critique (ou LCST pour "lower critical solution temperature") et insoluble au-dessus de la LCST. La température de transition du PNIPAAm est située aux alentours de 30-35°C, c'est-à-dire proche de la température physiologique. Cette propriété fait des hydrogels à base de PNIPAAm, des biomatériaux intéressants dans le domaine biomédical et permet d'envisager pour l'hydrogel développé au cours de ce travail des applications particulières exploitant l'aspect thermosensible du support. Le support solide résultant de la réticulation du PNIPAAm par de la polylysine est un hydrogel thermosensible ayant une température de transition aux alentours de 35°C. Lorsque la température est amenée au-dessus de 35°C, les chaînes polymères subissent une réorganisation et de l'eau est expulsée de l'hydrogel. Lors de cette transition, on peut supposer que les vésicules immobilisées sur ce support sont affectées par cette réorganisation des chaînes de polymère. L'application développée au cours de ce travail consiste donc à immobiliser sur le support polymère/polylysine des vésicules encapsulant un composé fluorescent et à déclencher la libération du composé encapsulé par une augmentation de la température au-dessus de

la LCST de l'hydrogel. Un tel système pourrait présenter des applications dans le domaine de la libération contrôlée de médicaments[33].

1.4 Les techniques utilisées

1.4.1 Principe d'utilisation de la fluorescence du tryptophane pour les tests d'affinité

Le design des peptides amphiphiles inclut volontairement un seul tryptophane, et ce dans un but analytique. Dans la littérature, le tryptophane de peptides modèles ou biologiques, tels que la mélittine est fréquemment utilisé comme sonde afin de déterminer l'affinité de ces peptides pour les membranes lipidiques[34,35]. En effet, comme le maximum d'émission du tryptophane dépend de la polarité du milieu dans lequel il se trouve, on observe un déplacement de ce maximum d'émission lorsque le tryptophane passe du milieu aqueux au milieu hydrophobe la membrane. Au fur et à mesure que la proportion de peptides liés augmente, on observe un déplacement progressif du maximum vers les courtes longueurs d'onde ou déplacement hypsochrome.

Les courbes d'affinité du peptide pour un type de membrane représenteront donc la variation du maximum d'émission du tryptophane en fonction du rapport molaire d'incubation lipide/peptide (R_i) (Fig. 1.11).

Le pourcentage de peptide lié pourra être estimé de la façon suivante

$$\%\, lié = \frac{\left(\lambda_{libre} - \lambda_{observée}\right)}{\left(\lambda_{libre} - \lambda_{lié}\right)} \times 100$$

où λ_{libre} correspond à la longueur d'onde associée au maximum d'émission du tryptophane en milieu aqueux et $\lambda_{lié}$ à la longueur d'onde associée au maximum d'émission du tryptophane lié à la membrane (c'est-à-dire à la longueur d'onde correspondant au plateau de la courbe d'affinité, lorsque l'on considère que tous les

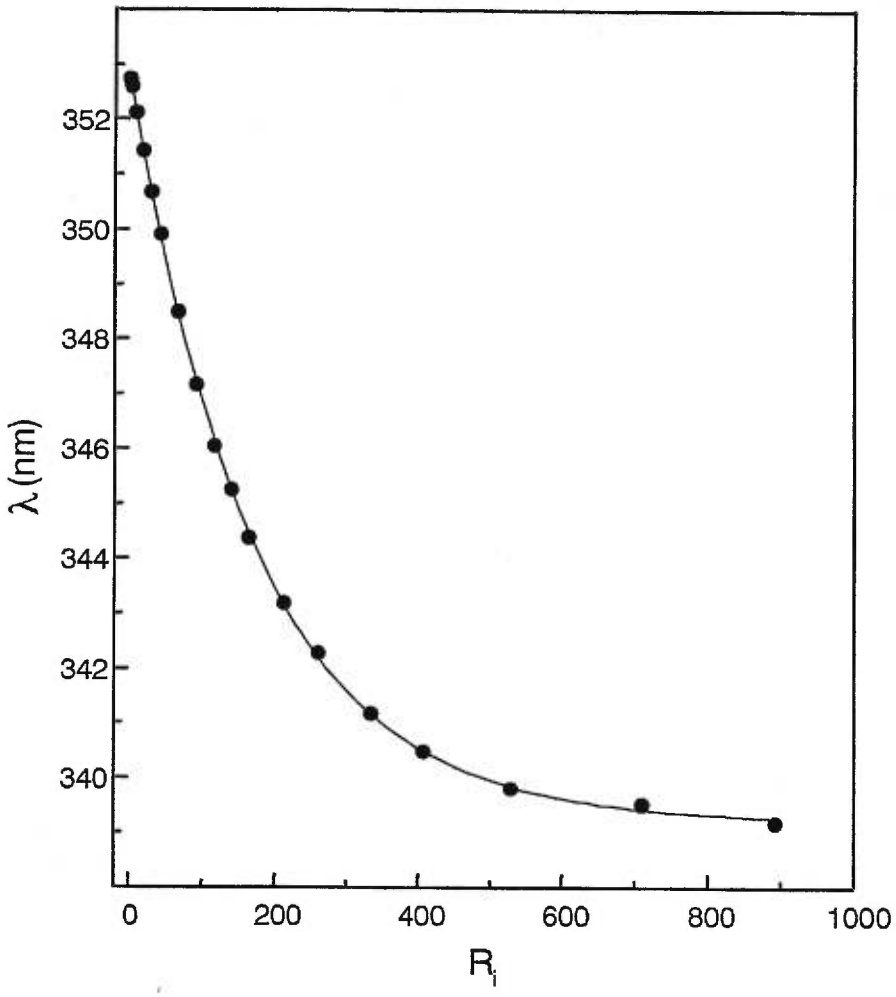

Figure 1.11 Courbe d'affinité de $K_2A_2L_3A_{19}WK_6$ pour des vésicules de POPC:POPG (85:15)[36].

peptides sont liés). On fait alors l'approximation que $\lambda_{observée}$ est directement proportionnelle au pourcentage de peptide lié. Ce pourcentage nous permettra d'obtenir les isothermes de liaison des peptides aux membranes.

1.4.2 Technique d'analyse de fuite

La technique d'analyse de fuite permet de suivre la libération de matériel encapsulé dans des vésicules suite à une perturbation. C'est une approche simple pour examiner si l'imperméabilité des vésicules est conservée durant l'immobilisation ou l'insertion des peptides modèles. Dans notre cas, nous utilisons une molécule fluorescente pour sonder la perméabilité des vésicules. Cette approche est basée sur la propriété d'auto-extinction de la fluorescence de la sonde. Deux sondes fluorescentes ont été utilisées au cours de ce travail: la calcéine et la sulforhodamine B (SRB) (Fig. 1.12). Ces deux sondes présentent les propriétés requises pour ces expériences de fuite[37]. Les deux composés fluorescents sont des espèces chargées, ce qui fait que la membrane lipidique est pratiquement imperméable à ces sondes, et leur fluorescence est auto-éteinte à haute concentration. Afin de caractériser l'auto-extinction de la sonde, nous calculerons le facteur Q, l'efficacité de l'extinction de la fluorescence:

$$Q = (1 - \frac{I_B}{I_T}) \text{x} 100$$

où I_B représente l'intensité de fluorescence résiduelle provenant de la sonde encapsulée à haute concentration et I_T l'intensité de fluorescence totale, correspondant à 100% de fuite, obtenue suite à la destruction de toutes les vésicules par addition de Triton X-100. La figure 1.13 représente la variation de Q en fonction de la concentration pour les deux sondes utilisées. A haute concentration, il y a existence d'interaction fluorophore-fluorophore et extinction de la fluorescence. On a une valeur de Q d'environ 90%. Lorsque la concentration de la sonde encapsulée diminue, on a une diminution de l'auto-extinction et donc du facteur Q. La concentration de sonde à l'intérieur des vésicules sera choisie en fonction de la mesure à effectuer et de la sonde utilisée.

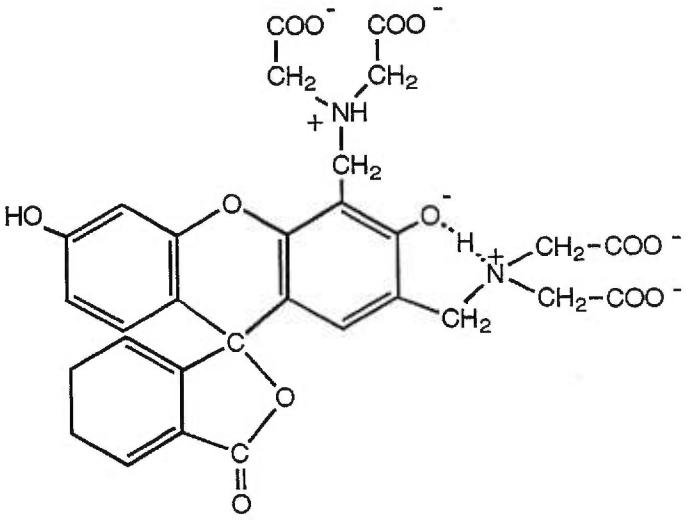

(A)

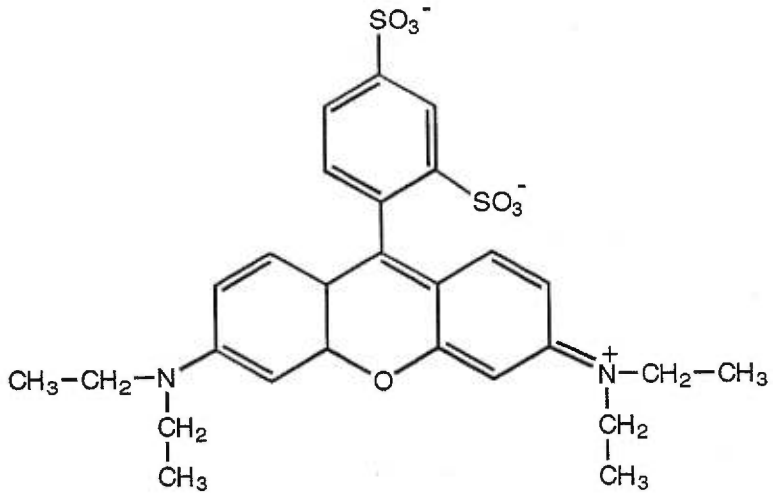

(B)

Figure 1.12 Structure de la calcéine (A) et de la SRB (B).

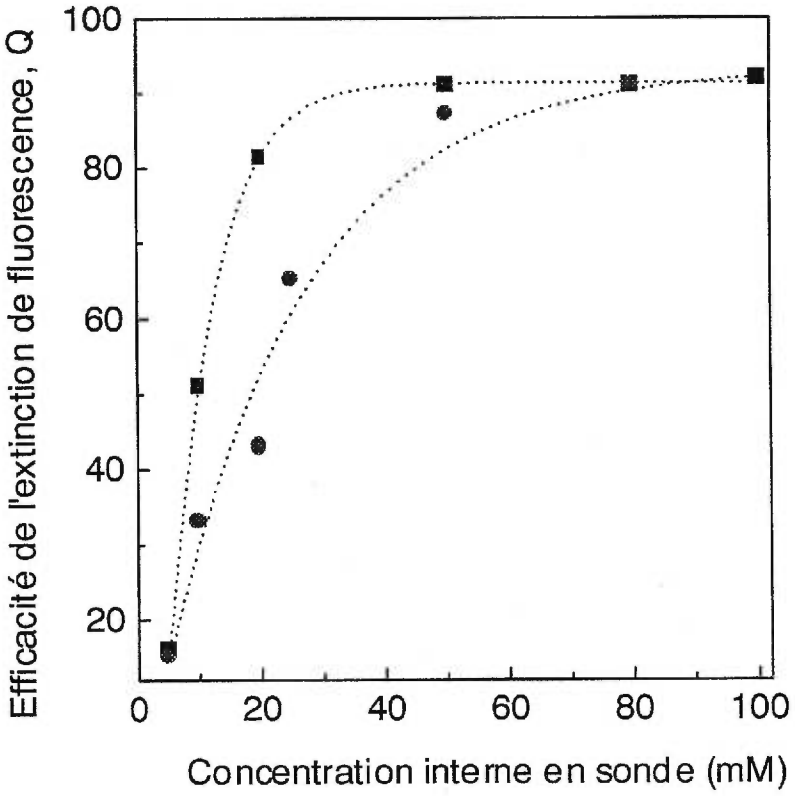

Figure 1.13 Variation de l'efficacité de l'auto-extinction de la calcéine (●) et de la SRB (■) encapsulées dans des vésicules de POPC en fonction de leur concentration interne (pH 6)[37].

Dans un premier temps, nous utiliserons la technique de fuite afin de caractériser la libération d'un composé fluorescent sous l'effet d'une perturbation lors de l'interaction avec un peptide. On pourra simplement suivre la libération de la sonde via l'augmentation de la fluorescence (Fig. 1.14). Le fluorophore est encapsulé à haute concentration à l'intérieur des vésicules, ce qui mène à l'auto-extinction de sa fluorescence (I_B). L'addition de peptide, si elle perturbe la perméabilité de la membrane induit la libération du fluorophore à l'extérieur de la vésicule. Le fluorophore se retrouve alors dilué dans le milieu aqueux, ce qui entraîne une augmentation de l'intensité de fluorescence (I_F). On peut alors calculer un pourcentage de fuite qui nous renseigne sur la quantité de sonde libérée. Ce pourcentage est calculé selon l'expression suivante:

$$\% \ fuite = \frac{(I_F - I_B)}{(I_T - I_B)} \times 100$$

Les concentrations de lipides et de sonde doivent remplir deux conditions, l'auto-extinction de la sonde encapsulée doit être maximale et on doit se trouver dans la région linéaire de fluorescence lorsque toute la sonde est libérée. Lorsqu'une vésicule libère une fraction de son contenu, la concentration de sonde encapsulée diminue. Afin de pouvoir négliger l'influence de la sonde encapsulée, il faut s'assurer que la concentration interne reste suffisamment élevée même en cas de fuite importante. En se plaçant à une concentration de sonde encapsulée élevée, de l'ordre de 80 mM, on assure une bonne auto-extinction de la sonde encapsulée, même pour des fuites importantes.

Lors d'une deuxième approche, la technique de fluorescence a été utilisée pour caractériser l'intégrité des vésicules suite à leur immobilisation sur un support solide. Pour ce type de caractérisation, nous chercherons à déterminer l'efficacité de l'extinction de fluorescence. Q nous renseignera sur l'évolution de la concentration interne des vésicules. Pour plus de sensibilité de la mesure, on peut se placer à une concentration interne de sonde plus faible, à la limite du plateau correspondant au maximum d'extinction. Une faible diminution de la concentration interne de sonde se traduira alors par une baisse significative de Q.

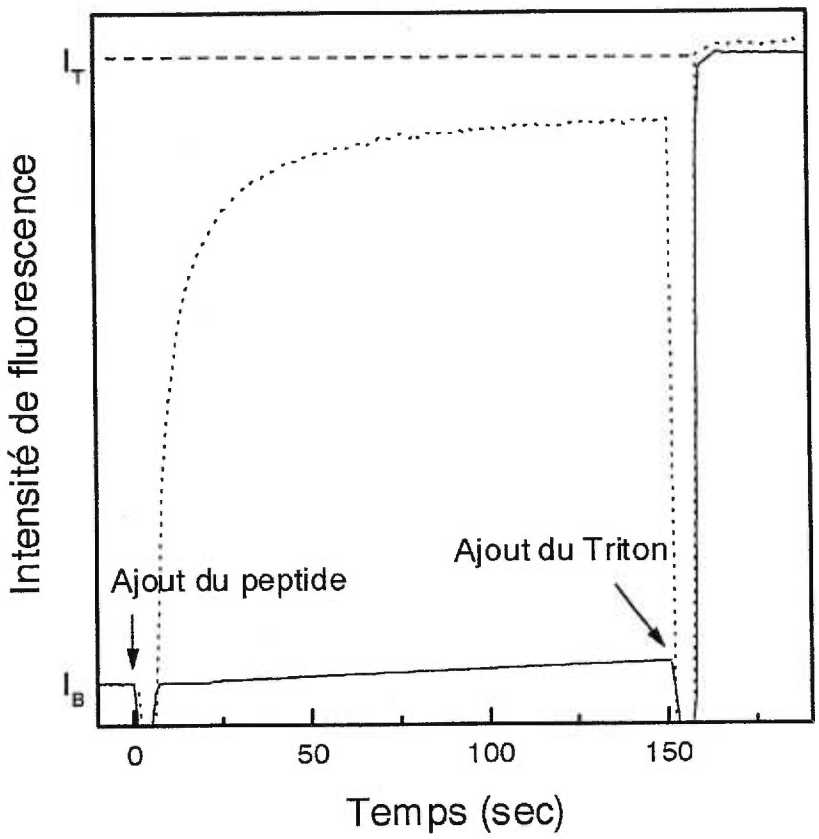

Figure 1.14 Variation de l'intensité de fluorescence de la calcéine lors de la fuite induite par l'addition de mélittine en présence de vésicules de POPC (----) et par l'addition de $K_2A_2L_3A_{19}WK_6$ en présence de vésicules de POPC:POPG (85:15) (—).

1.4.3 La spectroscopie infrarouge

Au cours de ce travail, la spectroscopie infrarouge à transformée de Fourier (FTIR) sera utilisée pour déterminer la LCST des polymères linéaires et réticulés.

Pour caractériser les interactions impliquées dans la transition se produisant à la LCST, nous avons suivi le comportement de bandes associées à différents groupements chimiques en fonction de la température. Nous avons tout d'abord étudié les bandes d'absorption associées à l'élongation C–H des chaînes acyles (υ_{C-H}) situées entre 2700 et 3100 cm^{-1} (Fig. 1.15). Le déplacement associé à υ_{C-H} est un outil utile pour suivre la réorganisation des chaînes alkyles avec la température. Les modes de vibration associés à l'élongation antisymétrique et symétrique des CH_2 sont sensibles à l'ordre des chaînes carbonées[38-40]. En suivant le déplacement du maximum de ces bandes en fonction de la température, on pourra obtenir des informations quant à l'implication de ces groupements dans la transition, ainsi que des informations quant à leur ordre conformationnel. Plusieurs facteurs peuvent influencer les bandes υ_{C-H}, tels que l'introduction de conformères gauche, le couplage vibrationnel interchaîne ainsi que la librotorsion qui introduit des angles de torsion entre deux méthylènes[41,42]. Cependant, le facteur le plus important reste l'ordre conformationnel.

La seconde région du spectre du polymère étudiée est située entre 1500 et 1700 cm^{-1} et correspond à des vibrations caractéristiques du groupement amide. L'infrarouge est une technique utilisée depuis 1950 pour étudier la conformation des peptides et des protéines. Il existe 9 modes de vibration possibles pour le groupement amide. La vibration Amide I située entre 1600 et 1700 cm^{-1} correspond à la vibration d'élongation C=O du groupe amide couplé dans le plan au cisaillement N–H et l'élongation C–N (Fig. 1.16). La fréquence exacte de cette vibration dépend de la nature de la liaison hydrogène impliquant le groupement C=O. La bande Amide II est aussi sensible à la conformation du groupement amide. Au cours de cette étude, nous avons suivi l'état de liaison du carbonyle du groupement amide à l'aide de la bande Amide I qui est la plus affectée par la transition. Certaines études ont proposé que la bande Amide I des systèmes polymères semblables à ceux utilisés dans le travail inclut trois composantes, reflétant chacune un

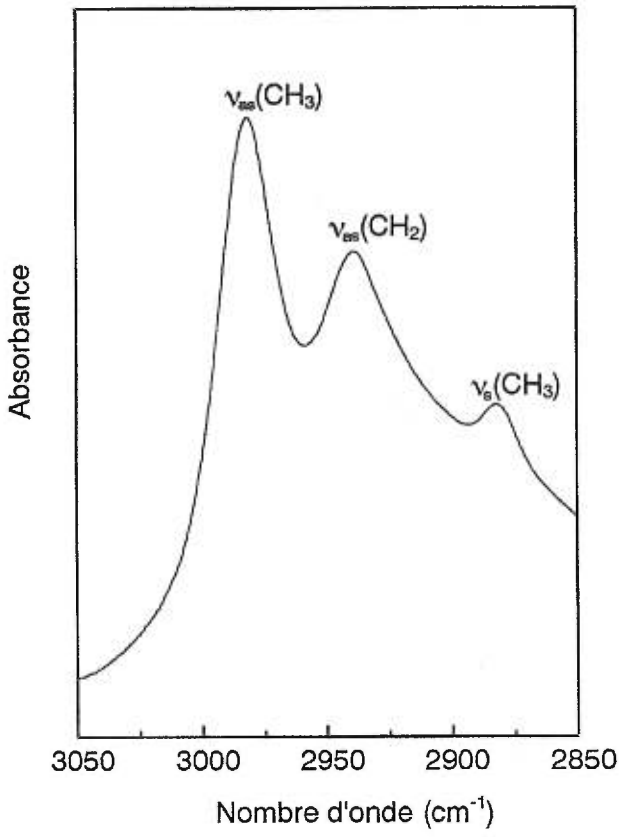

Figure 1.15 Région située entre 2850 et 3050 cm^{-1} du spectre FTIR correspondant aux bandes d'absorption associées à l'élongation C-H des chaînes acyles pour le poly(*N*-isopropylacrylamide-co-*N*-acryloxysuccinimide) (98-2) à 25°C corrigé pour l'eau.

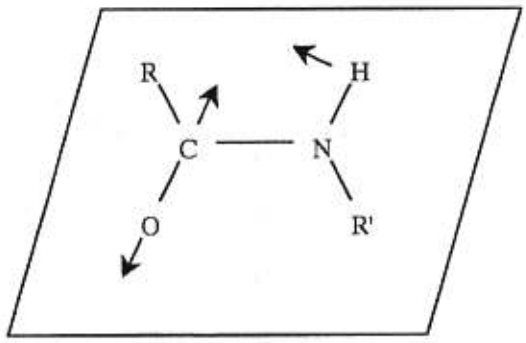

Figure 1.16 Mode de vibration Amide I du groupement amide.

état de liaison hydrogène différent pour le carbonyle impliqué. Aussi, au cours de ce travail, nous décomposerons la bande en trois composantes et pourrons alors suivre les proportions des états de liaison du carbonyle en fonction de la température. La caractérisation des états de liaison du carbonyle nous renseignera quant à la nature des interactions impliquées dans le phénomène de LCST et viendra compléter les informations obtenues dans la région des C–H sur les groupements hydrophobes.

1.5 Description des projets

Au cours de ce travail, nous avons développé deux types de supports solides permettant d'immobiliser des vésicules lipidiques intactes. Les deux systèmes font appel à des stratégies d'immobilisation différentes tout en impliquant dans les deux cas une ancre peptidique. Dans un des deux systèmes, l'ancre entre le support et les vésicules est un peptide amphiphile, dans l'autre, l'ancre utilisée est un polypeptide cationique. La première partie de cette thèse sera consacrée à l'étude du système polymère/peptide amphiphile, de la conception à l'application. La deuxième partie traitera du système polymère/polylysine, c'est à dire de l'hydrogel thermosensible.

Dans le deuxième chapitre, nous caractériserons les quatre peptides développés afin de jouer le rôle d'ancre amphiphile entre le support solide et les vésicules. Leur conformation en solution et en présence de lipides sera déterminée. Leur affinité pour les vésicules en fonction de la proportion de lipides chargés négativement sera déterminée, ainsi que leur effet sur la perméabilité de la membrane. Nous essayerons aussi de déterminer la nature de l'interaction peptide/lipide. Le peptide possédant les caractéristiques les plus adaptées à l'immobilisation de vésicules sera identifié.

Dans le troisième chapitre, nous étudierons les performances du système complet constitué du peptide le plus performant greffé sur des billes de PS. Nous déterminerons l'affinité du support solide pour des vésicules contenant différentes proportions de lipides chargés négativement. Le système sera ensuite appliqué à l'immobilisation d'une enzyme membranaire modèle, la γ-GT. La γ-GT, reconstituée dans des liposomes

contenant 50 % de lipides chargés négativement sera immobilisée sur le support solide. L'activité de l'enzyme sera alors mesurée en fonction du nombre de cycle de réutilisation.

La suite de la thèse sera consacrée à l'étude du système à base de l'hydrogel thermosensible. Nous commencerons par le quatrième chapitre en traitant de la détermination de la LCST dans un hydrogel. Cette température est facile à déterminer pour les chaînes linéaires de polymère, la séparation de phase étant observable à l'œil nu. En ce qui concerne les systèmes réticulés, insolubles, tels que les hydrogels, cette température de transition est beaucoup plus difficile à déterminer. Au cours de ce travail, nous avons donc mis au point une méthode spectroscopique simple permettant de déterminer cette LCST et de comprendre un peu mieux le phénomène. La spectroscopie FTIR permet d'identifier les groupements du polymère impliqués dans la transition et de déterminer plus précisément les interactions mises en jeu.

Dans le cinquième chapitre, nous détaillerons la synthèse et la caractérisation de différents hydrogels à base de PNIPAAm et de polylysine de différentes longueurs. La capacité de ces différents hydrogels à immobiliser des vésicules intactes sera alors déterminée. L'hydrogel le plus performant sera utilisé pour une application de libération contrôlée du contenu des vésicules immobilisées, en fonction de la température.

Dans le sixième chapitre, nous conclurons quant à l'ensemble des résultats obtenus au cours de ce travail. Nous envisagerons les améliorations possibles des systèmes développés, ainsi que les applications potentielles de ces deux systèmes.

1.6 Références

1. Horvàth, C. *High-Performance Liquid Chromatography*; Harcourt Brace Javanovich: Academic Press, Inc., 1986.

2. Loidl-Stahlhofen, A.; Kaufmann, S.; Braunschweig, T.; Bayerl, T. M. *Nature Biotechnology* **1996**, *14*, 999-1002.

3. Pidgeon, C.; Venkataram, U. V. *Anal. Biochem.* **1989**, *176*, 36-47.

4. Sandberg, M.; Lundahl, P.; Greijer, E.; Belew, M. *Biochim. Biophys. Acta* **1987**, *924*, 185-192.

5. Loidl-Stahlhofen, A.; Ulrich, A. S.; Kaufmann, S.; Bayerl, T. M. *Eur. Biophys. J.* **1996**, *25*, 151-153.

6. Yang, Q.; Wallstén, M.; Lundahl, P. *Biochim. Biophys. Acta* **1988**, *938*, 243-256.

7. Pidgeon, C.; Cai, S. J.; Bernal, C. *J. Chromatogr. A* **1996**, *721*, 213-230.

8. Zhang, Y.; Xiao, Y.; Kellar, K. J.; Wainer, I. W. *Anal. Biochem.* **1998**, *264*, 22-25.

9. Messing, R. A. *Immobilized Enzymes for Industrial Reactors*; Academic Press: New York, 1975.

10. Katchalski, E.; Silman, I.; Goldman, R. *Adv. Enzymol. Relat. Areas Mol. Biol.* **1971**, *34*, 445-536.

11. Kino, Y.; Sawa, M.; Kasai, S.; Mito, M. *J. Surg. Res.* **1998**, *79*, 71-76.

12. Kattar, J. I. S.; Sarma, T. A.; Singh, D. P. *Enzyme Microb. Technol.* **1999**, *25*, 564-568.

13. Drumheller, P. D.; Hubbell, J. A. *Anal. Biochem.* **1994**, *222*, 380-388.

14. Yang, Q.; Wallstén, M.; Lundahl, P. *J. Chromatogr.* **1990**, *506*, 379-389.

15. Yang, Q.; Lundahl, P. *J. Chromatogr.* **1990**, *512*, 377-386.

16. Gotoh, T.; Shidara, M.; Iwanaga, T.; Kikuchi, K.; Hozawa, M. *J. Ferment. Bioeng.* **1994**, *77*(3), 268-273.

17. Gotoh, T.; Kikuchi, K. *J. Chem. Eng. Jpn.* **1998**, *31*(5), 860-863.

18. Bayerl, T. M.; Bloom, M. *Biophys. J.* **1990**, *58*, 357-362.

19. Sackmann, E. *Science* **1996**, *271*, 43-48.

20. Lingler, S.; Rubinstein, I.; Knoll, W.; Offenhäusser, A. *Langmuir* **1997**, *13*, 7085-7091.

21. Plant, A. L. *Langmuir* **1999**, *15*, 5128-5135.

22. Théato, P.; Zentel, R. *Langmuir* **2000**, *16*, 1801-1805.

23. Zhang, Y.; Zeng, C.-M.; Li, Y.-M.; Hjertén, S.; Lundahl, P. *J. Chromatogr. A* **1996**, *749*, 13-18.

24. Schilcher, K.; Hinterdorfer, P.; Gruber, H. J.; Schindler, H. *Cell Biology International* **1997**, *21*, 769-778.

25. Yang, Q.; Liu, X.-Y.; Ajiki, S.-I.; Hara, M.; Lundahl, P.; Miyake, J. *J. Chromatogr. B* **1998**, *707*, 131-141.

26. Yang, Q.; Liu, X.-Y.; Miyake, J.; Toyotama, H. *Supramol. Sci.* **1998**, *5*, 769-772.

27. Ong, S.; Qiu, X.; Pidgeon, C. *J. Phys. Chem.* **1994**, *98*, 10189-10199.

28. Chui, W.-K.; Wainer, I. W. *Anal. Biochem.* **1992**, *201*, 237-245.

29. Gennis, R. B. *Biomembranes Molecular Structure and Function*; Édition Springer-Verlag: New York, 1989.

30. Wiedmann, T.; Salmon, A.; Wong, V. *Biochim. Biophys. Acta* **1993**, *1167*, 114-120.

31. Dempsey, C. E. *Biochim. Biophys. Acta* **1990**, *1031*, 143-161.

32. Nezil, F. A.; Bloom, M. *Biophys. J.* **1992**, *61*, 1176-1183.

33. Bochot, A.; Fattal, E.; Gulik, A.; Couarraze, G.; Couvreur, P. *Pharm. Res.* **1998**, *15*(9), 1364-1369.

34. Georghiou, S.; Thompson, M.; Mukhopadhyay, A. K. *Biochim. Biophys. Acta* **1982**, *688*, 441-452.

35. Surewicz, W. K.; Epand, R. M. *Biochemistry* **1984**, *23*, 6072-6077.

36. Percot, A.; Zhu, X. X.; Lafleur, M. *Biopolymers* **1999**, *50*, 647-655.

37. El Jastimi, R.; Lafleur, M. *Biospectroscopy* **1999**, *5*, 133-140.

38. Mantsch, H. H.; McElhaney, R. N. *Chem. Phys. Lipids* **1991**, *57*, 213-226.

39. Casal, H. L.; Cameron, D. G.; Mantsch, H. H. *Can. J. Chem.* **1983**, *61*, 1736-1742.

40. Li, H.; Zhang, X.; Zhang, R.; Shen, J.; Zhao, B.; Xu, W. *Macromolecules* **1995**, *28*, 8178-8181.

41. Kodati, V. R.; El Jastimi, R.; Lafleur, M. *J. Phys. Chem.* **1994**, *98*, 12191-12197.

42. Umemura, J.; Cameron, D. G.; Mantsch, H. H. *J. Phys. Chem.* **1980**, *84*, 2272-2277.

CHAPITRE 2

DESIGN AND CHARACTERIZATION OF ANCHORING AMPHIPHILIC PEPTIDES AND THEIR INTERACTIONS WITH LIPID VESICLES

Aline Percot, X.X. Zhu and Michel Lafleur, Biopolymers, **50**, 647-655 (1999).

Running title: Design and characterization of anchoring amphiphilic peptides

Keywords: amphiphilic peptides, peptide conformation, membrane permeability, peptide-lipid interactions

2.1 Abstract

In an effort to develop a polymer/peptide assembly for the immobilization of lipid vesicles, we have made and characterized four water-soluble amphiphilic peptides designed to associate spontaneously and strongly with lipid vesicles without causing significant leakage from anchored vesicles. These peptides have a primary amphiphilic structure with the following sequences: AAAAAAAAAAAAWKKKKKK, AALLLAAAAAAAAAAAAAAAAAAWKKKKKK, KKAALLLAAAAAAAAAAAAAAAAAAWKKKKKK and its reversed homologue KKKKKKWAAAAAAAAAAAAAAAAAALLLAAKK. Two of the four peptides have their hydrophobic segments capped at both termini with basic residues to stabilize the transmembrane orientation and to increase the affinity for negatively charged vesicles. We have studied the secondary structure and the membrane affinity of the peptides as well as the effect of the different peptides on the membrane permeability. The influence of the hydrophobic length and the role of lysine residues were clearly established. First, a hydrophobic segment of 24 amino acids, corresponding approximately to the thickness of a lipid bilayer, improves considerably the affinity to zwitterionic lipids compared to the shorter one of 12 amino acids. The shorter peptide has a low membrane affinity since it may not be long enough to adopt a stable conformation. Second, the presence of lysine residues is essential since the binding is dominated by electrostatic interactions as illustrated by the enhanced binding with anionic lipids. The charges at both ends, however, prevent the peptide from inserting spontaneously in the bilayer since it would involve the translocation of a charged end through the apolar core of the bilayer. The direction of the amino acid sequence of the peptide has no significant influence on its behavior. None of these peptides perturb membrane permeability even at an incubation lipid to peptide molar ratio of 0.5. Among the four peptides, AALLLAAAAAAAAAAAAAAAAAAWKKKKKK is identified as the most suitable anchor for the immobilization of lipid vesicles.

2.2 Introduction

The immobilization of lipid vesicles on a solid support can lead to a wide range of applications including the development of chromatographic methods,[1,2] enzymatic reactions on polymer resins with reconstituted enzymes in immobilized bilayers,[3] controlled drug release systems[4,5] and immobilizing devices for cells and cellular aggregates.[6] Several approaches have been developed for the immobilization of lipid membranes. Micro-glass beads were coated with lipids to provide a spherical supported vesicle (SSV).[7] Lipids were also immobilized covalently[1,2] or sterically[8] on a solid matrix to develop immobilized artificial membranes (IAM). Alternatively, anchors linked to solid supports could be used to immobilize vesicles or cells, an approach which has already been explored using lipidic anchors to graft polymers on vesicles.[9,10] Even so, stable immobilization with minimum perturbation remains a challenge. Our strategy is to develop stable peptide/polymer assemblies in which amphiphilic peptide anchors are used as alternative and versatile linkers.

The literature on model peptide-membrane interactions is rich and the knowledge that has been developed is useful for *de novo* design of peptides. For our applications, the best-suited anchoring peptides should be water-soluble and able to associate with lipid bilayers spontaneously and strongly. The peptides should not perturb the permeability of the membrane since the immobilized vesicles may be used as microscopic containers. These specific features have to be characterized to identify suitable peptides. Since the secondary amphiphilic peptides are often biologically active,[11] our designed peptides were inspired by the proteins and peptides with a primary amphiphilic topology that corresponds to a sequence of polar and apolar segments.[12] We designed peptides made of a hydrophobic segment of alanine and leucine and hydrophilic end(s) that include lysine residues. We have synthesized and characterized several peptides which are listed in Table I and referred to as $K_6WA_{19}L_3A_2K_2$, $K_2A_2L_3A_{19}WK_6$, $A_2L_3A_{19}WK_6$ and $A_{12}WK_6$.

Peptide	Primary structure
$K_6WA_{19}L_3A_2K_2$	KKKKKKWAAAAAAAAAAAAAAAAAAALLLAAKK
$K_2A_2L_3A_{19}WK_6$	KKAALLLAAAAAAAAAAAAAAAAAAWKKKKKK
$A_2L_3A_{19}WK_6$	AALLLAAAAAAAAAAAAAAAAAAWKKKKKK
$A_{12}WK_6$	AAAAAAAAAAAAWKKKKKK

Table I The primary structures of the model peptides

If the hydrophobic segment adopts a helical structure, the length of the longer segment with 24 amino acids would be long enough to span typical bilayers. In our studies, we used 1-palmitoyl-2-oleoyl-*sn*-glycero-3-phosphatidylcholine (POPC) as a model membrane because its hydrophobic thickness (26 Å [13]) is typical of that measured for biological membranes. The unavoidable small mismatch between the length of the apolar segment of the peptide and the hydrophobic thickness of the bilayer may be counterbalanced by the lipids either by stretching or by disordering their hydrocarbon chains.[13-15] The shorter segment with 12 amino acids would correspond roughly to half a bilayer. Alanine residues were used since they are known to form very stable α-helices.[16,17] For the longer hydrophobic segments, three alanine residues were replaced with leucine units to increase the hydrophobicity of the sequence and to promote the formation a of α-helix.[18-21] For $K_6WA_{19}L_3A_2K_2$ and $K_2A_2L_3A_{19}WK_6$, two alanine units were inserted between the leucine residues and the charged end to smooth out the change in hydrophilicity. For $A_2L_3A_{19}WK_6$, the same hydrophobic segment was retained. For all the peptides, a tryptophan residue was inserted between the hydrophilic and the hydrophobic segment as a convenient fluorescent probe to study peptide binding.[22,23] In addition, the presence of tryptophan residues at the hydrophilic/hydrophobic bilayer interface is common in natural peptides/proteins[24] and is believed to provide enhanced stabilization of peptides in bilayers.[15,25] Lysine residues

were chosen for the hydrophilic part since this amino acid favors helix conformation and helps to solubilize the hydrophobic block. Moreover, the presence of positive charges on the peptides is also expected to increase their affinity for biomembranes since the latter generally contain a significant proportion of negatively charged lipids. For $K_6WA_{19}L_3A_2K_2$ and $K_2A_2L_3A_{19}WK_6$, the two hydrophilic ends with lysine residues were thought to enhance their transmembrane stability.[13] $K_2A_2L_3A_{19}WK_6$ and its reversed homologue $K_6WA_{19}L_3A_2K_2$ were compared (the reversed peptide refers to a peptide with the same primary amino acid sequence but with the C-terminal and the N-terminal group inverted). In the cases of $A_2L_3A_{19}WK_6$ and $A_{12}WK_6$, only the C-terminal ends include lysine residues.

In order to evaluate the potential of these peptides as efficient vesicle anchors, we have characterized their secondary structures in the free and vesicle-bound forms using CD. The affinity of the peptides for zwitterionic and for negatively charged vesicles has been determined by the use of tryptophan fluorescence. Finally, the potential influence of the peptides on vesicle permeability was examined.

2.3 Materials and methods

2.3.1 Peptides synthesis and purification

The peptides were synthesized using standard procedures for solid phase Fmoc (9-fluorenylmethoxycarbonyl) chemistry. Automated synthesis was carried out using an Advanced ChemTech synthesizer 396 MPS. The resin used was an Fmoc-Lys(Boc)-Wang resin from Applied Biosystems Inc. (Foster City, CA). The peptides were purified by reverse-phase high performance liquid chromatography on a Waters C-18 column with a trifluoroacetic acid-acetonitrile-water mixture as the eluent. The purified peptides were identified by mass spectrometry. The matrix-assisted laser desorption ionization time-of-flight mass spectrometry experiments were carried out in a TOF Spec2E (Micromass, Manchester, UK).

2.3.2 Preparation of vesicles

POPC and 1-palmitoyl-2-oleoyl-*sn*-glycero-3-phosphatidylglycerol (POPG) were purchased from Avanti Polar Lipids (Birmingham, AL), calcein (2,4-bis-[N,N'-di(carboxymethyl) aminomethyl] fluorescein) from Molecular Probes Inc. (Eugene, OR), 4-(2-Hydroxyethyl)-1-piperazineethanesulfonic acid (HEPES) and Triton X-100 from Sigma (St. Louis, MO), and ethylenediaminetetraacetic acid (EDTA) from Aldrich (Milwaukee, WI).

The lipid stock solutions were prepared by dissolving each lipid in a 95/5 (v/v) benzene/methanol solvent and the lipid mixtures were obtained by mixing appropriate volumes of the stock solutions. The lipids were lyophilized from the benzene/methanol solutions and then hydrated with the calcein-containing buffer. Large unilamellar vesicles (LUV's) were prepared as previously described[26] by extrusion through polycarbonate filters of 100 nm pore size. Phospholipid concentrations were determined by the Fiske-SubbaRow phosphorus assay.[27]

2.3.3 Binding studies

Intrinsic fluorescence of the single tryptophan of these peptides was used to quantify the binding of the peptide to lipid vesicles.[22,23] The binding studies were conducted as reported.[26] To describe the process briefly: 5 μM peptide suspensions were prepared in a pH 7.4 buffer (20 mM HEPES, 2 mM EDTA, 100 mM NaCl). LUV's were prepared in the same buffer and diluted to about 10 mM. Lipid aliquots were added stepwise to the peptide solution. Spectra were recorded after each lipid addition. The wavelength of excitation was fixed at 280 nm and each spectrum was the result of 3 scans with an integration time of 0.3 s/nm. The spectra of blanks without the peptide were also recorded and subtracted from the tryptophan emission spectra to eliminate the Raman band of water and diffusion effects. The emission wavelength was measured as the middle point at 3/4 height of the band in the emission spectra. This wavelength ($\lambda_{3/4}$) was determined by fitting the emission band with three peaks using GRAMS software

(Galactic Industry, Salem) and determining $\lambda_{3/4}$ on the simulated spectra. This method led to reproducible results and minimized the influence of the correction with the blank.

In a different protocol, $K_6WA_{19}L_3A_2K_2$ and $K_2A_2L_3A_{19}WK_6$ were colyophilized with POPC to examine an alternative way of preparing the peptide/lipid complexes. The lipids and the peptide were dissolved separately in a 70/30 (v/v) benzene/methanol mixture. An aliquot of the peptide solution was lyophilized alone while a similar aliquot was added to the POPC solution, vigorously stirred and then lyophilized. The two samples were then hydrated and the lipid dispersion was extruded as described previously. The spectra were recorded under the conditions described above. The exact concentration of the peptide was determined by measuring the absorbance at 280 nm ($\varepsilon = 5600\ M^{-1}cm^{-1}$).

2.3.4 Leakage experiments

The leakage experiments were carried out by measuring the calcein release as previously described.[26] The phospholipids were hydrated with a dye-containing pH 7.4 buffer (80 mM calcein, 100 mM HEPES, 5 mM EDTA, 30 mM NaCl) and separated from free calcein by size exclusion chromatography. The eluted LUV dispersion was diluted into an isotonic external buffer (100 mM HEPES, 5 mM EDTA, 170 mM NaCl, pH 7.4) to obtain a final lipid concentration of about 10-20 μM in the cuvette. The high concentration (80 mM) of the encapsulated marker led to self-quenching of its fluorescence, resulting in a low background intensity of the vesicle dispersion (I_B). The peptide was added to the lipid dispersion in various ratios. The leakage of the dye was monitored by measuring the increasing fluorescence intensity. The fluorescence intensity measured after 10 minutes (I_F) was used in the calculation. The experiments were normalized relative to the total fluorescence intensity (I_T), measured after complete disruption of all the vesicles by Triton X-100 (0.1 vol%). The percentage of released calcein was calculated according to the following equation:

$$\%\ release = 100\,\frac{(I_F - I_B)}{(I_T - I_B)} \qquad (1)$$

The fluorescence intensity of calcein was monitored using an excitation wavelength of 490 nm, an emission wavelength of 513 nm and a response time of 0.3 s. The experiments were done at room temperature with continuous sample stirring.

2.3.5 CD Experiments

The sample preparation was carried out in a pH 7.4 buffer (5 mM HEPES and 30 mM NaCl) or in the buffer used for the binding experiments, with a peptide concentration of 20 μM. The LUV's were prepared as described above but their extrusion was performed on a 50 nm pore size filter to minimize light diffusion. They were incubated for 45 minutes with the peptide prior to data acquisition. The CD spectra were obtained between 185 and 260 nm at 25°C on a Jasco 710 spectropolarimeter. All measurements were carried out with 1 mm path length cells. Each spectrum was the average of 20 scans. CD and scattering due to the LUV's were corrected by subtracting the lipid spectra from that of the corresponding peptide-lipid suspensions. The observed ellipticity was expressed as the mean residue ellipticity $[\theta]$, normalized to units of deg cm^2 $dmol^{-1}$. The α-helical contents (f_H) were calculated by the use of the following equation:

$$f_H = 100 \frac{[\theta]_{222}}{[\theta]_{max}} \qquad (2)$$

where $[\theta]_{222}$ is the experimentally-observed mean residue ellipticity at 222 nm and $[\theta]_{max}$ the maximal mean residue ellipticity value of the peptide. This value is dependent on the chain length and can be estimated by $[\theta]_{max} = [\theta]_{\infty}(n-4)/n$, where n is the number of residues and $[\theta]_{\infty}$ the ellipticity at 222 nm for a 100% α-helical peptide[28] (estimated to be -40000 deg cm^2 $dmol^{-1}$ based on polylysine adopting exclusively an α-helical secondary structure).

2.4 Results and discussion

2.4.1 Binding of the peptides to lipid bilayers

The binding of $K_6WA_{19}L_3A_2K_2$, $K_2A_2L_3A_{19}WK_6$, $A_2L_3A_{19}WK_6$ and $A_{12}WK_6$ to bilayers was monitored by the use of the hypsochromic shift of the maximum emission wavelength of their single tryptophan upon binding to lipid vesicles (Figure 2.1). Figure 2.1A shows the binding of $K_6WA_{19}L_3A_2K_2$ and $K_2A_2L_3A_{19}WK_6$ to bilayers made respectively of POPC, a zwitterionic lipid, POPG, a negatively charged lipid, and a POPC:POPG (85:15) mixture. Free $K_2A_2L_3A_{19}WK_6$ exhibits a maximum emission wavelength around 353 nm, indicating the exposure of the tryptophan to the aqueous surrounding.[22,26,29] A progressive down shift of this maximum can be observed when lipid vesicles are added to the peptides. This shift is associated with the transfer of the tryptophan to a less polar environment and is representative of the peptide binding to the bilayer. The proportion of added lipids is expressed in terms of a lipid/peptide molar incubation ratio (R_i). For $K_2A_2L_3A_{19}WK_6$ incubated with POPC there is a slight decrease of the emission wavelength $\lambda_{3/4}$ of about 1 nm. When 15% of negatively charged lipids are present in the lipid matrix, a shift of $\lambda_{3/4}$ by about 13.5 nm is observed. For pure POPG vesicles, the $\lambda_{3/4}$ shift is abrupt and a plateau at 340 nm is reached at an R_i of 9. The plateau indicates that the complete peptide binding is achieved. These results clearly show that the presence of negatively charged lipids strongly increases the affinity of $K_2A_2L_3A_{19}WK_6$ for the lipid vesicles and that the peptide/bilayer interactions are essentially electrostatic. Similar results were obtained with the reversed peptide. $K_6WA_{19}L_3A_2K_2$ displays comparable shifts of its tryptophan fluorescence maximum, indicating a very similar binding to these membranes. The $\lambda_{3/4}$ of $K_6WA_{19}L_3A_2K_2$ are however always slightly shorter than those measured with $K_2A_2L_3A_{19}WK_6$; this could be attributed to a more polar surrounding of the tryptophan residue because of the presence of two additional positive charges. Figure 2.1B displays the binding isotherms obtained for $A_2L_3A_{19}WK_6$ with the same vesicles. A significant and progressive decrease of $\lambda_{3/4}$ is observed with neutral bilayers. However, a plateau is not well defined. When negative charges are present in the bilayer (POPC:POPG = 85:15), a smaller amount of lipids is

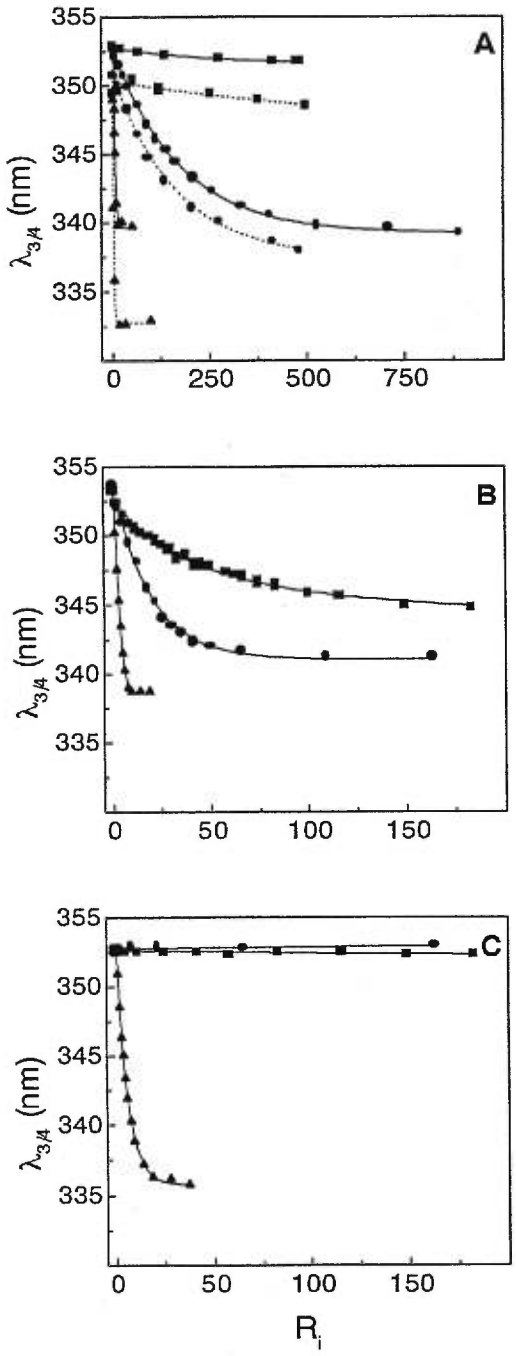

Figure 2.1 Binding isotherms determined by the shift of the fluorescence band maximum of the tryptophan of (A) $K_2A_2L_3A_{19}WK_6$ (—) and $K_6WA_{19}L_3A_2K_2$ (---), (B) $A_2L_3A_{19}WK_6$, and (C) $A_{12}WK_6$ to vesicles in the fluid phase: POPC (■), POPG (▲) and POPC:POPG (85:15) (●).

needed to bind the peptides since a plateau is reached at an R_i of 50. For pure POPG vesicles, the plateau is obtained at 339 nm at an R_i of 9. Figure 2.1C illustrates the results obtained for the shorter peptide $A_{12}WK_6$. In this case, no shift of $\lambda_{3/4}$ was observed when POPC or POPC:POPG (85:15) vesicles were added, suggesting the absence of binding. However, an abrupt shift from 352 nm to 336 nm occurred in the presence of POPG vesicles and a plateau is observed from an R_i of 20. It is concluded that the hydrophobic segment is too short to lead to any significant insertion of the peptide into the lipid vesicles and the absence of hydrophobic interaction is most likely the origin of the weaker membrane affinity of this peptide as compared to $K_6WA_{19}L_3A_2K_2$, $K_2A_2L_3A_{19}WK_6$ and $A_2L_3A_{19}WK_6$.

The comparison of the binding of $K_6WA_{19}L_3A_2K_2$, $K_2A_2L_3A_{19}WK_6$ and $A_2L_3A_{19}WK_6$ to vesicles of various compositions indicates that the presence of lysine residues at both ends – as in the case of $K_6WA_{19}L_3A_2K_2$ and $K_2A_2L_3A_{19}WK_6$ – limits considerably the association with vesicles as compared to $A_2L_3A_{19}WK_6$. This is especially pronounced in the case of the electrically neutral phosphatidylcholine membranes. $K_6WA_{19}L_3A_2K_2$ and $K_2A_2L_3A_{19}WK_6$ have a long hydrophobic segment which was initially designed to be in a transmembrane conformation guided by the terminal lysines. However, one hydrophilic end must travel across the bilayer to adopt this position; this translocation is most likely unfavored thermodynamically and may prevent the insertion of the peptide. In order to ascertain this hypothesis, we have tried to facilitate the insertion of $K_6WA_{19}L_3A_2K_2$ and $K_2A_2L_3A_{19}WK_6$ in a zwitterionic membrane by colyophilizing the peptides with POPC from a mixture of organic solvents. As a reference sample, an identical aliquot of the peptide in the same mixture was also lyophilized. The comparison between the emission spectra of the two hydrated samples indicates the insertion of the peptide in the POPC bilayers when the sample preparation includes a colyophilization step (Figure 2.2). The insertion is inferred from the change in the tryptophan environment probed by the shift of the maximum of the fluorescence toward shorter wavelength when the peptide is colyophilized with the lipid relative to the spectrum of the free peptide. The value of $\lambda_{3/4}$ shifts from 353 nm for the free peptide to 342 nm in the presence of POPC at an R_i of 562, a value typically

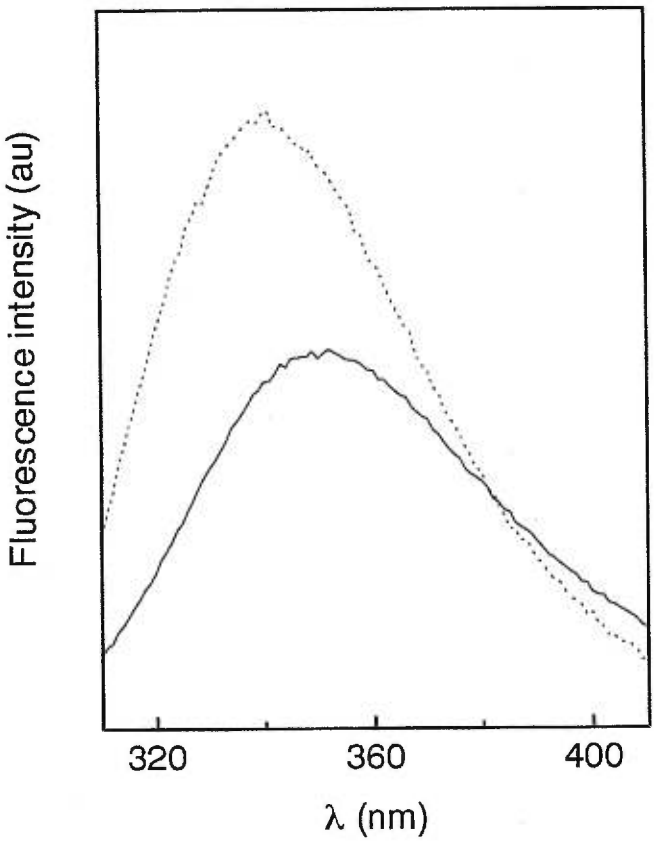

Figure 2.2 Fluorescence emission spectra for $K_2A_2L_3A_{19}WK_6$ with (---) and without (—) POPC. The peptide and the lipid were cosolubilized in a mixture of organic solvents, colyophilized and then hydrated. R_i = 562.

observed for peptides interacting with bilayers (Figure 2.1). The same result was obtained for $K_6WA_{19}L_3A_2K_2$, with a shift of the wavelength from 351 to 339 nm at an R_i of 130 (data not shown). These results reinforce the conclusion that the presence of lysine residues at both ends of the peptide is unfavorable for its spontaneous insertion in bilayers.

The changes in the $\lambda_{3/4}$ of the fluorescence spectra have been used to obtain the binding isotherms of $K_2A_2L_3A_{19}WK_6$ and $A_2L_3A_{19}WK_6$ to vesicles made of POPC/POPG mixture (Figure 2.3). The proportion of bound peptide was estimated by assuming a linear relationship with the shift of $\lambda_{3/4}$. From the total peptide and lipid concentrations and the proportion of bound peptide, the equilibrium concentration of free peptide (C_{eq}) can be calculated. The extent of binding, defined as the molar amount of peptide bound per mole of total lipids (X_b), was also calculated. We have corrected this value as previously suggested[30] by estimating that about 60% of the total lipids are in the outer half layer and therefore exposed to the peptide. An effective binding (X_b*) is expressed by

$$X_b^* \cong \frac{X_b}{0.6} \qquad (3)$$

A plot of X_b* versus C_{eq} yields the conventional binding isotherm. The curves display a non-linear behavior. This anticooperativity of the binding can be attributed to the variation of the electrical potential at the membrane surface upon peptide binding. A model has been developed[30] to distinguish between the long-distance interactions between the peptide and the membrane (described by the Gouy Chapman approach) and the short-distance interactions (described by a binding constant, associated to the transfer of the free peptide from the membrane neighborhood to the bilayer bound form). This approach allows us to describe the non-linear binding curves obtained for $K_2A_2L_3A_{19}WK_6$ and $A_2L_3A_{19}WK_6$.

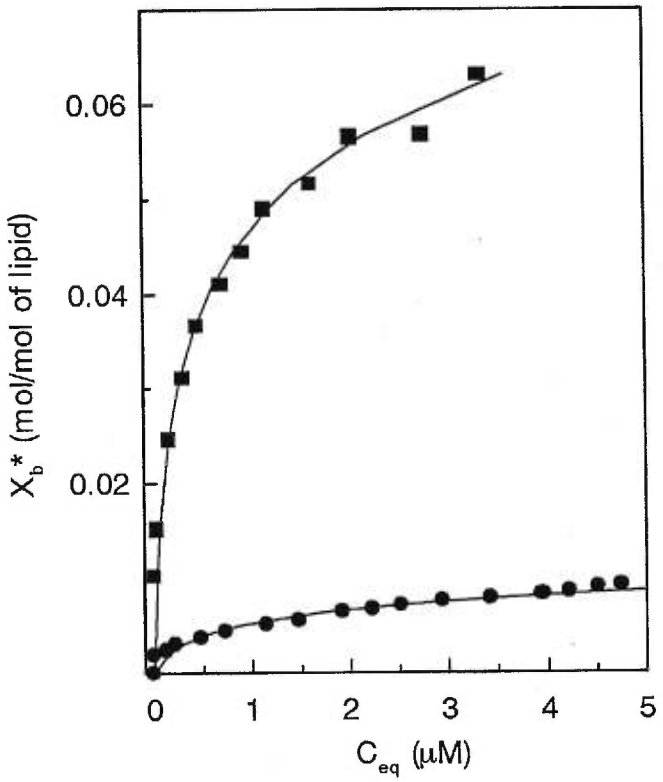

Figure 2.3 Isotherms of $K_2A_2L_3A_{19}WK_6$ (●) and $A_2L_3A_{19}WK_6$ (■) binding to POPC:POPG membranes. The lines represent the theoretical binding isotherms calculated as described in the text.

Peptide	z_P	K_P (M^{-1})
$K_2A_2L_3A_{19}WK_6$	+5.6	2.0
$A_2L_3A_{19}WK_6$	+2.2	$1.3x10^4$

Table II Effective charges and surface partition constants of the peptides

We calculated a surface partition constant K_P of 2.0 M^{-1} and $1.3x10^4$ M^{-1} for $K_2A_2L_3A_{19}WK_6$ and $A_2L_3A_{19}WK_6$, respectively, reflecting the higher membrane affinity of $A_2L_3A_{19}WK_6$ than $K_2A_2L_3A_{19}WK_6$. For $A_2L_3A_{19}WK_6$, the binding constant is in the same order of magnitude as that calculated for melittin.[30] This natural peptide interacts strongly with bilayers and hydrophobic interactions play a significant role in this interaction as illustrated by its strong binding to POPC.[31] In the case of $K_2A_2L_3A_{19}WK_6$, the binding constant is much smaller. Constants in the range of 1 to 10 M^{-1} have been calculated for a β-amyloid peptide.[32] These small binding constants have been associated with rather weak hydrophobic binding. As expected, the effective charge z_P is smaller for $A_2L_3A_{19}WK_6$ than for $K_2A_2L_3A_{19}WK_6$. This could be observed in the binding isotherms where the curves show a greater anticooperativity for $K_2A_2L_3A_{19}WK_6$ than for $A_2L_3A_{19}WK_6$. These effective charges are smaller than the real ones as previously observed for melittin which carries a real charge of +5 or +6 and has an effective one of +1.9.[30]

2.4.2 Peptide conformation

An α-helix structure is characterized by a distinct minimum at 222 nm (n-π* electronic transition of the amide carbonyl) in the CD spectrum.[33] The helical contents of the free and bilayer-bound peptides were calculated from Eq. (2) and listed in Table III. The secondary structure of $K_6WA_{19}L_3A_2K_2$, $K_2A_2L_3A_{19}WK_6$ and $A_2L_3A_{19}WK_6$ in

aqueous solution is about 50 % of α-helix (Figure 2.4). It is proposed that the helix involves mainly the apolar segment, as alanine and leucine are helix-promoting amino acids and as the helical structure is stable upon binding (Table III).

	Buffer	POPC:POPG	
Peptide	f_H (%)	R_i	f_H (%)
$K_6WA_{19}L_3A_2K_2$	48	430	42
$K_2A_2L_3A_{19}WK_6$	49	580	38
$A_2L_3A_{19}WK_6$	45	150	45
$A_{12}WK_6$	22	610	28

Table III α-Helical contents of the free and bound peptides

Free $A_{12}WK_6$ is mainly a disordered coil as indicated by the shape of the spectrum and the weak ellipticity at 222 nm. We have verified the stability of the secondary structure of these four peptides in the presence of POPC:POPG (85:15) membranes. The samples were prepared with a high R_i to promote membrane binding. As the lipid concentration is quite high in most of the cases (Figure 2.4A and 2.4C), the spectra are considered only between 215 and 250 nm, a range where the lipid contribution can be corrected. No significant change was observed at 222 nm for the spectra of the four peptides with and without lipids (Figure 2.4). The experiments were done with various R_i (data not shown) and the ellipticity remained roughly constant, with a standard deviation of 8 % around the average value obtained for the free peptide. The hydrophobic segment of $A_{12}WK_6$ appears to be too short to adopt a stable α-helix conformation even in the presence of lipids; it should be noted however that the

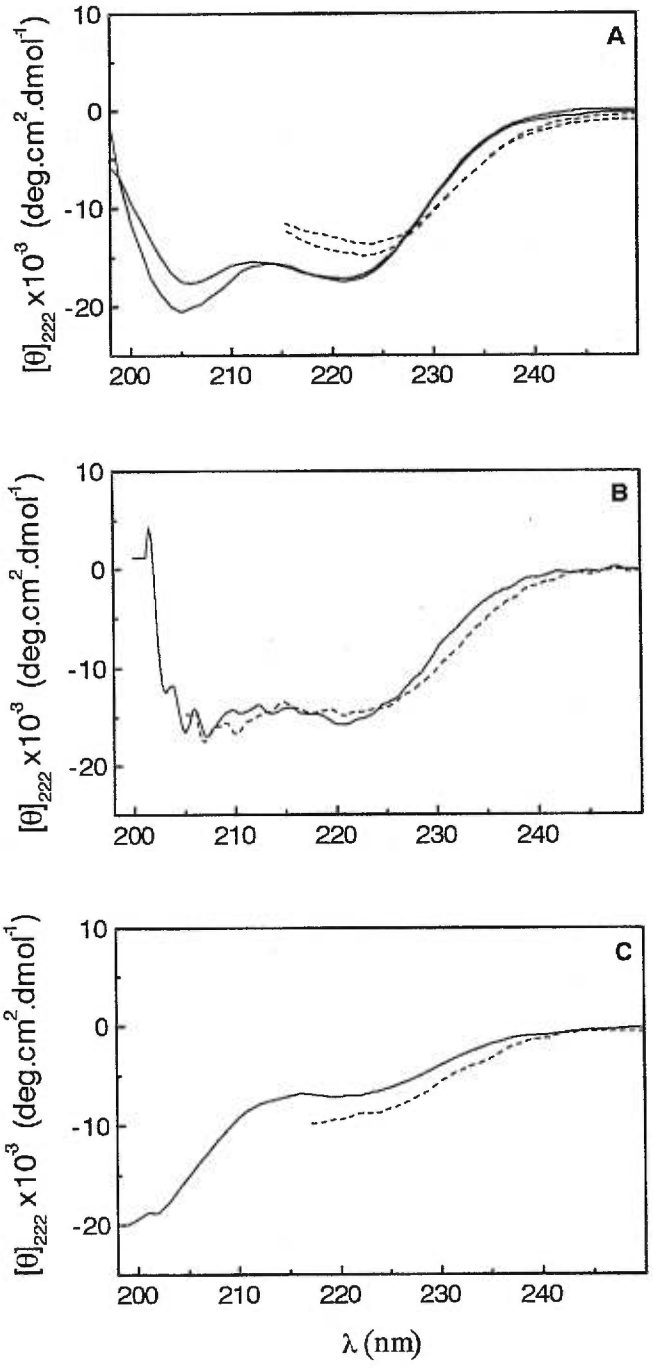

Figure 2.4 CD spectra of (A) $K_6WA_{19}L_3A_2K_2$ and $K_2A_2L_3A_{19}WK_6$, (B) $A_2L_3A_{19}WK_6$ and (C) $A_{12}WK_6$ free in the buffer (—) and with POPC:POPG (85:15) vesicles (---).

proportion of bound peptide is not known and it can be quite low despite the high R_i because of its very weak membrane affinity. $K_6WA_{19}L_3A_2K_2$, $K_2A_2L_3A_{19}WK_6$ and $A_2L_3A_{19}WK_6$ do not change their conformation when associated with charged membranes, indicating that the helical structure is stable upon membrane binding. Because of the high helical content of the peptides in aqueous environment, no considerable helicity increase was expected upon vesicle binding. Actually, only a small increase of the helical content by about 12 % was observed for $K_2A_2L_3A_{19}WK_6$ in the presence of trifluoroethanol or at lower temperature (data not shown).

2.4.3 Leakage experiments

In order to determine whether $K_6WA_{19}L_3A_2K_2$, $K_2A_2L_3A_{19}WK_6$ and $A_2L_3A_{19}WK_6$ perturb the membrane permeability, we have evaluated the release of calcein trapped in LUV's. The percentage of released calcein was calculated according to Eq. (1). The measurements were performed for $K_6WA_{19}L_3A_2K_2$ and $K_2A_2L_3A_{19}WK_6$ with POPC:POPG (85:15) vesicles and for $A_2L_3A_{19}WK_6$ with POPC and POPC:POPG (85:15) vesicles. We did not observe any significant release even when the amount of peptide reached an R_i of about 0.5 (corresponding to 2 peptides for a single lipid); the observed release even under these conditions was similar to the passive release obtained in the absence of peptide (i.e., less than 9 % over a 10-minute period). Therefore, it is concluded that the association of these peptides with lipids do not alter the membrane permeability.

2.5 Conclusions

We have designed and studied four potential anchoring peptides with primary amphiphilic character. First, the length of the hydrophobic segment is important. A peptide with a short hydrophobic segment such as $A_{12}WK_6$ can only interact with negatively charged bilayers, while $A_2L_3A_{19}WK_6$ with a longer hydrophobic segment can

bind with both neutral and negatively charged bilayers. The hydrophobic interactions can play a role in the peptide binding only when the hydrophobic segment is sufficiently long. Therefore, the longer hydrophobic segment with 24 amino acids is more suitable for anchoring peptides.

Second, the vesicle binding is strongly dependent on the electrostatic interactions and is enhanced by the presence of anionic lipids in the bilayer. This can be attributed to the lysine residues which were expected to improve the binding to negatively charged membranes. But the presence of lysines at both ends of the peptides prevented the spontaneous insertion of the apolar segment since the translocation of a charged end through the apolar core of the bilayer would be required. This unfavorable phenomenon limits the binding of the peptide with bilayers as illustrated by the drastic decrease in the values of the surface partition equilibrium constants from $A_2L_3A_{19}WK_6$ to $K_2A_2L_3A_{19}WK_6$. This is coherent with the proposed translocation mechanism for the insertion of membrane integral proteins with primary amphiphilic structures.[34] No significant effect of the direction of the peptide sequence was observed on the interaction of the peptide with vesicles but the direction of the sequence will constitute a crucial factor to take into account when the peptide is immobilized on a resin. The results on $A_2L_3A_{19}WK_6$ convincingly show its insertion in zwitterionic and negatively charged membranes.

This study identifies $A_2L_3A_{19}WK_6$ as a suitable anchoring peptide for the peptide/polymer systems since it associates spontaneously with all types of membranes with a strong affinity and without perturbing their permeability. The grafting of this peptide on solid polymer resins is presently in progress in our laboratories.

Financial support from the Natural Sciences and Engineering Research Council (NSERC) of Canada and the Fonds FCAR (Quebec) is gratefully acknowledged.

2.6 References

1. Pidgeon C. & Venkataram U. V. (1989) Anal. Biochem. 176, 36-47.
2. Ong S., Qiu X. & Pidgeon C. (1994) J. Phys. Chem. 98, 10189-10199.
3. Gotoh T., Shidara M., Iwanaga T., Kikuchi K. I. & Hozawa M. (1994) J. Ferment. Bioeng. 77, 268-273.
4. Takeoka S., Ohno H., Hayashi N. & Tsuchida E. (1989) J. Controlled Release 9, 177-186.
5. Stevenson W. T. K. & Sefton M. V. (1994) TRIP 2, 98-104.
6. Drumheller P. D. & Hubbell J. A. (1994) Anal. Biochem. 222, 380-388.
7. Bayerl T. M. & Bloom M. (1990) Biophys. J. 58, 357-362.
8. Yang Q. & Lundahl P. (1994) Anal. Biochem. 218, 210-221.
9. Wu X. S., Hoffman A. S. & Yager P. (1992) Polymer 33, 4659-4662.
10. Klibanov A. L., Maruyama K., Beckerleg A. M., Torchilin V. P. & Huang L. (1991) Biochim. Biophys. Acta 1062, 142-148.
11. Segrest J. P., De Loof H., Dohlman J.G., Brouillette C. G. & Anantharamaiah G. M. (1990) Proteins Struct. Funct. Genet. 8, 103-117.
12. Cornut I., Thiaudière E. & Dufourcq J. (1993) The Amphipathic Helix, Epand R.M. Eds., CRC Press, Boca Raton. Fl., 173-219.
13. Nezil F. A. & Bloom M. (1992) Biophys. J. 61, 1176-1183.
14. Zhang Y. P., Lewis R. N. A. H., Henry G. D., Sykes B. D., Hodges R. S. & McElhaney R. N. (1995) Biochemistry 34, 2348-2361.
15. Killian J. A., Salemink I., de Planque M. R. R., Lindblom G., Koeppe II R. E. & Greathouse D. V. (1996) Biochemistry 35, 1037-1045.
16. Marqusee S., Robbins V. H. & Baldwin R. L. (1989) Proc. Natl. Acad. Sci. USA 86, 5286-5290.
17. Gratzer W. B. & Doty P. (1962) J. Am. Chem. Soc. 85, 1193-1197.
18. Chung, L. A. & Thompson T.E. (1996) Biochemistry 35, 11343-11354.
19. Kiyota T., Lee S. & Sugihara G. (1996) Biochemistry 35, 13196-13204.

20. Iwata T., Lee S., Oishi O., Aoyagi H., Ohno M., Anzai K., Kirino Y. & Sugihara G. (1994) J. Biol. Chem. 269, 4928-4933.
21. Padmanabhan S., Marqusee S., Ridgeway T., Laue T. M. & Baldwin R. L. (1990) Nature 344, 268-270.
22. Surewicz W. K. & Epand R. M. (1984) Biochemistry 23, 6072-6077.
23. Georghiou S., Thompson M. & Mukhopadhyay A. K. (1982) Biochim. Biophys. Acta 688, 441-452.
24. Landolt-Marticorena C., Williams K. A., Deber C. M. & Reithmeier R. A. F. (1993) J. Mol. Biol. 229, 602-608.
25. Yau W-M., Wimley W. C., Gawrisch K. & White S. H. (1998) Biochemistry 37, 14713-14718.
26. Benachir T., Monette M., Grenier J. & Lafleur M. (1997) Eur. Biophys. J. 25, 201-210.
27. Fiske C. H. & SubbaRow Y. (1925) J. Biol. Chem. 66, 375-400.
28. Lyu P. C., Sherman J. C., Chen A. & Kallenbach N. R. (1991) Proc. Natl. Acad. Sci. USA 88, 5317-5320.
29. Liu L. P. & Deber C. M. (1997) Biochemistry 36, 5476-5482.
30. Beschiaschvili G. & Seelig J. (1990) Biochemistry 29, 52-58.
31. Dufourcq J. & Faucon J. F. (1977) Biochim. Biophys. Acta 467, 1-11.
32. Terzi E., Hölzemann G. & Seelig J. (1994) Biochemistry 33, 7434-7441.
33. Marqusee S. & Baldwin R. L. (1987) Proc. Natl. Acad. Sci. USA 84, 8898-8902.
34. Singer S. J., Maher P. A. & Yaffe M. P. (1987) Proc. Natl. Acad. Sci. USA 84, 1960-1964.

CHAPITRE 3

IMMOBILIZATION OF LIPID VESICLES ON POLYMER SUPPORT *VIA* AN AMPHIPHILIC PEPTIDIC ANCHOR: APPLICATION TO A MEMBRANE ENZYME

Aline Percot, X.X. Zhu and Michel Lafleur, Bioconjugate Chemistry (2000).

Running title: Immobilization of lipid vesicles on polymer support

Keywords: polymer support, amphiphilic peptide, immobilization, lipid vesicle, membrane enzyme

3.1 Abstract

To immobilize lipid vesicles on a polymer support, we have used a peptidic anchor with the following sequence: Ala-Ala-Leu-Leu-Leu-Ala-Ala-Ala-Ala-Ala-Ala-Ala-Ala-Ala-Ala-Ala-Ala-Ala-Ala-Ala-Ala-Ala-Ala-Ala-Ala-Ala-Trp-Lys-Lys-Lys-Lys-Lys-Lys. This amphiphilic peptide was previously designed in our group to interact spontaneously and strongly with vesicles without perturbing their permeability. At the end of the solid-phase peptide synthesis the peptide was left on the polymer beads and this novel polymer-peptide system was used for vesicle immobilization. It was shown that this polymer-peptide system could immobilize as much as 200 μmol of lipids per gram of dry resin. The amount of immobilized vesicles was decreased by a reduction of the proportion of the negatively-charged lipids in the vesicles, indicating the importance of electrostatic interactions in the immobilization of the vesicles. The integrity of the vesicles was mostly preserved after the immobilization. This new polymer-peptide system was used easily and successfully to immobilize a membrane-bound enzyme, γ-glutamyl transpeptidase. The activity of the membrane-bound enzyme was studied by monitoring the release of p-nitroaniline. After 8 cycles, 50 % of the activity of the enzyme was still retained, indicating the strong immobilization of the enzyme in its active form. The polymer-peptide support could be regenerated by washing with ethanol and reused.

3.2 Introduction

The immobilization of lipid vesicles on a solid support can lead to a wide range of applications including chromatographic techniques (1-4), controlled drug release systems (5-7), immobilizing devices for cells (8) and enzymatic reactions (9-11). Several approaches have been developed for the immobilization of lipid membranes, including covalent binding (1) and entrapment (11-13). However, most of the existing techniques imply chemical modifications (1) or detergent dialysis (long and perturbing for

biomolecule as enzyme) (11-13).

In the present study, we present an alternative device providing a strong, spontaneous and simple way to immobilize vesicles. A peptidic anchor covalently attached to a polymer resin is used to bind lipid vesicles through electrostatic and hydrophobic interactions. We have previously designed an amphiphilic peptide with the sequence: Ala-Ala-Leu-Leu-Leu-Ala-Ala-Ala-Ala-Ala-Ala-Ala-Ala-Ala-Ala-Ala-Ala-Ala-Ala-Ala-Ala-Ala-Ala-Ala-Ala-Ala-Ala-Ala-Trp-Lys-Lys-Lys-Lys-Lys-Lys ($A_2L_3A_{19}WK_6$) (14). This peptide has a hydrophobic segment of 24 amino acids and a short hydrophilic part made of 6 lysine residues. A tryptophan was inserted between the hydrophilic and the hydrophobic segment to help the positioning of the peptide in the membrane (15) and to serve as a convenient fluorescent probe (16). This amphiphilic peptide was found to interact spontaneously and strongly with various types of membranes (zwitterionic and negatively-charged) without perturbing their permeability. Therefore, it is a suitable anchoring peptide in our newly designed polymer-peptide supports. Even though the hydrophobic segment plays a role in the membrane affinity, the binding of vesicles by this peptide has been shown to be strongly dependent on the electrostatic interactions and can be enhanced by the presence of anionic lipids in the bilayer (14). The sense of the peptide was also an important parameter when the peptide was grafted on a solid surface. In our system, the lysine extremity is attached on the polymer resin and acts as a biocompatible spacer between the polymer surface and the hydrophobic segment.

The 31 amino acid peptide $A_2L_3A_{19}WK_6$ can be attached onto a functional polymeric resin by solid phase peptide synthesis (SPPS) without the final cleavage, leaving resin beads coated with the peptides (Figure 3.1). The polymer support in this application should have good thermal and mechanical stability and good resistance to solvent or microbial attack. The polystyrene (PS) beads used for SPPS are stable and insoluble in aqueous buffer. The strong amide bond formed between the polymer and the peptide is also stable and is resistant to mild treatments such as ethanol washing. In order to evaluate the potential use of this polymer-peptide system as an efficient vesicle-supporting system, we have studied its affinity for bilayers of various lipid compositions. In addition, to examine the effect of the charges of the peptidic anchor, two polymer-peptide systems were synthesized. In one case, the ε-amino side group of

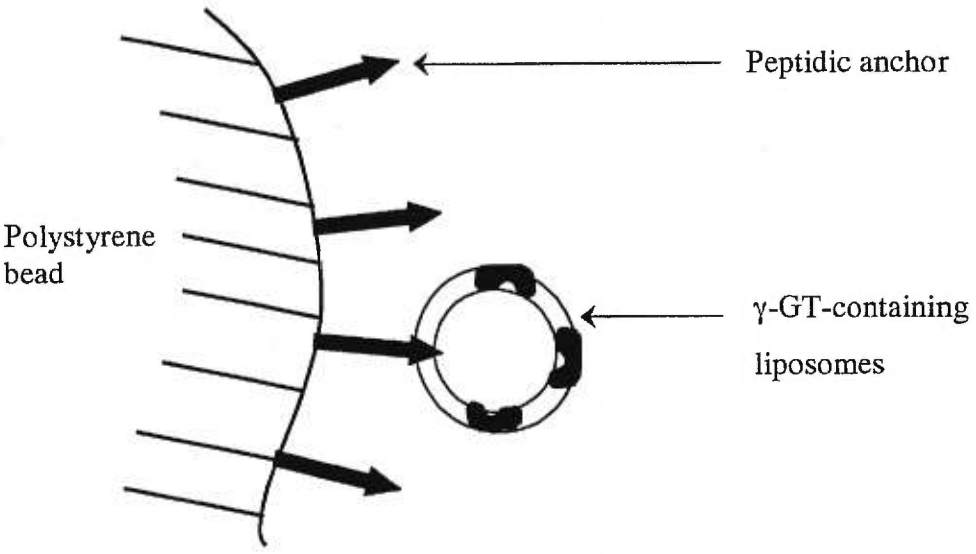

Figure 3.1 Schematic representation of the peptide-polymer system which is used to immobilize the enzyme-containing liposomes.

lysine and the side chain of tryptophan were deprotected at the end of the peptide synthesis so that the lysine residues carried positive charges (deprotected $A_2L_3A_{19}WK_6$). In the other case, the protecting groups were left on at the end of the synthesis leading to neutral residues (protected $A_2L_3A_{19}WK_6$). The membrane-immobilization ability and the permeability of the immobilized vesicles were studied for both grafted peptides.

Immobilization of enzymes on insoluble supports offers the great advantages of continuous operation, improved enzyme stability and reusability, and easy recovery of the product. Most of the devices developed for enzyme immobilization involve direct attachment of the enzyme on a polymeric support (17, 18). This is appropriate for water-soluble enzymes, but many enzymes exist in cell membranes and a bilayer environment is needed for them to remain active (19, 20). Generally, liposomes can be formed and trapped in a polymer matrix by the detergent removal method, by freeze-thawing, or by cross-linking (21, 22). These techniques are complicated to perform and may perturb the activity of the enzymes. The polymer-peptide system developed here can be easily used to immobilize membrane-bound enzymes. γ-Glutamyl transpeptidase (γ-GT) was used as a model membrane enzyme. It was incorporated in vesicles that were subsequently immobilized on the polymer support. The activity of the immobilized enzyme was tested for repeated operations in a batch reactor. We report here the results of a novel biocatalytic system consisting of a membrane enzyme reconstituted in lipid vesicles immobilized on polymer beads *via* a peptidic anchor.

3.3 Materials and methods

3.3.1 Material

1-Palmitoyl-2-oleoyl-*sn*-glycero-3-phosphatidylcholine (POPC) and 1-palmitoyl-2-oleoyl-*sn*-glycero-3-phosphatidylglycerol (POPG) were purchased from Avanti Polar Lipids (Birmingham, AL), sulforhodamine B (SRB) from Molecular Probes Inc. (Eugene, OR), and ethylenediaminetetraacetic acid (EDTA) from Aldrich (Milwaukee,

WI). The 4-(2',4'-dimethoxyphenyl-Fmoc-aminomethyl)phenoxyacetamido-ethyl (Fmoc Amide) resin and the methylbenzhydrylamine (MBHA) resin were purchased from Perkin Elmer Applied Biosystems (Foster City, CA). 4-(2-Hydroxyethyl)-1-piperazineethanesulfonic acid (HEPES) and Triton X-100, L-γ-glutamyl-*p*-nitroanilide, glycylglycine, bovine kidney γ-glutamyl transpeptidase (EC 2.3.2.2) and a protein assay kit were purchased from Sigma (St. Louis, MO).

3.3.2 Peptide synthesis

The peptides were synthesized using the standard procedures for solid phase chemistry (23). Automated synthesis was carried out on an Advanced ChemTech synthesizer 396 MPS. Both peptides were synthesized with the 9-fluorenylmethoxycarbonyl (Fmoc) strategy. The protected peptide was synthesized on the Fmoc Amide resin whereas the deprotected peptide was synthesized on the MBHA resin. The deprotection step was achieved by classical treatment of the beads with trifluoroacetic acid (92.5 %) and triisopropylsilane (2.5 %). In the case of the protected polymer-peptide system, the tert-butyloxycarbonyl (Boc) protective groups were not eliminated from the side amino groups for the lysines and the tryptophan. At the end of the synthesis, both the protected and unprotected peptides were left covalently attached on the resin.

3.3.4 Binding studies

Lipid stock solutions were prepared by dissolving each lipid in a 95/5 (v/v) benzene/methanol solvent and the lipid mixtures were obtained by mixing appropriate volumes of the stock solutions. The lipids were then lyophilized from the benzene/methanol solutions and hydrated with the binding buffer (20 mM HEPES, 100 mM NaCl, 2 mM EDTA, pH 7.4). Large unilamellar vesicles (LUV's) were prepared as previously described by extrusion through polycarbonate filters of 100 nm pore size (24).

The amount of vesicles bound to the polymer beads was determined by a centrifugation assay. The dry polymer beads (around 5 mg) were hydrated with the binding buffer for 15 min. The LUV's were added to the polymer beads to obtain a final lipid concentration of ca. 10 mM, and a final volume of ca. 3 mL. They were incubated at room temperature for 3 h with constant agitation. The samples were then centrifuged (10 min, 2200 × g) to settle the polymer beads. The quantity of immobilized lipids was determined by measuring the phospholipid concentration in the supernatant using the Fiske-SubbaRow phosphorus assay (25). A control experiment showed that, in the absence of the polymer, all the lipids remained in the supernatant after incubation and centrifugation.

3.3.5 Leakage experiments

Two methods were used to estimate the integrity of the immobilized vesicles. In both approaches, the release of a dye (SRB) entrapped in the vesicles was measured. SRB-containing vesicles were prepared by hydrating the lipids (POPC:POPG 50:50, molar ratio) with a dye-containing buffer (20 mM HEPES, 60 mM NaCl, 2 mM EDTA, pH 7.4, 30 mM SRB). They were immobilized on the polymer beads according to the protocol described above. The immobilized and unbound vesicles were separated by a centrifugation step.

First, the polymer-peptide beads with the immobilized vesicles were washed with ethanol to solubilize and recover all the immobilized lipids and the entrapped SRB. The SRB fluorescence intensity of the ethanol washing, as well as the quantity of lipids was measured. The fluorescence intensity relative to the amount of lipid (arbitrary unit per mole of lipid, au/mol) representative of the concentration of SRB trapped in the vesicles, was calculated for free and immobilized vesicles. Second, in another set of experiments, Triton-X (0.1 vol. %) a membrane-perturbing agent, was added to stirred beads on which vesicles were immobilized. Before the addition of the surfactant, the fluorescence of the SRB inside the vesicles was quenched because of its high concentration (26) and the perturbation of the permeability was monitored by the increased SRB fluorescence intensity in the cell.

The fluorescence measurements were performed at 25°C on a SPEX Fluorolog-2 spectrometer equipped for sample stirring. The fluorescence intensity of SRB was monitored with an excitation wavelength of 565 nm, an emission wavelength of 586 nm and a response time of 0.3 s. The excitation and emission bandpath widths were set at 1.5 and 0.5 nm, respectively.

3.3.6 Preparation and immobilization of γ-GT-bound liposomes

γ-GT was dissolved in the binding buffer (0.4 mg/mL). The protein concentration was determined by a modified Lowry protein assay with deoxycholate and trichloroacetic acid (27). In order to obtain γ-GT reconstituted in lipid bilayers, solid lipids (POPC:POPG 50:50, molar ratio) were hydrated with the enzyme-containing buffer. The lipid suspension (ca. 30 mM) was then freeze-thawed and extruded to obtain vesicles with a diameter of 100 nm. In parallel, about 10 mg of the dry peptide-coated beads were incubated in 1 mL of binding buffer. Afterwards, an aliquot of the γ-GT-lipid suspension was added to the polymer beads. The samples were incubated at room temperature for 3 h with constant agitation. To eliminate unbound enzymes and lipid vesicles, the polymer beads were washed 3 times with the binding buffer. After these washings, no lipid was found in the supernatant and only a residual enzyme activity could be detected. A cyclic activity assay was performed with these polymer beads bearing the γ-GT-containing vesicles. A solution (2.8 mL) containing 20 mM HEPES (pH 7.4), 100 mM NaCl, 2mM EDTA, 14.3 mM glycylglycine and 0.5 mM L-γ-glutamyl-*p*-nitroanilide was added to the polymer beads directly in a UV cell. This enzymatic reaction transforms the substrate L-γ-glutamyl-*p*-nitroanilide into *p*-nitroaniline as product, which should be released to the media. The amount of *p*-nitroaniline produced from the reaction was measured on a Varian Cary (1 Bio) UV-VIS Spectrophotometer at 410 nm for 10 min. An extinction coefficient of 8.80×10^3 M^{-1} cm^{-1} for *p*-nitroaniline was used (11). The temperature was controlled with a water-jacketed cell holder connected to a circulating bath thermostated at 25°C. The mixture was periodically stirred vigorously, and the polymer beads settled after each stirring step. The absorbance was measured as an indication of the amount of *p*-nitroaniline

released in the supernatant. An absolute activity could be calculated for the immobilized membrane-bound γ-GT and was expressed as μmol of *p*-nitroaniline liberated per minute per mL of hydrated resin. At the end of each enzymatic reaction, the supernatant containing the remaining substrate and the product was removed. The resin was washed by 1 mL of binding buffer, and fresh substrate was added to perform another cycle of the enzymatic reaction.

A control experiment was done with the same enzyme-containing buffer but without lipids to quantify the residual activity due to the enzyme directly adsorbed on the polymer-peptide system. The measured activities of the membrane-bound γ-GT and the adsorbed γ-GT were normalized to the activity of the membrane-bound enzyme during the first cycle.

Control experiments were also done to verify that the detected activity was due to the immobilized enzymes and not to the enzymes released during the activity assay. At steps N = 0, 5 and 10, the resin was treated exactly the same way as in an activity assay (10 min incubation at 25°C with stirring), but with no substrate added to the mixture. After this treatment, an activity assay was done on the recovered supernatant.

As a reference, the activity of the free enzyme in buffer was measured and its specific activity was expressed as μmol of *p*-nitroaniline liberated per minute per milligram of protein.

3.4 Results and discussion

3.4.1 Immobilization of liposomes

The performance of the polymer-peptide system was evaluated for the immobilization of fluid membranes with various lipid compositions. The liposomes were made of POPC, a zwitterionic lipid, and POPG, a negatively-charged lipid, allowing a modulation of the interfacial charge of the vesicles. To examine the contribution of electrostatic interactions, we compared the immobilization capacities of the polymer

beads grafted with the peptide in its deprotected and protected forms. A control experiment was also carried out with the bare resin without attached peptides.

Figure 3.2 shows the amount of immobilized lipids for membranes with varying proportions of the negatively-charged lipids. The amount of immobilized lipids increases with increasing POPG content in the lipid mixture for the polymer with the deprotected peptide $A_2L_3A_{19}WK_6$. In the case of pure POPG vesicles, this support system can immobilize as much as 200 μmol of lipids per gram of dry resin. For the bare resin, no lipids were retained in the pellet (data not shown), indicating that the peptidic anchors grafted on the polymer beads are essential in the immobilization of the vesicles. For the polymer beads coated with the protected $A_2L_3A_{19}WK_6$, almost no lipids were immobilized on the resin (less than 1 μmol/g of dry resin), indicating the importance of the electrostatic interactions between the solid support and the vesicles during the immobilization. The charges on both the peptide and the vesicle surface are very important to an efficient immobilization. The crucial role of electrostatics was already observed in the interactions between membranes and this peptide in its free form (14). The binding constant (K_p) of the free peptide to various POPC:POPG vesicles was estimated from the initial slope of the binding isotherms of the free peptide (14). As shown in Figure 3.2, this binding constant increases with the POPG content in the bilayer. For the free peptide, the affinity is 120 times higher for the POPG vesicles than for the POPC vesicles. This is consistent with the data obtained for the grafted peptide, where the quantity of immobilized lipid varies from insignificant quantity for POPC up to 200 $\mu mol/g_{dry\ resin}$ for POPG vesicles. The low affinity of the free peptide for the zwitterionic vesicles ($K_p \approx 1.1 \times 10^4\ M^{-1}$) helps to explain the fact that the polymer-peptide system did not bind zwitterionic vesicles.

The integrity of the immobilized vesicles was verified by encapsulating a fluorescent probe in POPC:POPG (50:50) vesicles. First, SRB and the lipids immobilized on the polymer beads were solubilized by vigorous washing with ethanol. The intensity of the SRB fluorescence divided by the quantity of lipids in the ethanol washing is representative of the concentration of encapsulated SRB. This parameter has been determined for the free vesicles (by diluting an aliquot in ethanol) and for the immobilized ones. For free vesicles containing 30 mM SRB, a fluorescence intensity per

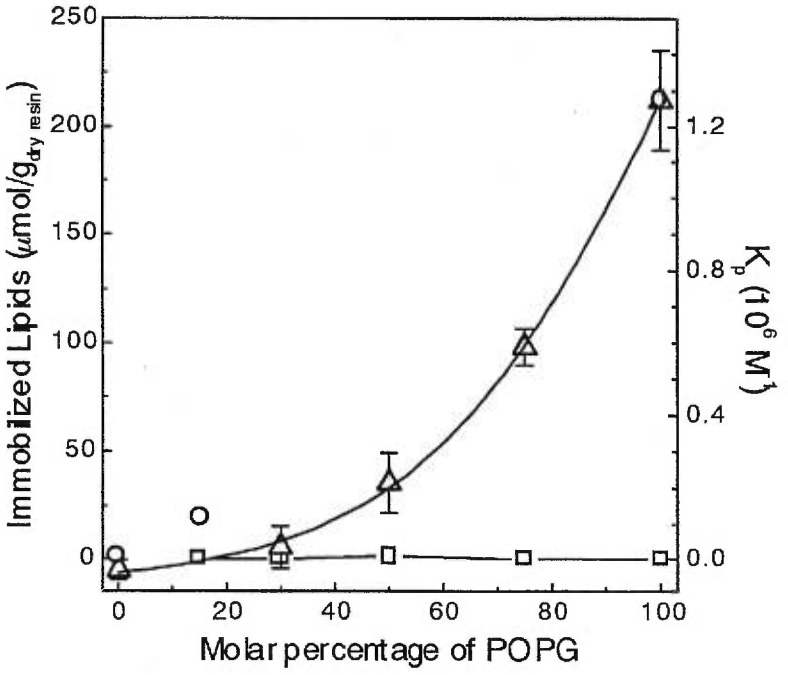

Figure 3.2 Quantity of immobilized lipids on the polymer support grafted with the deprotected $A_2L_3A_{19}WK_6$ peptidic anchor (△) and on the support grafted with protected $A_2L_3A_{19}WK_6$ (□) as a function of the POPG content in the vesicles made of POPC:POPG mixtures. The error bars represent the standard deviation on at least 3 measurements. The binding constant (K_p) of the free peptide (○) are shown for three POPC:POPG systems (14). The left and right vertical axes were normalized relative to the highest value (i.e., that obtained for pure POPG).

lipid of $1.07\pm0.04\times10^{13}$ au/mol was obtained. For the immobilized vesicles, it was $0.6\pm0.1\times10^{13}$, representing on average 57 % of the SRB remained in the bound vesicles. To verify that the SRB was indeed entrapped in the vesicles, in a second set of experiments, we added a surfactant to the pellet and measured the SRB fluorescence intensity. A rapid increase of the fluorescence intensity was observed after the addition of Triton. This showed that a significant quantity of SRB was still encapsulated at a high concentration in the vesicles after the immobilization step and that the SRB could be released by a membrane-disrupting detergent. However, this increase is hard to quantify because of the diffusion of the polymer beads. In addition, the integrity of the vesicles cannot be determined precisely because the SRB probe interacts with our solid support as inferred from a residual pink color of the beads, even after the ethanol washing. Therefore, the value obtained for the remaining entrapped SRB upon immobilization is underestimated. We can conclude from both results that the majority of the encapsulated SRB remains in the vesicles and that the vesicles immobilized on our polymer-peptide system can be used as small containers for further applications.

3.4.2 Enzymatic reaction of reconstituted γ-GT in liposomes immobilized on the polymer-peptide system

Vesicles containing POPC:POPG (50:50) were used as a matrix for the enzyme reconstitution. The enzyme-containing vesicles were then immobilized onto the resin bearing the deprotected $A_2L_3A_{19}WK_6$. After being washed to eliminate the unbound vesicles and enzymes, the beads were ready to be used as a biocatalytic system. This method is much simpler and less time-consuming than most of the classical immobilization methods as they need dialysis steps or chemical attachment of the enzyme (9-11).

The activity of the immobilized membrane-bound γ-GT was estimated to be 0.3 μmol min^{-1} mL^{-1} of hydrated resin for the initial cycle. This activity is in the same range as the activity detected by Gotoh et al (9) for the membrane-bound γ-GT immobilized by dialysis on Sepharose. The activity of the free enzyme under the same conditions (buffer, pH and temperature) was around 13 μmol mg^{-1} min^{-1}. If we assume that the

activity is not affected by the reconstitution in the bilayer or by the immobilization step, we could estimate that the quantity of active enzyme immobilized on the resin was about 0.02 mg per mL of hydrated resin. It should be noted that this amount corresponds to the "efficient" enzyme, which is likely limited to the enzyme present in the external layer of the membrane (11).

In Figure 3.3, the enzyme activity relative to that of the initial cycle (0.3 μmol min^{-1} mL^{-1} of hydrated resin) is plotted versus the number of cycles in a batch reactor approach as described in Materials and Methods. Significant activity was retained even after 12 cycles (more than 20 % of the initial activity). We can observe a linear loss of activity with the increasing number of cycles. This decrease of activity could result from a physical loss of enzyme from the system or from a deactivation of the enzyme retained in the system. To identify the origin of this decrease, the release of the enzyme during the activity assay was examined (see Materials and Methods). The activity measured on the supernatant actually corresponds to the loss of activity observed between two successive cycles. Therefore, the decrease of activity is most likely due to the physical loss of the enzyme. We could not detect any lipid in the supernatants, but because of the small amount of lipids involved, we could not distinguish whether the enzyme was released in its free form or along with lipid vesicles. The measured activities of the supernatant were much smaller than those observed with the polymer beads, clearly indicating that most of the enzymatic reaction was performed by the enzyme reconstituted in the vesicles immobilized on the resin.

To confirm that the enzymatic activity was due to the membrane-bound γ-GT and not to the γ-GT directly adsorbed on the resin, a control experiment was made without any lipids. The resin support was incubated with the enzyme under the same conditions, and the activity of the adsorbed enzyme was measured for repeated cycles in the same way. Even for N = 1, the activity detected was only 20% of the activity detected for membrane-bound enzyme.* As shown in Figure 3.3, the activity decreased linearly with the number of cycles, as in the case of the membrane-bound enzyme.

*Dans ce cas, l'enzyme utilisée est très stable, active en solution, adsorbée sur une surface ou solubilisée dans une membrane lipidique. L'adsorption non spécifique de l'enzyme conduit donc à une activité résiduelle mesurable.

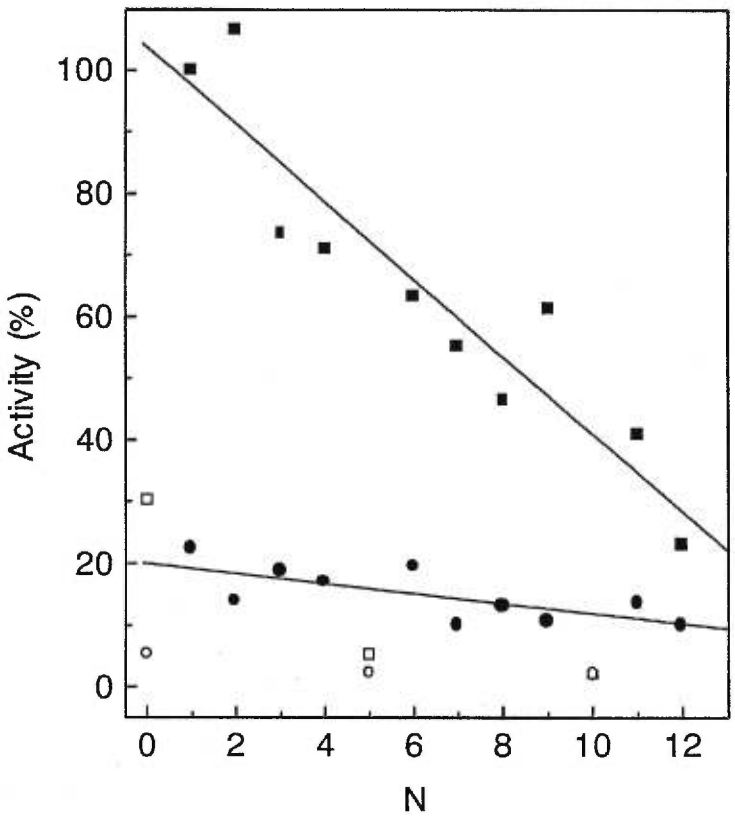

Figure 3.3 Relative activity for the immobilized membrane-active enzyme γ-GT (■) and for the adsorbed enzyme (●) on the polymer-deprotected $A_2L_3A_{19}WK_6$ system plotted as a function of the number of utilization cycles (N). As a control experiment, the loss of the enzyme was periodically probed (N = 0, 5 and 10) by measuring the enzymatic activity in the supernatant for the immobilized enzyme (□) and for the adsorbed enzyme (○). The activity assay was made at 25°C and the absorbance was measured at 410 nm.

The polymer-peptide system allows easy recovery of the products and the reutilization of the enzyme. The durability of the immobilized enzyme is very important for the applications. More than 50 % of its initial activity was still retained after 8 cycles. It is important to note that this polymer-peptide system can be reused. After 12 cycles of use, the resin can be regenerated by washing with ethanol and lyophilization and reused with similar performances.

3.5 Conclusions

We have developed and characterized a polymer-peptide system able to immobilize lipid vesicles. The amphiphilic peptidic anchor grafted on the resin was responsible for the immobilization of the liposomes and the interactions involved were mostly electrostatic. The quantity of immobilized vesicles increased with the content of negatively-charged lipids in the bilayer and reached 200 μmol/g of dry resin for POPG vesicles. Upon immobilization, the permeability of the vesicles was mostly maintained, and the vesicles could be used as small containers. This carrier can be easily regenerated by washing with ethanol and reused.

This polymer-peptide support is versatile since the peptide can interact strongly and spontaneously with many types of lipids. A membrane-active enzyme was shown to have retained its activity after being immobilized through vesicles bound to the polymer support *via* an amphiphilic peptide. This system offers an alternative method for enzyme immobilization and has several advantages compared with immobilization strategies by covalent binding or physical adsorption, including the preservation of the conformation and activity of membrane-active enzymes, the possibility to immobilize water-insoluble enzymes and minimal diffusion effects for the enzymes attached to the surface of the polymer beads. We have tested one model membrane-active enzyme with the new support system in this study. It is obvious that this type of polymer-peptide support may be potentially used for the immobilization of biological membranes and even cells, as drug carriers and column packing materials for the separation of biomolecules.

Acknowledgments

Financial support from the Natural Sciences and Engineering Research Council (NSERC) of Canada and Fonds FCAR from the Province of Quebec is gratefully acknowledged.

3.6 References

(1) Pidgeon, C., and Venkataram, U. V. (1989) Immobilized artificial membrane chromatography: supports composed of membrane lipids. *Anal. Biochem. 176*, 36-47.

(2) Ong, S., Qiu, X., and Pidgeon, C. (1994) Solute interactions with immobilized artificial membranes. *J. Phys. Chem. 98*, 10189-10199.

(3) Yang, Q., and Lundahl, P. (1994) Steric immobilization of liposomes in chromatographic gel beads and incorporation of integral membrane proteins into their lipid bilayers. *Anal. Biochem. 218*, 210-221.

(4) Zhang, Y., Xiao, Y., Kellar, K. J., and Wainer, I. W. (1998) Immobilized nicotinic receptor stationary phase for on-line liquid chromatographic determination of drug-receptor affinities. *Anal. Biochem. 264*, 22-25.

(5) Stevenson, W. T. K., and Sefton, M. V. (1994) Recent developments in polymer-based controlled release technology for therapeutic purposes. *TRIP 2*, 98-104.

(6) Wu, X. S., Hoffman, A. S., and Yager, P. (1992) Conjugation of phosphatidylethanolamine to poly(*N*-isopropylacrylamide) for potential use in liposomal drug delivery systems. *Polymer 33*, 4659-4662.

(7) Bochot, A., Fattal, E., Gulik, A., Couarraze, G., and Couvreur, P. (1998) Liposomes dispersed within a thermosensitive gel: a new dosage form for ocular delivery of oligonucleotides. *Pharm. Res. 15*, 1364-1369.

(8) Kino, Y., Sawa, M., Kasai, S., and Mito, M. (1998) Multiporous cellulose microcarrier for the development of a hybrid artificial liver using isolated hepatocytes. *J. Surg. Res. 79*, 71-76.

(9) Gotoh, T., and Kikuchi, K. (1998) Immobilization of biological membranes by sonication and freeze-thawing. *J. Chem. Eng. Jpn. 31*, 860-863.

(10) Monsan, P., and Combes, D. (1988) Enzyme stabilization by immobilization. *Methods Enzymol. 137*, 584-612.

(11) Gotoh, T., Shidara, M., Iwanaga, T., Kikuchi, K., and Hozawa, M. (1994) Immobilization of γ-glutamyl transpeptidase, a membrane enzyme, in gel beads *via* liposome entrapment. *J. Ferment. Bioeng. 77*, 268-273.

(12) Wallstén, M., Yang, Q., and Lundahl, P. (1989) Entrapment of lipid vesicles and membrane protein-lipid vesicles in gel bead pores. *Biochim. Biophys. Acta 982*, 47-52.

(13) Yang, Q., Wallstén, M., and Lundahl, P. (1990) Lipid-vesicle-surface chromatography. *J. Chromatogr. 506*, 379-389.

(14) Percot, A., Zhu, X. X., and Lafleur, M. (1999) Design and characterization of anchoring amphiphilic peptides and their interactions with lipid vesicles. *Biopolymers 50*, 647-655.

(15) Landolt-Marticorena, C., Williams, K. A., Deber, C. M., and Reithmeier, R. A. F. (1993) Non-random distribution of amino acids in the transmembrane segments of human type I single span membrane proteins. *J. Mol. Biol. 229*, 602-608.

(16) Georghiou, S., Thompson, M., and Mukhopadhyay, A. K. (1982) Melittin-phospholipid interaction studied by employing the single tryptophan residue as an intrinsic fluorescent probe. *Biochim. Biophys. Acta 688*, 441-452.

(17) Ding, Z., Chen, G., and Hoffman, A. S. (1998) Unusual properties of thermally sensitive oligomer-enzyme conjugates of poly(*N*-isopropylacrylamide)-trypsin. *J. Biomed. Mater. Res. 39*, 498-505.

(18) Chen, G., and Hoffman, A. S. (1993) Preparation and properties of thermoreversible, phase-separating enzyme-oligo(*N*-isopropylacrylamide) conjugates. *Bioconjugate Chem. 4*, 509-514.

(19) Gennis, R. B., and Jonas, A. (1977) Protein-lipid interactions. *Ann. Rev. Biophys. Bioeng. 6*, 195-238.

(20) Coleman, R. (1973) Membrane-bound enzymes and membrane ultrastructure. *Biochim. Biophys. Acta 300*, 1-30.

(21) Messing, R. A. (1975) *Immobilized Enzymes for Industrial Reactors.* Academic Press, New York.

(22) Weetall, H. H. (1975) *Immobilized Enzymes, Antigens, Antibodies, and Peptides.* Marcel Dekker, Inc., New York.

(23) Grant, G. A. (1992) *Synthetic Peptides: a user's guide.* W. H. Freeman and Company, New York.

(24) Benachir, T., Monette, M., Grenier, J., and Lafleur, M. (1997) Melittin-induced leakage from phosphatidylcholine vesicles is modulated by cholesterol: a property used for membrane targeting. *Eur. Biophys. J. 25*, 201-210.

(25) Fiske, C. H., and SubbaRow, Y. (1925) The colorimetric determination of phosphorus. *J. Biol. Chem. 66*, 375-400.

(26) El Jastimi, R., and Lafleur, M. (1999) A dual-probe fluorescence method to examine selective perturbations of membrane permeability by melittin. *Biospectroscopy 5*, 133-140.

(27) Peterson, G. L. (1977) A simplification of the protein assay method of Lowry *et al.* which is more generally applicable. *Anal. Biochem. 83*, 346-356.

CHAPITRE 4

A SIMPLE FTIR SPECTROSCOPIC METHOD FOR THE DETERMINATION OF THE LOWER CRITICAL SOLUTION TEMPERATURE OF *N*-ISOPROPYLACRYLAMIDE COPOLYMERS AND RELATED HYDROGELS

Aline Percot, X.X. Zhu and Michel Lafleur, Journal of Polymer Science: Part B: Polymer Physics, **38**, 907-915 (2000).

Running title: Linear and crosslinked poly(*N*-isopropylacrylamide)

Keywords: poly(*N*-isopropylacrylamide), hydrogel, FTIR, LCST

4.1 Abstract

Linear and crosslinked polymers based on *N*-isopropylacrylamide (NIPAAm) exhibit unusual thermal properties. Aqueous solutions of poly(*N*-isopropylacrylamide) (PNIPAAm) phase-separate upon heating above a lower critical solution temperature (LCST), whereas related hydrogels undergo a swelling-shrinking transition at an LCST. A linear copolymer made of NIPAAm/acryloxysuccinimide (98/2 mol/mol) and two hydrogels with different hydrophilicities were prepared. Fourier transform infrared (FTIR) spectroscopy was employed to determine the transition temperature and provide insights into the molecular details of the transition via the probing of characteristic bands as a function of temperature. The FTIR spectroscopy method described here allowed the determination of the transition temperature for both the linear and crosslinked polymers. The transition temperatures for PNIPAAm and the gel resulting from crosslinking with polylysine or *N,N'*-methylenebisacrylamide (MBA) were in the same range, 30-35°C. For the gels, the transition temperature increased with the hydrophilicity of the polymer matrix. The spectral changes observed at the LCST were similar for the free chains and the hydrogels, implying a similar molecular reorganization during the transition. The C–H stretching region suggests that the *N*-isopropyl groups and the backbone both underwent conformational changes and became more ordered upon heating above the LCST. An analysis of the amide I band suggests that the amide groups of the linear polymer were mainly involved in hydrogen bonding with water molecules below the LCST, the chain being flexible and disordered in a water solution. During the transition, around 20 % of the intermolecular hydrogen bonds between the polymer and water are broken and replaced by intramolecular hydrogen bonds. Similar changes were also observed at the LCST of a gel crosslinked with MBA.

4.2 Introduction

Several polymer solutions exhibit a critical behavior leading to a phase separation above the lower critical solution temperature (LCST) because the polymer becomes

insoluble in water at higher temperatures. Typical examples of thermosensitive polymers are poly(ethylene glycol),[1] ethyl(hydroxyethyl)cellulose[2] and *N*-substituted acrylamide.[3,4] For polymers based on *N*-isopropylacrylamide (NIPAAm), the LCST is around the physiological temperature. Consequently, both linear and crosslinked poly(*N*-isopropylacrylamide) (PNIPAAm) have recently been used in many biomedical applications, such as controlled drug release, immobilization of enzymes, biosensing and protein purification.[5-9] Experimentally, the LCST of PNIPAAm is between 30 and 35°C, the exact temperature being a function of the detailed structure of the macromolecule.[5] Related hydrogels show a similar behavior and shrink at high temperatures.[5,9-12] This swelling-shrinking phase transition occurs at an LCST (the term is conveniently used for both transition temperatures as these are related to a similar phenomenon). For several applications of these gels, a specific LCST is required, and efforts have been devoted to identifying the key parameters for its modulation. It has been recently shown that the LCST of linear PNIPAAm can be modulated by copolymerization with monomers of various degrees of hydrophilicity.[4] In the case of hydrogels, the control of the LCST is poorly understood.* For example, the effect of the crosslinker is not well-established.

The LCSTs of aqueous solutions of PNIPAAm can be studied by a variety of experimental techniques, including turbidity, calorimetry, light scattering, nuclear magnetic resonance (NMR) spectroscopy, viscosimetry, fluorescence and attenuated total reflection (ATR)/Fourier transform infrared (FTIR) spectroscopy.[5,13,14] In the case of hydrogels, the LCST is usually determined by the measurement of the swelling ratio as a function of temperature, a time-consuming approach that does not provide reproducible and precise results,[5] or by DSC, which becomes problematic when the transitions become broad and do not involve considerable energy.[11]

In this study, we developed a new and simple method to determine the LCST in both linear and crosslinked polymers via FTIR spectroscopy. This technique has been

*Complément de bibliographie: J.G.H. Joosten, J.L. McCarthy, and P.N. Pusey, *Macromolecules*, **24**, 6690 (1991); Y. Hu, K. Horie, and H. Ushiki, *Macromolecules*, **25**, 6040 (1992); S. Hirotsu, *Advances in Polymer Science*, **110**, 1 (1993); M. Asano, F.M. Winnik, T. Yamashita, and K. Horie, *Macromolecules*, **28**, 5861 (1995); F. Ikkai, and M. Shibayama, *Macromolecules*, **31**, 3275 (1998); T.L. Lowe, M. Benhaddou, and H. Tenhu, *Macromol. Chem. Phys.*, **200**, 51 (1999).

shown to be useful for probing transitions such as lipid bilayer transition,[15] for the self-association of aqueous surfactant,[16] and for studying hydrogen bonding in polymers.[17] In addition, changes in the infrared spectra provide information on the conformation and bonding state of the functional groups involved in the transition.

The studied polymer is a copolymer of NIPAAm and acryloxysuccinimide (NAS), a monomer used as a reacting site for amino groups of many biomolecules. This copolymer is often used for biological applications.[7-9,18,19] We determined the LCST for this linear copolymer with cloud-point determination and the new FTIR approach. We also investigated the molecular details of the transition using the infrared spectra.

The infrared method was also used for the characterization of two crosslinked copolymers with different hydrophilicities. The more hydrophilic one was crosslinked with polylysine (PL). The other gel was obtained from crosslinking with *N,N'*-methylenebisacrylamide (MBA), which was chosen for its structural similarity to NIPAAm. The LCSTs were determined, and the molecular changes occurring during the transition were examined.

4.3 Experimental

Acrylic acid (AA), *N*-hydroxysuccinimide (NHS), NIPAAm, PL, MBA and 2,2'-azoisobutyronitrile (AIBN) were purchased from Sigma (St. Louis, MO) and Aldrich (Milwaukee, WI). AA was purified by distillation.

4.3.1 Copolymerization

The coupling of AA with NHS was carried out as previously described.[20] The obtained NAS had the expected spectral characteristics.[21]

^{1}H NMR ($CDCl_3$, ppm): 2.85 (s, 4 H), 6.0-7.0 (m, 3 H). IR (KBr, cm^{-1}): 1800, 1775, 1735, 1260, 995, 870.

The synthesis of poly(*N*-isopropylacrylamide-co-*N*-acryloxysuccinimide) (PNIPAS) was carried out as previously described.[7,22] NIPAAm and NAS (the total

weight was about 1 g) were dissolved in 15 mL of a mixture of anhydrous tetrahydrofuran (THF) and anhydrous toluene (1/3, v/v) with a NIPAAm/NAS molar ratio of 98/2. AIBN (1 mol % of the comonomers) was added as the initiator for the polymerization. The reaction was carried out for 24 h at 55°C under nitrogen. 60 mL of THF were then added to the mixture to solubilize the copolymer. The mixture was added dropwise into 500 mL of petroleum ether to precipitate the copolymer. The precipitate was filtered under vacuum and dried at 42°C overnight.

The molecular weight of the copolymer was determined by size exclusion chromatography on a Waters 410 system with THF as the mobile phase. Polystyrene standards were used for calibration.

4.3.2 Synthesis of the hydrogel with MBA as the crosslinker

NIPAAm (6.80 mmol), NAS (0.14 mmol), and MBA (0.15 mmol) were dissolved in 5 mL of dimethyl sulfoxide (DMSO). The solution was purged with nitrogen for 15 min, and AIBN (0.02 g) was then added. The polymerization was carried out at 60°C for 1 h. The solid hydrogel was cut into small pieces that were washed with DMSO and THF. Finally, the gel particles were dried under vacuum at 50°C for 4 days.

4.3.3 Synthesis of the hydrogel with PL as the crosslinker

A poly(L-lysine) with a degree of polymerization of 288 was used to crosslink the aforementionned linear copolymer. 200 milligrams of the copolymer were swollen in 1 mL of *N,N'*-dimethylformamide. PL (about 50 mg) in a buffer (10 mL of 2(*N*-morpholino)ethanesulfonic acid buffer, 50 mM, pH 7.4) was added to the polymer and incubated at 10°C for 48 h with constant agitation at 40 rpm[7] and then at room temperature overnight. The resulting hydrogel was washed with water several times and lyophilized.

4.3.4 Cloud point determination of PNIPAS

The cloud point of the copolymer solution was measured using a Varian Cary (1 Bio) ultraviolet-visible spectrophotometer with a water-jacketed cell holder connected to a thermostated circulating bath. The cloud point was detected from the change in optical transmittance at 600 nm of a sample 1 cm thick referenced against distilled water. Solutions containing 20 % (w/w) copolymer in water were used. The temperature was raised from 20 to 45°C with a heating rate of 0.1°C/min.

4.3.5 Thermal FTIR spectroscopic study

For the copolymer, a solution containing 20 % (w/w) copolymer in water was prepared. For the hydrogels, the dry polymer was incubated in water at room temperature for 6 h, and the swollen gel particles were used for the FTIR experiments. An aliquot of the sample was placed between two CaF_2 windows separated by a 5-μm Teflon spacer. This cell was mounted on a brass holder whose temperature was computer-controlled with thermopumps. For each temperature, the sample was equilibrated 10 min prior to data acquisition. For each spectrum, 100 scans at a resolution of 2 cm^{-1} were recorded for both the sample and the background. The temperature was raised from 22 to 47°C, and a spectrum was recorded at each degree Celsius; the effective heating rate was about 0.07°C/min. The FTIR spectra were recorded on an FTS-25 Bio-Rad spectrometer equipped with a mercury-cadmium-telluride detector.

To eliminate the water contribution ($\nu_{O-H} \approx 3400$ cm^{-1}) in the methylene stretching region, a polynomial was fitted to simulate the edge of the water band and then subtracted in the C–H stretching vibration region. In the region of the amide bands (1720-1580 cm^{-1}), the spectra were corrected for the water contribution by subtraction of the water spectrum recorded at the same temperature under the same conditions. The subtraction was considered satisfactory when the region between 1750 and 2650 cm^{-1}, where there should be no absorption, was flat. The 1700-1590 cm^{-1} region of the corrected spectra was Fourier self-deconvolved to identify the number of components in

the amide I band. Subsequently, the amide I band was curve-fitted. These mathematical treatments were done with GRAMS software (Galactic Industry, Salem).

4.4 Results and discussion

4.4.1 Characterization of the copolymer

The PNIPAS copolymer was prepared with 2 mol % NAS (Fig. 4.1). The resulting copolymer had a molecular weight of 12,000 g/mol with a polydispersity index (I) of 3.2. All the experiments were performed on the unfractionated copolymer.

We measured the LCST of the linear copolymer by following the turbidity of the solution and by FTIR spectroscopy. A low heating rate was used for both techniques to ensure thermal equilibration and to prevent an artificial shift of the LCST from occurring when the heating rate is too fast. The concentration of the sample was also an important parameter. Because a plateau was observed on the phase diagram between 15 and 20 wt %,[23,24] a sample concentration of 20 % (w/w) was used.

The LCST of the copolymer was first determined from a plot of light transmittance versus temperature (Fig. 4.2A). The absolute LCST was defined as the minimum of the first derivative of the heating curve. The LCST value obtained for the copolymer is around 31°C and is in agreement with previous reports.[5]

FTIR spectra were recorded for the copolymer in water. The bands between 3000 and 2835 cm^{-1} were associated with the C–H stretching (ν_{C-H}) vibrations (Fig. 4.3A). The peaks at 2982 and 2882 cm^{-1} were assigned to the asymmetric and symmetric ν_{C-H} of the methyl groups, respectively. The peak at 2939 cm^{-1} was due to the antisymmetric ν_{C-H} of methylene groups of the polymer backbone.[14] The positions of these three peaks were sensitive to temperature. The maxima of these peaks are plotted versus the temperature in Fig. 4.2. As one can see, there is an abrupt shift upon heating toward lower frequencies for these three bands. The LCST was determined from the minimum of the first derivative of the curves, and a value of 31.3°C was obtained, in agreement with the

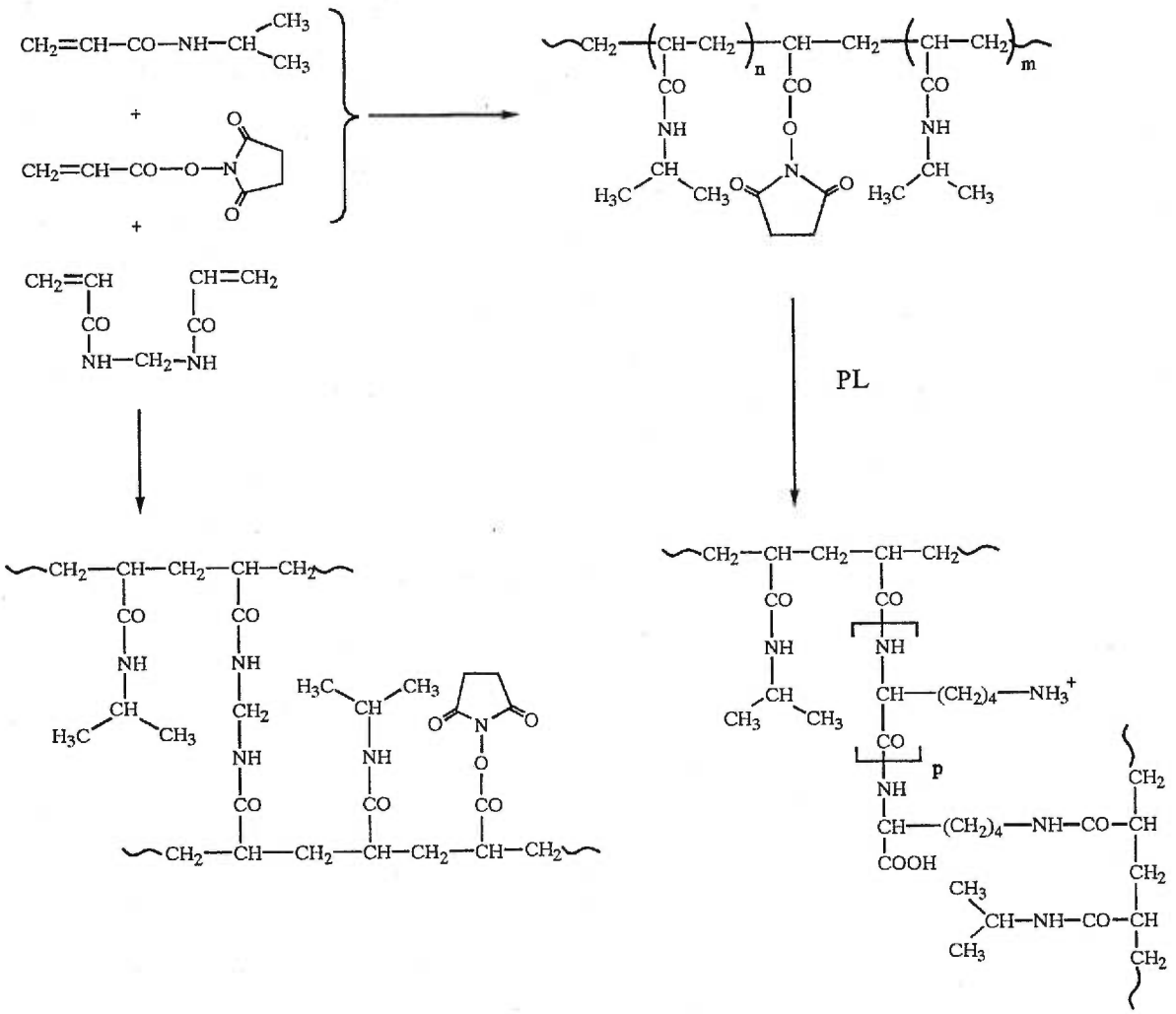

Figure 4.1 Preparation of the linear copolymer and related hydrogels.

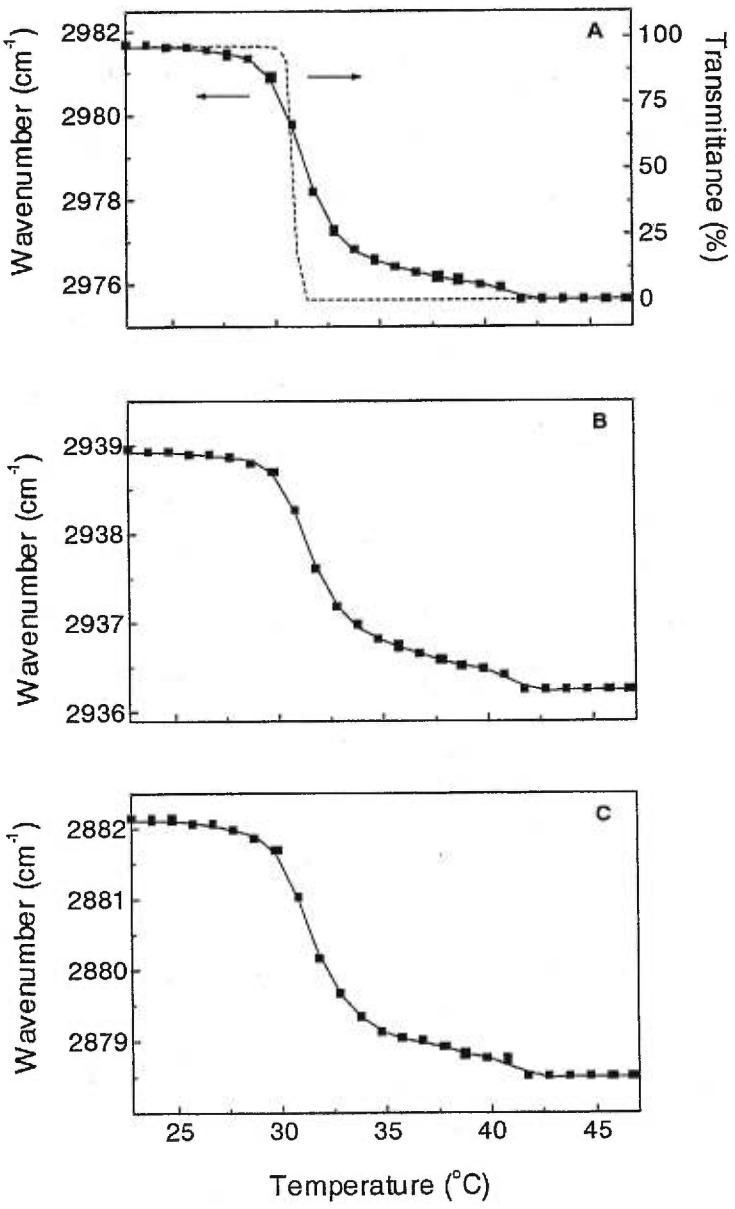

Figure 4.2 Determination by FTIR spectroscopy of the LCST of PNIPAS (–■–) following as a function of temperature the position of the (A) asymmetric and (C) symmetric ν_{C-H} bands of the *N*-isopropyl groups and (B) the asymmetric ν_{C-H} band of the methylene groups of the backbone. There was 20 % (w/w) polymer in water. The light transmittance of the same solution observed at 600 nm (----) is also shown in (A).

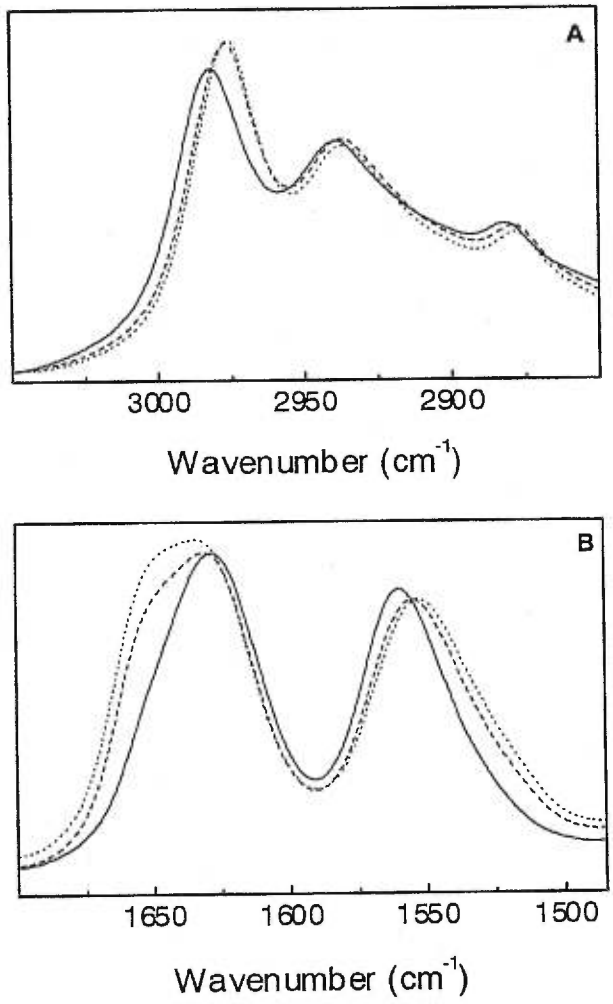

Figure 4.3 FTIR spectra of PNIPAS in (A) the ν_{C-H} region and (B) the amide I and II region at 25°C (—), 35°C (----) and, 45°C (·····).

determination by turbidity measurements. Therefore, the shift of these bands constituted a reliable probe for determining the LCST in the copolymer. Because the amplitude of the shift was larger (ca. 7 cm^{-1}) for the band corresponding to the asymmetric ν_{C-H} vibration of the methyl groups at 2982 cm^{-1}, it was used subsequently as a sensor for the LCST measurement.

The ν_{C-H} shift is a useful probe for monitoring the organizational changes of alkyl chains with temperature because the CH_2 antisymmetric and symmetric stretching modes are sensitive to changes in the conformation of hydrocarbon chains.[15,25,26] In the case of PNIPAS, the bands associated with both the lateral groups and the polymer backbone undergo a shift in their maxima. The abrupt shift toward lower frequencies is mainly interpreted as an increase of the conformational order during the transition, even though other phenomena may be involved.[16,27] This is related to the fact that PNIPAS exists as flexible and disordered coils in aqueous solutions below the LCST and collapses as ordered aggregates above the LCST.[5] Conformational changes during the transition have also been suggested by NMR spectroscopy.[28]*

The amide I and II bands could be associated with the amide groups on PNIPAS. As can be seen in Fig. 4.3B, the shape and position of these bands were sensitive to the precipitation occurring at the LCST. Because the amide I band appears to have been more affected by the transition and because it mainly involves the carbonyl stretching, which is sensitive to hydrogen bonding, we have focused our attention on this band. At 25°C, the amide I band is characterized by a relatively sharp band centered at about 1629 cm^{-1}. Upon heating, the band shifted toward a higher frequency because of the increased spectral contribution at approximately 1655 cm^{-1}. To get a more quantitative analysis, the amide I band was curve-fitted between 1700-1610 cm^{-1}; the limited range was used to circumvent the problems of overlapping contributions due to the succinimide groups (1735 cm^{-1}) and to the amide II band. Good fits were obtained using three components to

*Une seconde transition de faible amplitude semble apparaître entre 35 et 42°C sur les 3 courbes de la figure 4.2. Cette transition est aussi observée par diffusion quasi-élastique de la lumière, ainsi que par rhéologie (D. Lessard, communication personnelle). Celle-ci semble associée à une augmentation de la taille des aggrégats avec l'augmentation de la température.

simulate the band (Fig. 4.4A and 4.4C). Moreover, other studies have proposed that the amide I band includes three components.[14,17] All the spectra recorded at the different temperatures were simulated with three components whose frequencies, widths, and band shapes were free to vary. The maxima of the three bands resulting from the curve fittings are constant over the investigated temperature range. They were located around 1629±1, 1655±1, and 1678±2 cm^{-1} (the variation is expressed as the standard deviation calculated with 25 spectra). In addition, these values were close to the frequencies measured on the deconvolved spectra where at least two major components can be clearly identified (Fig. 4.4B and 4.4D). As proposed previously,[14,17] we assumed that the three components were associated with amide groups involved in different hydrogen bonding patterns. The band around 1629 cm^{-1} was associated with a strongly hydrogen-bonded carbonyl and could be attributed to intermolecular interactions between polymer chains and water molecules. This band is broad (around 40 cm^{-1}), reinforcing this association with the hydrated and disordered regions of the polymer. The band at 1655 cm^{-1} was attributed to weaker intramolecular hydrogen bonding within the polymer chains. It is proposed that the third band around 1678 cm^{-1} corresponds to free carbonyl groups.

If we assume that the absorptivity coefficients are similar for the three components, the areas of the three components can be transformed into the percentages of each type of carbonyl groups (Fig. 4.5A)*. Below the LCST, most of the carbonyl groups (ca.90%) were involved in hydrogen bonding with water. This is fully consistent with the fact that the polymer chain was solubilized in these conditions. There were only 5 % of the intramolecular hydrogen bonding carbonyl groups and 5 % of the free carbonyl groups. At the LCST, there was a decrease of the relative area of the band associated with the hydrogen bonds between the polymer carbonyl groups and the water, as recently observed by ATR/FTIR spectroscopy.[14] The relative intensity of the band associated with intramolecular hydrogen bonding increased. These results indicate that during the transition, about 20 % of the hydrogen bonds between the polymer and water molecules were replaced by intrapolymer ones. The proportion of free carbonyl groups appears to have been constant over the whole temperature range and was not affected by the LCST

*Cette hypothèse semble justifiée dans notre cas du fait que l'aire totale de la bande Amide I reste constante en fonction de la température.

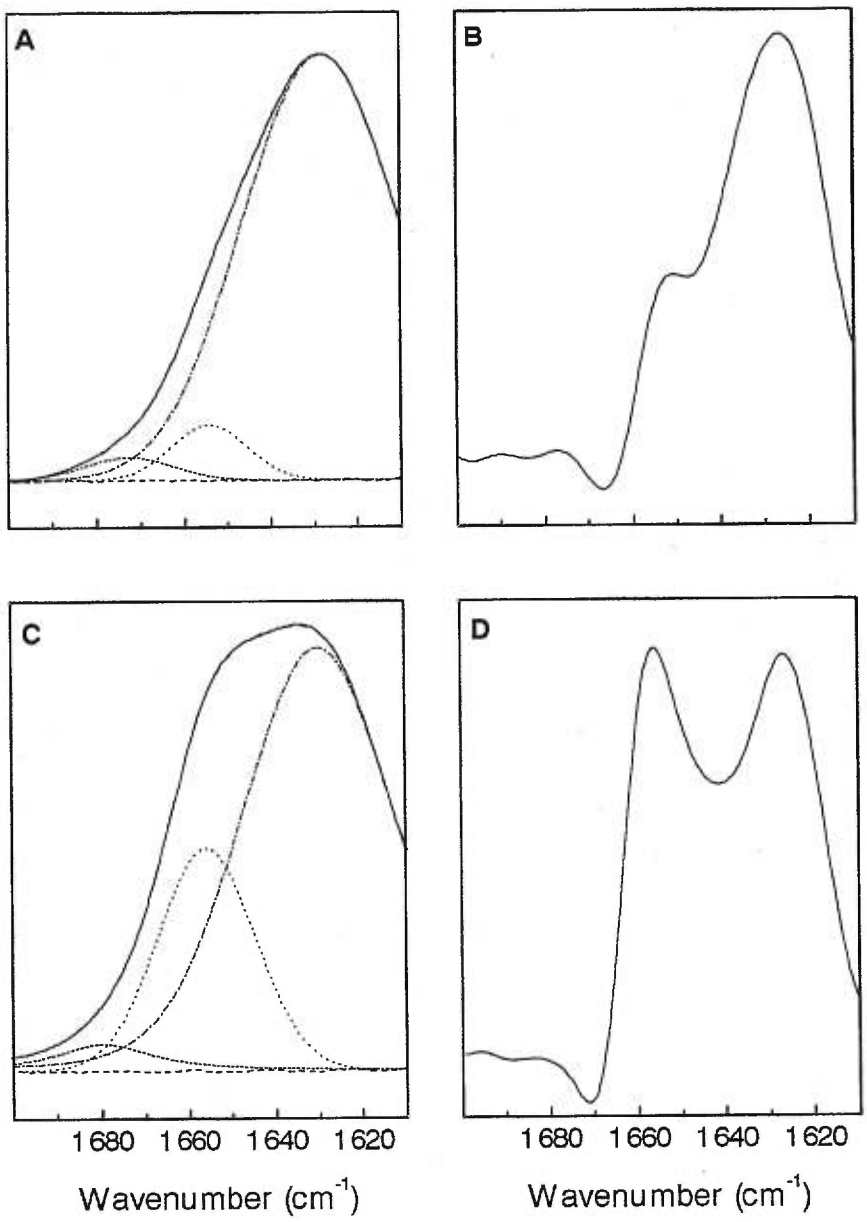

Figure 4.4 Amide I band of a PNIPAS solution (20 % w/w in water). A (25°C) and C (45°C) show the experimental (—) and simulated (·····) spectra. The three components obtained from the band fitting (-·-·- ; - - - ; ----) and the residual curve (– –) are also displayed. B (25°C) and D (45°C) show the corresponding deconvolved spectra.

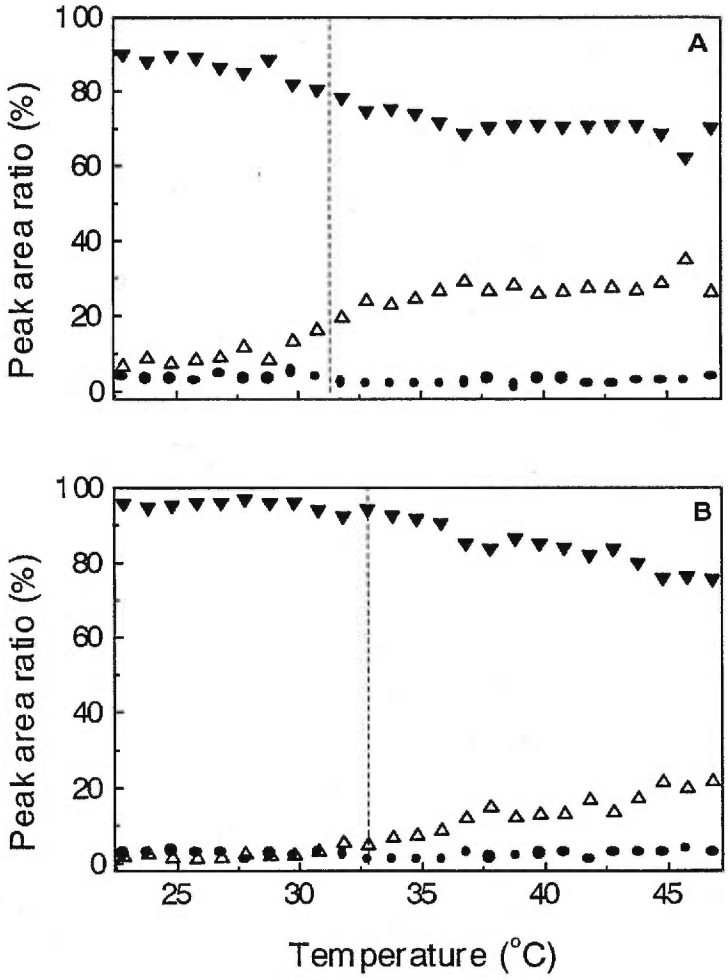

Figure 4.5 Thermal variations of the relative intensity of each amide I component for (A) PNIPAS and (B) the MBA-crosslinked hydrogel. ▼ = band at about 1630 cm^{-1} associated with intermolecular hydrogen bonds; Δ = band at about 1655 cm^{-1} associated with intramolecular hydrogen bonds; ● = band at about 1675 cm^{-1} associated with free carbonyl groups. The dashed lines (---) indicated the LCSTs for the systems.

phenomenon. The increase of intramolecular hydrogen bonds observed during precipitation of the polymer is supported by theoretical studies of phase separations occurring at the LCST, indicating that the origin of the transition is mainly associated with the reorganization of the hydrogen bonds.[29]

4.4.2 Characterization of the related hydrogels

Two different crosslinkers were used in the preparation of hydrogels to examine the influence of their nature on the LCST of the resulting gels (Fig. 4.1). MBA is regarded as a moderately hydrophilic crosslinker.[30] PL is cationic and was used because its amino groups can act as reactional groups for the crosslinking. Both hydrogels are thermosensitive: the transparent gels at low temperatures become opaque upon heating. As with the linear copolymers, FTIR spectroscopy was used to determine the LCST and to characterize the transition at a molecular level.

First, we determined the LCST by following the shift of the maximum of the three peaks located in the ν_{C-H} region. As with the linear polymer, the shift was more evident for the peak corresponding to the ν_{C-H} asymmetric vibration of the isopropyl groups (Fig. 4.6), but the symmetric ν_{C-H} band of the CH_3 and the antisymmetric ν_{C-H} of the methylene were also shifted in a similar way during the transition (data not shown). This shows that just as with the linear polymers, the FTIR method is a useful tool for determining LCSTs in hydrogels. The LCST obtained was in the same range that the LCST obtained for the linear copolymer was. For the MBA-crosslinked hydrogel, the LCST was 32.8°C whereas it was 34.8°C for the PL-crosslinked hydrogel. The higher LCST obtained for the PL-crosslinked gel compared to that of the MBA-crosslinked gel was attributed to the high hydrophilicity of PL. Other studies made on gels containing sodium acrylate as a comonomer have shown that the LCST increases with the proportion of ionic comonomer.[31] We found that the LCST of an hydrogel can also be efficiently modulated by varying the hydrophilicity of the crosslinker.

The extent of the shift of the three ν_{C-H} bands observed during the shrinking transition was very similar to that observed for the phase separation occurring with the linear copolymer, suggesting that the molecular reorganization occurring during these

transitions has a similar nature. The decrease in the ν_{C-H} mode frequency with increasing temperature (Fig. 4.6) could again be attributed to an increase of the conformational order. In addition, our results show that both the lateral groups and the backbone were implied in the transition. These results are in agreement with a previous NMR study that indicates that the protons of both the *N*-isopropyl groups and the backbone are involved in the transition.[28] In the case of PL-crosslinked gels, a shift of the ν_{C-H} band was observed at the LCST. In this case, the transition is less sharp (Fig. 4.6B). It has been reported that ionic gels contain heterogeneities,[28,32] and this phenomenon may explain a transition occurring over a larger range of temperatures for our cationic PL-crosslinked gel.

The amide region of the FTIR spectra was also examined. In this region, hydrogels had additional spectral contributions because both crosslinkers contain amide groups. The MBA crosslinker is formed of two amide groups but only 2 % of the MBA was added to the polymer matrix. For a complete reaction, these amide groups would contribute to approximately 4 % of the amide band and could thus be neglected. The spectra of this gel at 25 and 45°C are displayed in Fig. 4.7A. As for the linear copolymer, at 25°C, the amide I band was narrow and centered around 1634 cm^{-1}. Above the LCST (45°C), a contribution at 1656 cm^{-1} appeared. Each spectrum was resolved into three components, using the same curve-fitting method used for the linear copolymer, and their positions were 1634±2, 1656±1 cm^{-1}, and 1677±4 cm^{-1} (the variation is expressed as the standard deviation calculated with 25 spectra). The deconvolution confirmed the position of the two major components in these spectra. The relative bands areas were transformed into the percentage of each type of carbonyl groups (Fig. 4.5B). As for the ν_{C-H} bands, the behavior of the amide I band as a function of temperature was similar for the gel and the linear polymer. Below the LCST, the low frequency component represented about 95 % of the signal, suggesting that the majority of the carbonyl groups are involved in hydrogen-bonding with water. The areas of the two other components were small, indicating that very few amide groups were free or involved in intramolecular hydrogen bonding. During the transition occurring at the LCST, the 1634 cm^{-1} component lost some intensity relative to the 1656 cm^{-1} band; this change suggests that 20 % of the hydrogen bonds with water were broken and replaced by intramolecular hydrogen bonds.

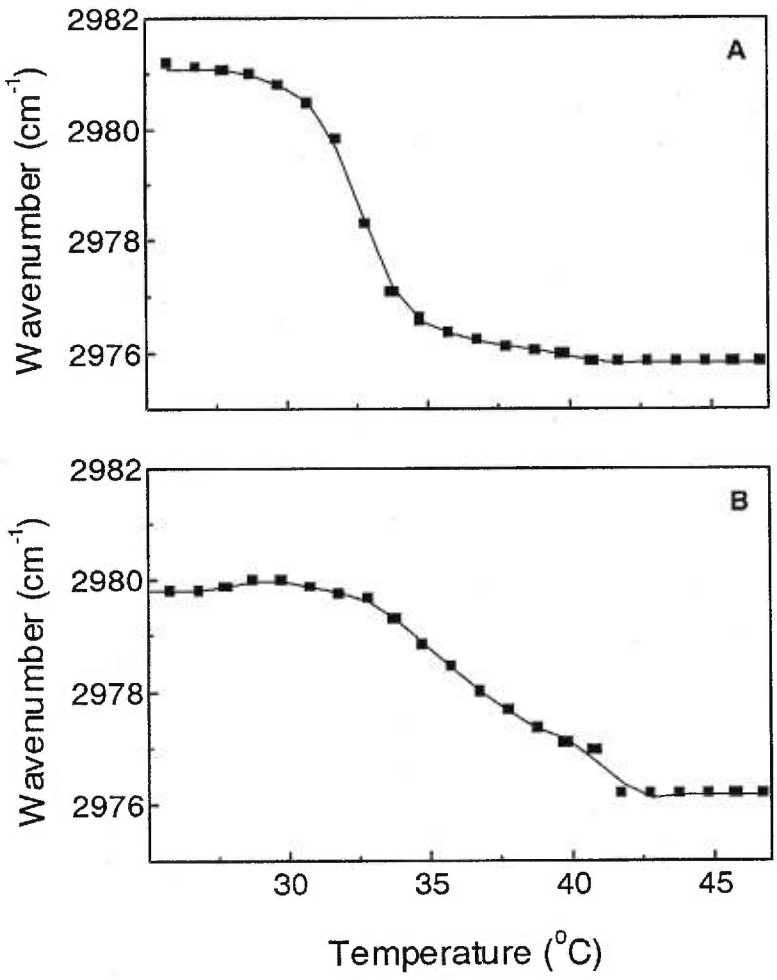

Figure 4.6 Thermal transitions determined by FTIR spectroscopy following the variation of the asymmetric ν_{C-H} band position of the *N*-isopropyl groups as a function of temperature for (A) the MBA-crosslinked gel and (B) the PL-crosslinked gel.

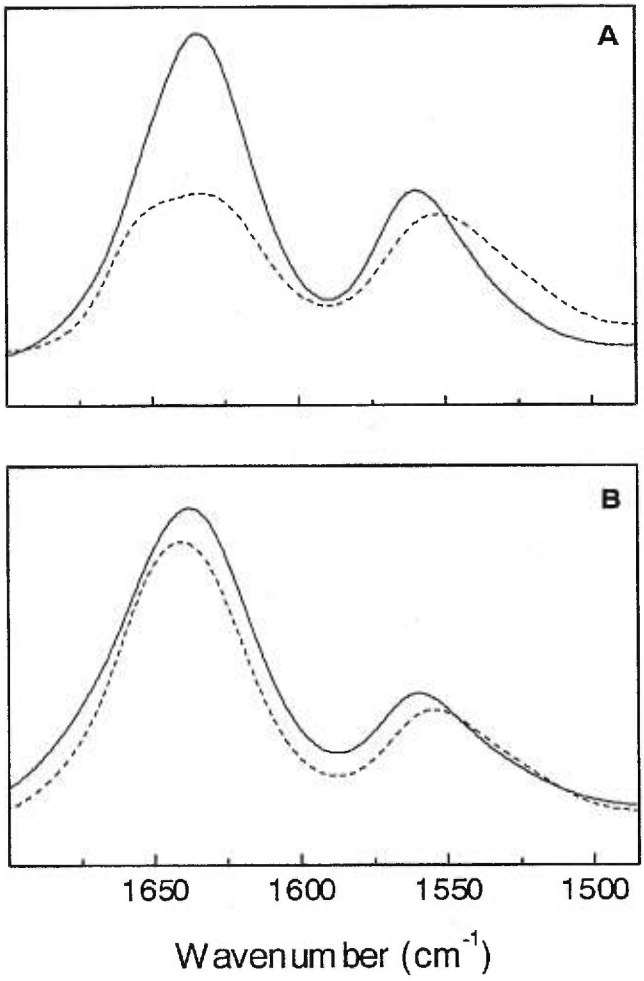

Figure 4.7 FTIR spectra of the amide I and II region of (A) the MBA-crosslinked hydrogel and (B) the PL-crosslinked hydrogel recorded at 25°C (—) and 45°C (----).

The proportion of hydrogen bonds involved in the transition was of the same order as in the linear copolymer.

Interestingly, the correction for the water contribution became more and more difficult above 45°C. This could be due to several phenomena, but it has been shown that water molecules trapped in restricted spaces have a different spectrum[33], leading to moreproblematic water subtractions. It is possible that such water-filled small spaces were formed during the gel condensation.

For the gel crosslinked by PL, the amide bands included a considerable contribution of the crosslinker because around 30 % of the amide groups of the gel belonged to the PL. Unlike the linear copolymer and the gel crosslinked by MBA, the shape of the amide I band was much less affected by the transition occurring at the LCST (Fig. 4.7B). A possible explanation is that the secondary structure of PL was not modified over the temperature range investigated and this hid the structural changes of the polymer. Some experiments were done on free PL by circular dichroism to examine its conformational stability with temperature, and no changes were observed below 45°C (data not shown). As we could not separate the different components of this amide I band, we found it would be too speculative to try to extract information on the hydrogen bonding state of the polymer carbonyl groups.

Our results show that the thermoshrinking transition observed in gels based on NIPAAm leads to similar spectral changes associated with alkyl and amide groups and, as a consequence, to similar structural changes as those involved in the linear copolymer transition. We also have shown that the gel LCST is sensitive to the hydrophilicity of the matrix.

4.5 Conclusions

FTIR spectroscopy has been shown to be a useful tool for determining the LCST of polymers as well as gels. The shift of the maxima of the asymmetric ν_{C-H} bands as a function of temperature provides reliable LCST for both linear copolymer of NIPAAm

(confirmed by the determination of the cloud point) and crosslinked hydrogels. The FTIR spectra also reveal that the molecular nature of the transition experienced by the linear copolymer and the gels is similar. Below the LCST, most of the carbonyls of the amide groups appear to be involved in hydrogen bonding with water. Above the LCST, about 20 % of these bonds are replaced by intramolecular bonds. In addition, our results suggest that both the lateral groups and the backbone undergo conformational changes during the transition.

Our findings also show that the LCST can be modulated by the hydrophilicity of the crosslinker. This tuning can be essential for the optimization of thermosensitive biomaterials. Both an accurate determination of the LCST and an improved molecular understanding of the associated phenomenon are of great importance for designing systems with well-defined properties. The proposed FTIR method could be applied to many other polymer matrixes through probing of the position of bands associated with functional groups involved in the molecular reorganization.

Acknowledgments

Financial support from the Natural Sciences and Engineering Research Council (NSERC) of Canada and Fonds FCAR of Quebec is gratefully acknowledged.

4.6 References

1. S. Saeki, N. Kuwahara, M. Nakata, and M. Kaneko, *Polymer*, **17**, 685 (1976).
2. A. Carlsson, G. Karlström, B. Lindman, and O. Stenberg, *Colloid Polym. Sci.* , **266**, 1031 (1988).
3. L. D. Taylor and L. D. Cerankowski, *J. Polym. Sci., Polym. Chem. Ed.*, **13**, 2551 (1975).
4. H. Y. Liu and X. X. Zhu, *Polymer*, **40**, 6985-6990 (1999).
5. H. G. Schild, *Prog. Polym. Sci.*, **17**, 163 (1992).
6. H Hayashi, K. Kono, and T. Takagishi, *Biochim. Biophys. Acta*, **1280**, 127 (1996).
7. J-P. Chen, D-H. Chu, and Y-M. Sun, *J. Chem. Tech. Biotechnol.*, **69**, 421 (1997).
8. J-P. Chen, *J. Chem. Technol. Biotechnol.*, **73**, 137 (1998).
9. Y-M. Sun, J-P. Chen, and D-H. Chu, *J. Biomed. Mater. Res.*, **45**, 125 (1999).
10. Y. H. Bae, T. Okano, and S. W. Kim, *J. Polym. Sci., Polym. Phys. Ed.*, **28**, 923 (1990).
11. K. Otake, H. Inomata, M. Konno, and S. Saito, *Macromolecules* , **23**, 283 (1990).
12. X. S. Wu, A. S. Hoffman, and P. Yager, *J. Polym. Sci., Polym. Chem. Ed*, **30**, 2121 (1992).
13. F. M. Winnik, *Macromolecules*, **23**, 233 (1990).
14. S-Y. Lin, K-S. Chen, and L. Run-Chu, *Polymer*, **40**, 2619 (1999).
15. H. H. Mantsch and R. N. McElhaney, *Chem. Phys. Lipids*, **57**, 213 (1991).
16. J. Umemura, D. G. Cameron, and H. H. Mantsch, *J. Phys. Chem.*, **84**, 2272 (1980).
17. D. J. Skrovanek, P. C. Painter, and M. M. Coleman, *Macromolecules*, **19**, 699 (1986).
18. J. P. Chen, H. J. Yang, and A. S. Hoffman, *Biomaterials*, **11**, 625 (1990).
19. X. S. Wu, A. S. Hoffman, and P. Yager, *Polymer*, **33**, 4659 (1992).
20. P. Ferruti, A. Bettelli, and A. Feré, *Polymer*, **13**, 462 (1972).
21. A. Pollak, H. Blumenfeld, M. Wax, R. L. Baughn, and G. M. Whitesides, *J. Am. Chem. Soc.*, **102**, 6324 (1980).
22. H. J. Yang, C-A. Cole, N. Monji, and A. S. Hoffman, *J. Polym. Sci., Polym. Chem. Ed.*, **28**, 219 (1990).

23. M. Heskins and J. E. Guillet, *J. Macromol. Sci., Chem.*, **8**, 1441 (1968).

24. C. Boutris, E. G. Chatzi, and C. Kiparissides, *Polymer*, **38**, 2567 (1997).

25. H. L. Casal, D. G. Cameron, and H. H. Mantsch, *Can. J. Chem.*, **61**, 1736 (1983).

26. H. Li, X. Zhang, R. Zhang, J. Shen, B. Zhao, and W. Xu, *Macromolecules*, **28**, 8178 (1995).

27. V. R. Kodati, R. El-Jastimi, and M. Lafleur, *J. Phys. Chem.*, **98**, 12191 (1994).

28. T. Tokuhiro, T. Amiya, A. Mamada, and T. Tanaka, *Macromolecules*, **24**, 2936 (1991).

29. M. Yu and H. Nishiumi, *J. Phys. Chem.*, **96**, 842 (1992).

30. M. C. Chandy and V. N. R. Pillai, *Polym. Int.*, **37**, 39 (1995).

31. Y. Liu, J. L. Velada, and M. B. Huglin, *Polymer*, **40**, 4299 (1999).

32. R. Lundberg, *Encyclopedia of Polymer Science and Engineering*, Vol. 8, p. 393, Wiley-Interscience, New York (1987).

33. M. Lafleur, M. Pigeon, M. Pézolet and J. P. Caillé, *J. Phys. Chem.*, **93**, 1522 (1989).

CHAPITRE 5

NEW HYDROGELS BASED ON *N*-ISOPROPYLACRYLAMIDE COPOLYMERS CROSSLINKED WITH POLYLYSINE: MEMBRANE IMMOBILIZATION SYSTEMS

AlinePercot, Michel Lafleur and X. X. Zhu, Polymer (2000).

Running title: New Hydrogels for Membrane Immobilization

Keywords: *N*-isopropylacrylamide, polylysine, lipid vesicle, immobilization, controlled release

5.1 Abstract

New hydrogels based on *N*-isopropylacrylamide copolymerized with an activated monomer have been developed as vesicle immobilizing devices. In order to provide a strong and reversible interaction between the solid support and the lipid vesicles, we chose polylysine, a cationic polypeptide as the anchoring element. Our systems are based on *N*-isopropylacrylamide copolymerized with an activated monomer and then crosslinked with polylysine. The innovative feature of this approach is that the polypeptide plays many key roles: i) it is used as crosslinker, ii) its positive charges act as anchor sites, and iii) as an hydrophilic molecule, polylysine improves the swelling properties of the gel and therefore the capacity of vesicle binding. Several hydrogels were synthesized with varying monomers ratios and polylysine lengths. The characterization of the systems includes an estimation of the ability of the gels to immobilize vesicles and of the integrity of the adsorbed vesicles. The most efficient gel is made of a copolymer containing 6 mol % of activated monomer crosslinked with a long polylysine (degree of polymerization of 288). This hydrogel can immobilize up to 1000 μmol of lipids per gram of dry gel. Control experiments show clearly that the nature of the anchoring interaction is electrostatic. As an illustration of the potential applications of such a system, we show that vesicles can be immobilized in a gel-packed column and the release of their content is triggered by an increase of the temperature.

5.2 Introduction

The immobilization of membranes on solid supports leads to several applications. Solid-supported membranes can be used as containers for controlled drug release systems [1], as a stationary phase for chromatographic devices [2-5], as continuous operating systems performing enzymatic processes [6,7] or as artificial organs [8]. Different methods have been used to immobilize lipid membranes on a solid support. Lipids can be immobilized by covalent bonding [2], by entrapment in a solid

matrix [4,8] or by ionic binding. This latter interaction is advantageous in several ways. As an interfacial phenomenon, the electrostatic interaction is less likely to perturb the integrity of the membrane. The binding is usually strong, stable, and reversible; consequently, the solid support can easily be washed and reused. Positively charged matrices are suitable to immobilize cells as biomembranes generally contain negatively charged lipids [9].

We have designed and developed hydrogels based on poly-*N*-isopropylacrylamide crosslinked with polylysine as vesicle immobilizing systems. Poly(*N*-isopropylacrylamide) (PNIPAAm) has been selected for the development of the immobilization system because it is hydrophilic and nondenaturing for many proteins [10]. Aqueous solutions of PNIPAAm have a lower critical solution temperature (LCST) around 30-35°C [10]. Because of their thermal sensitivity, homo- and copolymers of *N*-isopropylacrylamide (NIPAAm) have been used in immunoassays, bioseparations, controlled release systems, and enzyme bioreactors [10-15]. Related NIPAAm hydrogels retain their thermo-sensitivity [10], and this property can be exploited to control the release from vesicles immobilized on the gel. A key feature of our systems is that polylysine was used both as the crosslinker and the membrane anchor. It is a water-soluble polycation extensively used for biological applications. This polypeptide can interact with ionic sites on vesicles or cell surfaces [16]. It was shown that there is a tight binding between polylysine and negatively charged lipids and this interaction depends on the degree of polymerization (DP) of the peptide [17-19]. The DP may also influence the crosslinking reaction, the swelling of the resulting gels and the number of anchoring sites. Therefore, we have examined the effect of the DP of polylysine on the properties of the hydrogels to optimize the performance of these systems.

To crosslink PNIPAAm with polylysine, *N*-acryloxysuccinimide (NAS) was used as the reactive comonomer since the succinimide group is chemically stable but shows high reactivity and selectivity toward amine nucleophiles [11,12,20]. Since the degree of crosslinking may affect the mechanical properties of the hydrogel obtained, various amounts of NAS were used in the preparation of the copolymers to optimize the resulting gel properties.

We report here the preparation of NIPAAm/NAS copolymers and related gels. The characterization of the membrane immobilization ability of different gels is also discussed. The most efficient gel is used in an application involving thermally controlled release.

5.3 Materials and methods

All chemicals and biochemicals including NIPAAm and acrylic acid (AA) were purchased from Sigma (St. Louis, MO, USA) and Aldrich (Milwaukee, WI, USA), unless otherwise mentioned. AA was purified by distillation in the presence of an inhibitor. Ninhydrin was purchased from Baker Analyzed (Phillipsburg, NJ, USA), sulforhodamine B (SRB) from Molecular Probes (Eugene, OR, USA), and 1-palmitoyl-2-oleoyl-*sn*-glycero-3-phosphatidylcholine (POPC) and 1-palmitoyl-2-oleoyl-*sn*-glycero-3-phosphatidylglycerol (POPG) from Avanti Polar Lipids (Birmingham, AL, USA).

5.3.1 Synthesis of N-acryloxysuccinimide

The coupling of AA with *N*-hydroxysuccinimide (NHS) was carried out as described previously [21]. NHS (0.014 mol) and AA (0.014 mol) were dissolved in 20 ml of anhydrous chloroform. Dicyclohexycarbodiimide (DCC) (0.014 mol) dissolved in anhydrous chloroform (10 ml) was slowly added to this solution. The mixture was stirred for 45 h at room temperature. The insoluble dicyclohexylurea was removed by filtration. NAS was purified by chromatography on a silica gel column. The product displays the expected spectral characteristics [11]: ^{1}H NMR ($CDCl_3$) 2.85 (s, 4 H), 6.0-7.0 ppm (m, 3 H); IR (KBr) 1800, 1775, 1735, 1260, 995, 870 cm^{-1}.

5.3.2 Synthesis of poly(N-isopropylacrylamide-co-N-acryloxysuccinimide)

The copolymer was prepared by dissolving NIPAAm and NAS (total weight about 1 g) in 15 ml of a mixture of anhydrous tetrahydrofuran (THF) and anhydrous toluene 1/3 (v/v); the NAS proportions were 2 or 5 mol %. 2,2'-Azoisobutyronitrile (AIBN) (1 mol % of the monomers) was added as the initiator for the polymerization, performed under nitrogen at 55°C for 24 h. THF (60 ml) was added to the mixture to solubilize the copolymer. The mixture was then added drop-wise into 500 ml petroleum ether to precipitate the copolymer. The precipitate was filtered under vacuum and dried at 42°C overnight [22]. The homopolymer of NIPAAm was synthesized similarly in toluene.

5.3.3 Crosslinking of the copolymers by polylysine

A long poly(L-lysine) with a DP of 288 (PLℓ) and a short one with a DP of 19 (PLs) were used as crosslinkers. 200 mg of the copolymer were swollen in 1 ml of dimethylformamide. Polylysine (about 50 mg) in 10 ml of 2-*N*-morpholinoethanesulfonic acid (MES) buffer (50 mM, pH 7.4) was added to the polymer and incubated at 10°C during 48 h with constant agitation at 40 rpm [14] and then at room temperature overnight. The resulting gels were repeatedly washed with water and then lyophilized.

5.3.4 Characterization of the copolymers

The molecular weights of the linear copolymers were determined by size exclusion chromatography (SEC) using THF as the mobile phase and polystyrene as standards. The LCST was determined by measuring the turbidity at 500 nm of a solution containing 0.2 % (w/w) copolymer in water as the sample was heated up.

The succinimide group content of the copolymer before and after crosslinking was monitored by FTIR spectroscopy. The NAS content was calculated from the ratio of the intensity of a band associated with the succinimide group at 1735 cm^{-1} to that of the

band at 2876 cm^{-1} corresponding to the acrylamide monomer. Calibration curves were made from spectra of NAS and NIPAAm mixtures of varyingratios. A quadratic function was used to fit the baseline in both regions prior to the determination of the intensity. The samples were prepared as KBr pellets and the spectra were recorded on a Bio-Rad FTS-25 FTIR spectrometer equipped with a mercury-cadmium-telluride detector. For each spectrum, 100 scans were collected with a nominal resolution of 2 cm^{-1}.

5.3.5 Characterization of the synthesized gels

The succinimide content was determined by FTIR as described above. The unreacted polylysine in the wash was assayed with the Lowry protein assay [23]. The polylysine immobilized in the hydrogel was estimated as the difference between the amount used as reactant and the recovered quantity in the wash.

The swelling ratio (SR) of the gels was measured gravimetrically. The gels were equilibrated in water at room temperature overnight. The swelling ratio was determined by

$$\mathrm{SR} = \frac{w_S - w_D}{w_D} \qquad (1)$$

where w_S and w_D are the dry and the swollen weights of the gel, respectively.

5.3.6 Acetylation of hydrogel amino groups

The gel was swollen in an aqueous solution of sodium acetate (450 mg/ml, pH 7.5) and stirred for 5 h. Acetic anhydride (60 times in excess) was then added to the mixture. The acetylation was carried out between 0 and 4°C during 3 h while the pH was maintained at 7.5 [24]. Several hours were needed for the reaction because of the limited diffusion of the reactants in the gel. The sample was then centrifuged, washed with water several times and lyophilized. The amount of amino-group substitution was measured by the ninhydrin procedure of Brown and Green [25], using PLs as the standard. To a known weight of acetylated gel were added 75 µl of a ninhydrin solution

in ethanol (50 g/l), 100 µl of a solution of phenol in ethanol (4 g/ml) and 75 µl of a KCN solution in pyridine (20 µM). The mixture was well vortexed and heated at 100°C for 5 min. The absorbance was measured in the supernatant at 568 nm. The result was compared to that obtained on PNIPAS6-PLℓ before acetylation.

5.3.7 Interaction of the free and grafted PL with the vesicles

First of all, the binding of free PLℓ and PLs to lipid vesicles was determined by a centrifugation assay [26]. The polylysine was dissolved in a MES buffer and added to a suspension of POPC:POPG (85:15) multilamellar vesicles (MLV). The samples were then freeze-and-thawed five times and centrifuged to isolate the free polylysine from that bound to the vesicles. The polylysine concentration in the supernatant was measured by the Lowry protein assay [23].

Two aspects were examined for the immobilization of lipid vesicles on the crosslinked gels: the amount of lipids retained by the gel, and the integrity of the immobilized lipid vesicles. In order to perform these assays, dye-containing vesicles were prepared by hydrating the lipids with a buffer (50 mM HEPES, 5 mM ethylenediaminetetraacetic acid (EDTA), 10 mM NaCl, pH 7.4) containing SRB (80 mM SRB) [27]. The lipid suspension (ca. 30 mM) was then freeze-and-thawed and extruded to obtain vesicles of 100 nm in diameter. The SRB-containing vesicles were separated from the free SRB by size exclusion chromatography using a column filled with Sephadex G-50 fine gel swollen in an isosmotic external buffer (50 mM HEPES, 5 mM EDTA, 134 mM NaCl, pH 7.4). The dry gel (between 2 and 7 mg) was swollen in 2 ml of external buffer and vigorously stirred for an hour to grind the gel. The size distribution of the resulting particles depends on the mechanical properties of the gel, as discussed later. The lipid vesicles were added to the gel particles and the samples were incubated at 25°C for 1.5 h with constant agitation. The samples were then centrifuged to pellet the gel. The quantity of immobilized lipids was determined by measuring the phospholipid concentration in the supernatant using the Fiske-SubbaRow phosphorus assay [28]. A control experiment showed that all the lipids remained in the supernatant after incubation and centrifugation in the absence of the gel.

The self-quenching property of the entrapped dye was used to estimate the integrity of the immobilized vesicles. The fluorescence of SRB inside the vesicles is quenched because of its high concentration [29]. If the vesicle permeability is affected by its interaction with the gel, SRB would leak out and the internal concentration of the probe would decrease: this dilution would lead to an increase of fluorescence. This perturbation can be probed by the self-quenching efficiency (Q) of the remaining entrapped SRB. This parameter is calculated according to

$$Q = \left(1 - \frac{I_0}{I_T}\right) x100 \qquad (2)$$

where I_0 is the initial fluorescence intensity of the SRB after vesicle immobilization and I_T is the total fluorescence intensity measured after complete disruption of all the vesicles by Triton X-100 (0.1 vol %). The Q values were calculated for the pellet (i.e. on the bound-vesicles) as well as for the remaining free vesicles in the supernatant. In the case of the pellet, an aliquot of the vesicle-containing gel was re-suspended in the external buffer in a fluorescence cell.

The fluorescence measurements were performed at 25°C on a SPEX Fluorolog-2 spectrometer equipped for sample stirring. The fluorescence intensity of SRB was monitored with an excitation wavelength of 565 nm, an emission wavelength of 586 nm and a response time of 0.3 s. The excitation and emission bandpath widths were set at 1.5 and 0.5 nm, respectively.

5.3.8 Controlled release with temperature

The SRB containing vesicles were prepared and immobilized on the swollen gel as described above. The vesicle-containing gel (about 750 mg) was packed in a glass column (10 x 7 mm) thermostated by a water bath. The column was connected to a flow-through cuvette placed in a Hitachi Model 100-60 UV-VIS Spectrophotometer and the absorbance was measured at 565 nm to detect the SRB release. For some collected fractions, self-quenching of the SRB was determined as described above to determine whether the released SRB is free or still encapsulated in vesicles. The phospholipid concentration in the collected fractions was determined using the Fiske-SubbaRow

phosphorus assay [28]. The flow rate was 25 ml/h. The mobile phase was the external buffer (50 mM HEPES, 5 mM EDTA, 134 mM NaCl, pH 7.4). The gel was first washed at room temperature for 20 min with buffer, the temperature of the column was then increased to 50°C. At the end of the experiment, when a flat baseline was recovered, the column was washed by ethanol.

5.4 Results and discussion

5.4.1 Synthesis and characterization of the copolymers

NAS was copolymerized with NIPAAm to introduce reactive groups towards the primary amine groups of polylysine (Fig. 5.1). The degree of crosslinking should depend on the amount of NAS residues in the copolymer. We have used 2 and 5 mol % of NAS in the feed to examine the impact of this parameter. The complete polymerization was confirmed by NMR spectroscopy, inferred by the disappearance of protons associated with the C=C double bond. In addition, the inclusion of succinimide groups in the copolymers was established by the presence of three peaks at 1814, 1784 and 1739 cm^{-1} in the IR spectra (Fig. 5.2D). These bands were observed in the NAS monomer spectrum (Fig. 5.2B) but absent in that of the pure PNIPAAm polymer (Fig. 5.2C). In order to estimate the proportion of NAS in the copolymer, we have developed a method based on band intensity ratios from the IR spectra. The band at 2876 cm^{-1} is due to the symmetric stretching vibration of the methyl group of *N*-isopropylacrylamide (Fig. 5.2A and 5.2C). Its intensity was used to probe the NIPAAm content, the very small contribution of NAS at this wave number (Fig. 5.2B) being neglected. Three bands were observed in the carbonyl stretching region of the NAS monomer spectrum (Fig. 5.2B). These bands, at 1800, 1775 and 1735 cm^{-1}, were also well resolved in the spectra of the copolymer but slightly shifted upon polymerization (Fig. 5.2D). The vibrational coupling of the two cyclic carbonyl should lead to two bands in this region, corresponding to the antisymmetric and symmetric coupled C=O stretching vibration [30]. The third band

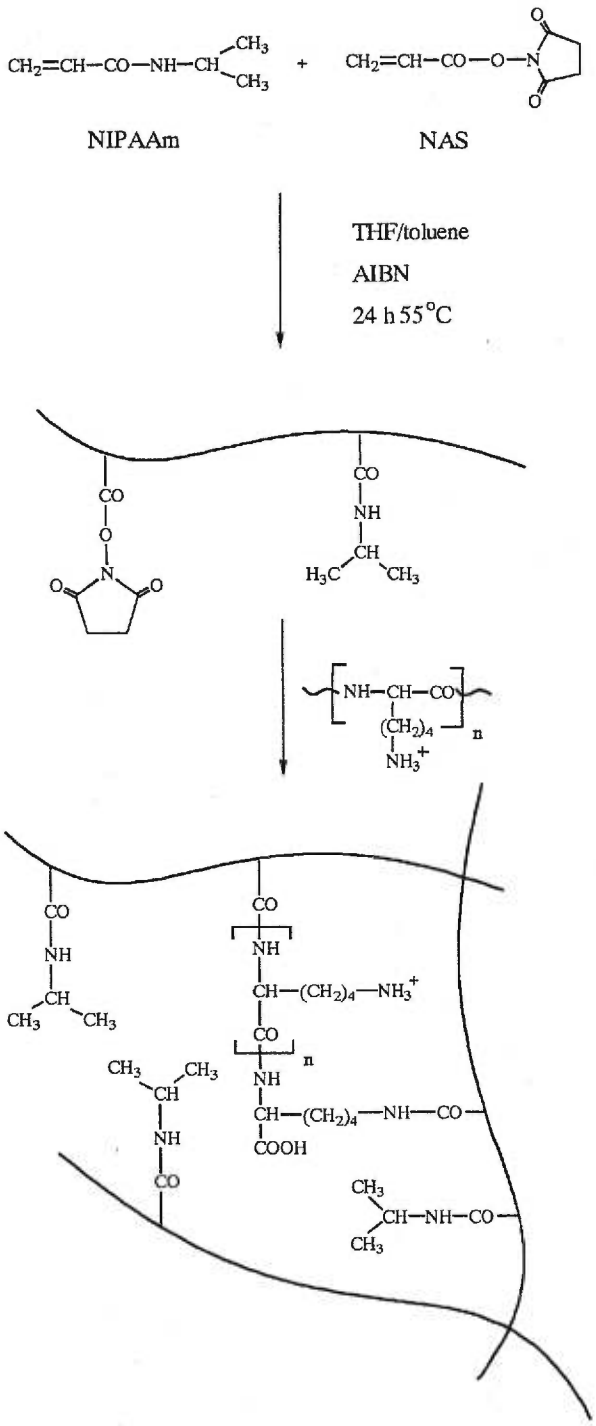

Figure 5.1 Synthetic schemes of the copolymers (PNIPAS) and the crosslinking of PNIPAS by polylysine.

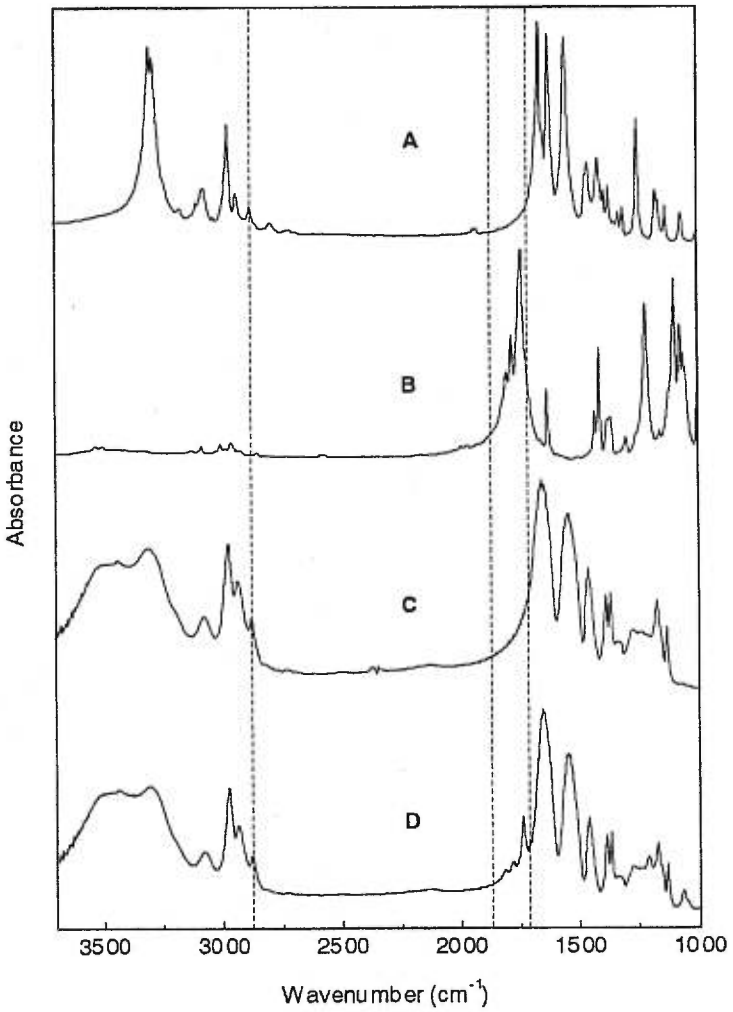

Figure 5.2 IR spectra of the monomers, NIPAAm (A) and NAS (B), and the polymers, PNIPAAm (C) and PNIPAS6 (D). The dashed lines (----) indicate the band at 2876 cm^{-1} associated with the symmetric stretching vibration of the methyl group of NIPAAm and the region between 1710 and 1837 cm^{-1} which includes the bands associated with the succinimide group.

could be attributed to the ester carbonyl of the NAS group. As proposed previously [14], we have used the band at 1735 cm^{-1} to probe NAS, since it is the most intense. A calibration curve was established from the intensity ratio of the band associated with the succinimide group at 1735 cm^{-1} and the band associated with the acrylamide monomer at 2876 cm^{-1} (Fig. 5.3 and 5.4). Using this curve, we have estimated that the NAS/NIPAAm ratios of the two copolymers prepared were 4 and 6 mol % of NAS; these copolymers are referred to as PNIPAS4 and PNIPAS6, respectively (Table IV).

Copolymer	NAS (mol %)	Yield (%)	M_n (g/mol)	M_w/M_n	LCST (°C)
PNIPAS4	4	81	12000	3.2	33.5
PNIPAS6	6*	73	32000	2.5	34.1

*Valeur obtenue par extrapollation de la courbe de calibration de la figure 5.4.

Table IV Characterization of the copolymers

These ratios are consistent with the reactivity ratios of the monomers (0.277 for NIPAAm and 1.934 for NAS [22]). The content of NAS has also been estimated by determining the concentration of the NHS anions generated by the reaction of succinimide group of the polymer with isopropylamine, measuring its absorbance at 259 nm [11,22,31]. This method was found very sensitive to the reaction conditions (pH, reaction time), especially in the case of gels where the reactants have to diffuse in a polymer matrix. In this case, systematic underestimation of the content of NAS was observed. We believe that the IR method proposed here provides more reliable estimates of the NAS proportions.

The copolymers have a lower molar mass (M_n) than the homopolymer of NIPAAm. The M_n was 12 000 and 32 000 for PNIPAS4 and PNIPAS6, respectively, with identical copolymerization conditions. The same phenomenon was observed by Chen et al. [32] for copolymerization with various NAS/NIPAAm ratios: the M_n

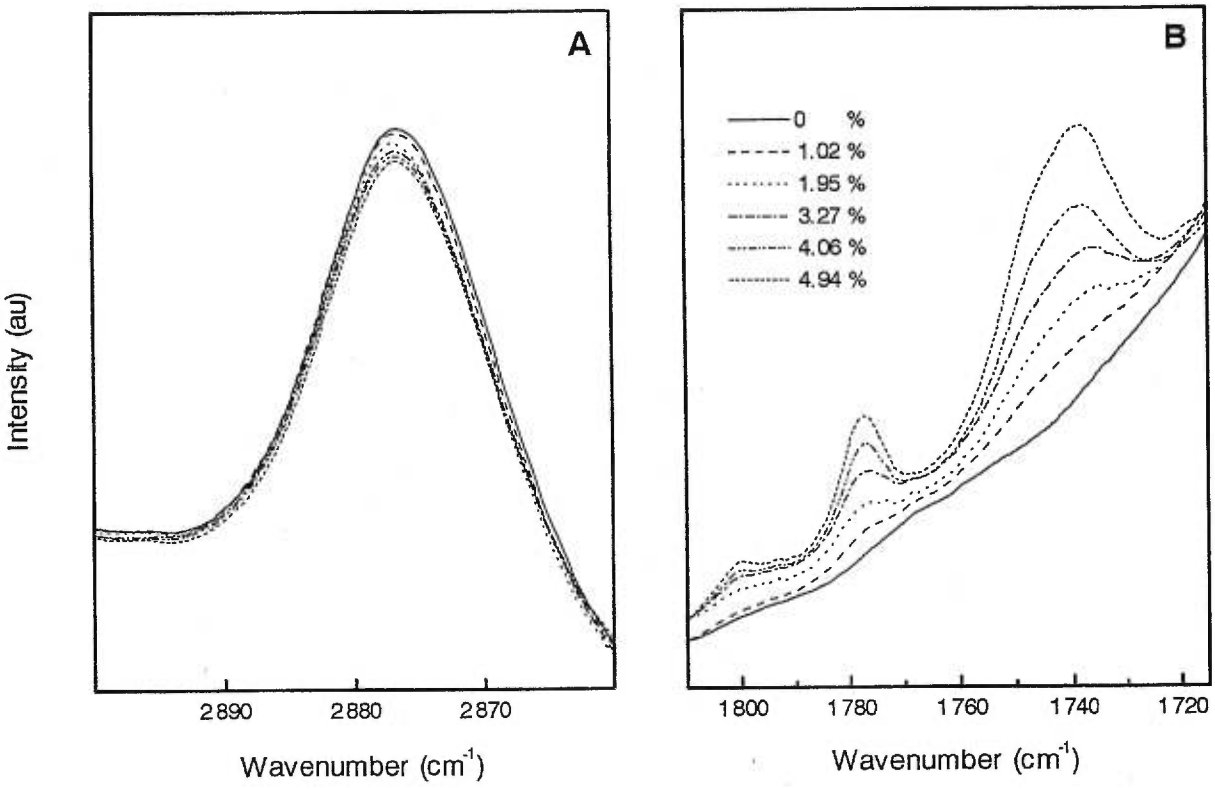

Figure 5.3 IR spectra of standard mixtures of NAS/NIPAAm monomers with defined ratios. (A) The band at 2876 cm^{-1} is associated with NIPAAm and used to normalize the spectra. (B) Bands at 1800, 1775 and 1735 cm^{-1} are associated with the succinimide group.

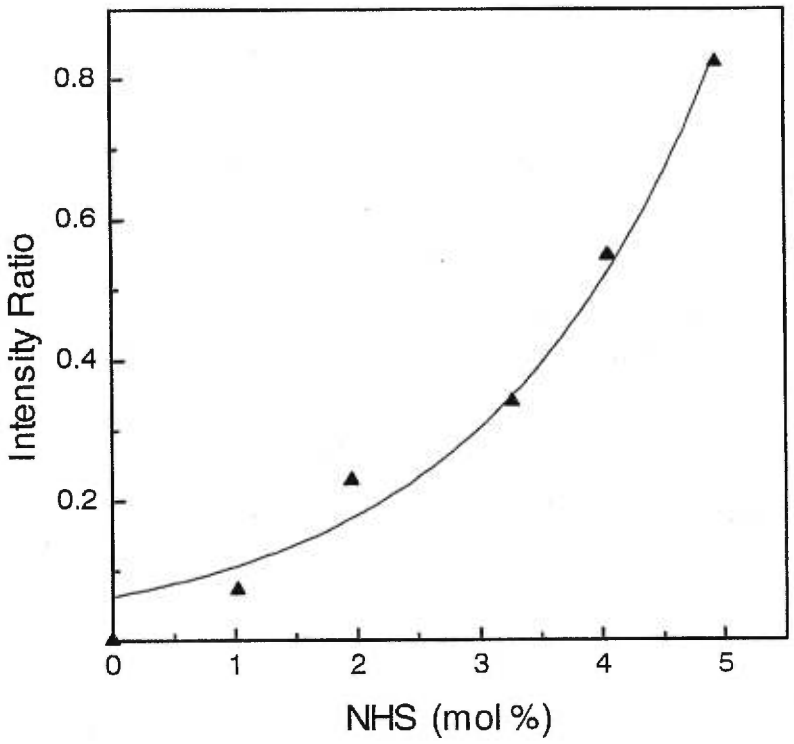

Figure 5.4 Calibration curve obtained from the variation of the intensity ratios of the band at 1735 cm^{-1} assigned to the succinimide group to the NIPAAm band at 2876 cm^{-1} in the IR spectra of NAS/NIPAAm monomer mixtures.

*L'écart type des points expérimentaux par rapport à la courbe de calibration simulée est de 0.04.

obtained were in the same range as ours, and increased with increasing NAS/NIPAAm ratio. We have tried to improve the M_n of PNIPAS4 by varying the THF/toluene ratio used for the polymerization since THF has a high chain transfer activity [11,20]. The optimal ratio was 1/3 (v/v) in agreement with Yang et al. [22]. Changes in the initiator concentration and the initial concentrations of the monomers did not lead to any significant improvement of the M_n. The LCST's of the copolymers were around 33-35°C (Table IV). The small difference between the LCST's of PNIPAS4 and PNIPAS6 may be due to the chemical composition and the molar mass of the copolymers [20].

5.4.2 Crosslinking of the copolymers with polylysine

Two polylysines with different DP's were used as crosslinking agents (Fig. 5.1). Table V summarizes the characteristics of the synthesized gels.

One gel was made with PNIPAS4 copolymer crosslinked by PLℓ and is referred to as PNIPAS4-PLℓ. In this case, all the succinimide groups reacted during the crosslinking reaction as inferred from the complete disappearance of the IR bands at 1814, 1784 and 1739 cm^{-1}. It was calculated that 250 mg of polylysine were bound per gram of dry gel. The charges introduced by the lysine residues increase considerably the hydrophilicity of the polymer matrix and can explain the high swelling ratio observed: the gel can take up water, as much as 42 times of its dry weight. However, the resulting gel is soft, sticky and difficult to manipulate. The low molecular weight of the copolymer PNIPAS4 (12 000 g/mol) may explain the softness of the gel.

The gels PNIPAS6-PLℓ and PNIPAS6-PL*s* resulted from the crosslinking of PNIPAS6 with PLℓ and PL*s*, respectively. Both gels were resilient and easy to grind. Based on the IR determination, about 50 % of the initial NAS have reacted in both cases. The presence of unreacted NAS is likely due to the slow diffusion of polylysine in the gels as the crosslinking proceeded. For PNIPAS6-PLℓ, 270 mg of PLℓ per gram of dry gel were grafted. As expected, the swelling was high as a consequence of the insertion of the polylysine charges in the gel. The gel PNIPAS6-PL*s* contains 125 mg of short

Gel	Unreacted NAS (mol %)	Amount of PL ($mg/g_{dry\ gel}$)	SR	Vesicle composition POPC/POPG (mol/mol)	Q_{pellet} (%)	$Q_{supernatant}$ (%)	Immobilized Lipids ($\mu mol/g_{dry\ gel}$)
PNIPAS4-PLℓ	0	250	42	85/15	88±2*	85±2	70±30
PNIPAS6-PLℓ	2.6	270	46	85/15	93±6	80±10	1000±100
"	"	"	"	100/0	57±9	92.0±0.6	13±6
PNIPAS6-PLℓAc	–	"	1	85/15	79±8	92±4	4±2
PNIPAS6-PLs	3.0	125	21	85/15	83±6	94.8±0.3	6±4

*the uncertainties represent the standard deviation of at least 3 measurements.

Table V Characterization of the gels and immobilization and of the permeability of the vesicles at 25°C.

polylysine per gram of dry gel; this is about 50 % of the polylysine content compared to PNIPAS6-PLℓ. In parallel, the swelling of this gel was smaller by a factor of 2, probably as a result of the limited charge content.

5.4.3 Immobilization of vesicles

The ability of the different gels to immobilize vesicles was evaluated (Table V). The absolute quantity of immobilized lipids is reported in µmole of immobilized lipids per gram of dry gel. Measurement of the self-quenching efficiency Q of a fluorescent probe encapsulated in the vesicles was used to verify the integrity of the immobilized membranes. The experiments were performed with membranes containing 15% of POPG, a negatively charged lipid, and 85% of POPC, a zwitterionic lipid. For all these experiments, the gels were ground in small particles in order to maximize the gel surface accessible for interacting with lipids. Because of the poor mechanical properties of PNIPAS4-PLℓ, this gel could not be properly ground and very coarse heterogeneous particles were obtained in this case.

Our results indicate clearly that the hydrogels are suitable for vesicle immobilization (Table V). The best performing gel is PNIPAS6-PLℓ. In this case, about 1000±100 µmol of lipids can be immobilized per gram of dry gel (this corresponds to 21 µmol of lipid/ml of swollen gel). If less lipids were present during the incubation step, all the lipid vesicles were immobilized illustrating the high anchoring efficiency of the gel. The maximal load for our gel is in the same range as that reported for lipids immobilized sterically by reverse phase evaporation on Sephacryl S-1000 beads [4]. The very good ability of PNIPAS6-PLℓ to immobilize vesicles is directly linked to the presence of the polylysines since they provide strong anchoring sites and ensure a good swelling of the gel, and therefore a good accessibility to the sites. The main anchoring force of the vesicles on the hydrogel seems to be of electrostatic nature, as demonstrated by two findings. First, the quantity of the neutral POPC vesicles immobilized is much lower (a reduction of 97 %) than that of vesicles containing negatively charged lipids (Table V). Second, the a was chemically modified to neutralize the positive charges of polylysine by

acetylation: the resulting acetylated gel is referred to as PNIPAS6-PLℓAc. This gel showed very poor swelling and immobilized a very limited quantity of lipids. These results highlight the prime importance of the lysine charges in our designed gel.

In order to characterize the accessibility of the binding sites to the 100 nm LUV, we have characterized the stoichiometry of the free amino groups per accessible POPG in our gels (Table VI). The free amino group content is defined as the total number of amino groups on polylysine in the gel minus those that are involved in the crosslinking (deduced from the amount of NAS that reacted). The accessible POPG molecules were associated to the POPG on the external leaflet of the membrane, assuming homogeneous lipid distributions and that 60% of the lipids were on the outer leaflet. As a preliminary characterization, we estimate the NH_3^+/POPG stoichiometry for free polylysine in solution. The long polylysine binds to POPG-containing vesicles in a stoichiometric manner since we find approximately one lysine per accessible POPG. In the case of the short polylysine, there is only 0.1 lysine per POPG molecule (Table VI).

Free Polylysine		Bound Polylysine	
Polylysine	NH_3^+/POPG	Gel	NH_3^+/POPG
PLℓ	1	PNIPAS4-PLℓ	210
		PNIPAS6-PLℓ	20
PLs	0.1	PNIPAS6-PLs	1090

Table VI Stoichiometry of the immobilization of vesicles by free and bound polylysine

As polylysine was added in excess in the centrifugation assay, we conclude that PLs has a smaller affinity for POPC/POPG (85/15) vesicles than PLℓ. The affinity of the polypeptide for these vesicles is very dependent on the peptide length. Different behaviors for long and short polylysine were associated with conformation effects

[17,19]. Once grafted on the polyacrylamide, a ratio of 20 amino groups per accessible POPG was found for PNIPAS6-PLℓ. This ratio, which is lower than that obtained with the free PLℓ, suggests that not all the amino groups are accessible to the vesicles and the vesicle concentration is probably not homogeneous throughout the gel.

Preservation of the membrane integrity during the immobilization process was also examined by looking at the potential release of a dye (Table V). For all the POPC:POPG vesicles, the Q value of the SRB entrapped in lipid vesicles remained high for both the immobilized vesicles and those remaining free in the supernatant. This indicates that the interaction between polylysine and the lipids does not affect the permeability of the vesicles. Therefore our designed system presents the advantage that the immobilized vesicles can be used as small containers. During the measurement of Q, the immobilized vesicles were emptied from their content and, interestingly, different kinetics of SRB-release induced by the addition of Triton-X could be observed for free and immobilized vesicles (Fig. 5.5). In the case of the free vesicles, a rapid and complete release of the fluorophore occurred within the first 2-3 seconds following the addition of the detergent. Conversely, the SRB release was much more progressive for the gel-immobilized vesicles and extended over one minute. In this case, the detergent needs to diffuse in the matrix to disrupt the vesicles and its diffusion coefficient modulates the efflux from the vesicles. Therefore, this hydrogel system offers the possibility of controlled release by choosing different disrupting agents.

It was found that the gel prepared from a copolymer containing less NAS monomer (here 4 %) was less suitable than PNIPAS6-PLℓ. PNIPAS4-PLℓ was soft and sticky, and as a consequence was difficult to grind. Despite a good swelling and a reasonable content of polylysine, this gel could immobilize less lipids than PNIPAS6-PLℓ. This lower efficiency was related to the bigger size of the gel particles leading to a limited effective surface for vesicle anchoring. This poor immobilization ability of the gel is illustrated by the high value of free amino groups per POPG (Table VI). It should be noted that our anchoring approach preserves also in this case the integrity of the vesicles after immobilization as indicated by the high self-quenching coefficient of the entrapped fluorophore (Table V). Our results also indicate that long polylysine is a more suitable

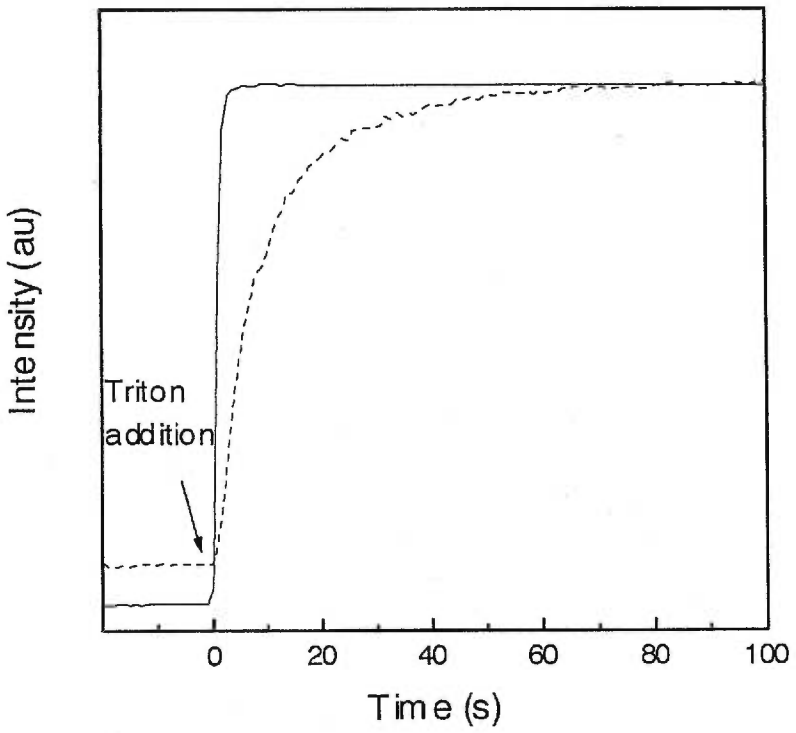

Figure 5.5 Fluorescence quenching measurements: the SRB release induced by the addition of Triton-X as a function of time for free POPC/POPG vesicles (—) and for the same vesicles after immobilization on PNIPAS6-PLℓ (--).

crosslinking agent. Few lipids were immobilized on PNIPAS6-PL*s*, the gel made from the crosslinking of PNIPAS6 with PL*s*. Only a small quantity of lysine was found in this gel. This leads to a limited number of anchoring sites as well as a reduced swelling. As a consequence, the gel could immobilize only very few lipid vesicles. Actually, the immobilization of lipids by this gel is comparable to the acetylated gel.

5.4.4 Thermally controlled release

As an illustration of the potential use of PNIPAS6-PLℓ as a thermosensitive support, we show that the content of immobilized vesicles can be released in a controlled manner using a thermal trigger. First, a column was filled with PNIPAS6-PLℓ. The vesicle immobilization step was done in suspension by mixing gel particles and POPC/POPG (85/15) vesicles. The vesicle-containing gel was then packed in a thermostated column. Afterwards, a 20-min elution at room temperature did not release any lipids or SRB (Fig. 5.6). After 20 min, the temperature of the column was raised to 50°C, over the transition temperature of the gel. An increase of the absorbance at 565 nm was then observed on the elution profile (Fig. 5.6), probing for the release of SRB. Since almost no lipids were detected in the collected fractions, we concluded that the released SRB was free. This was confirmed by a very low SRB self-quenching in the collected fractions. After 10 min, the baseline was recovered. Therefore, the thermosensitivity of the gel can be efficiently used for thermally controlled release. We believe that upon heating, the gel shrinks, and the reorganization perturbs the immobilized vesicles which release a fraction of their SRB content. After the elution, the column was washed by ethanol and the immobilized lipids and remaining SRB could be recovered in the washing.

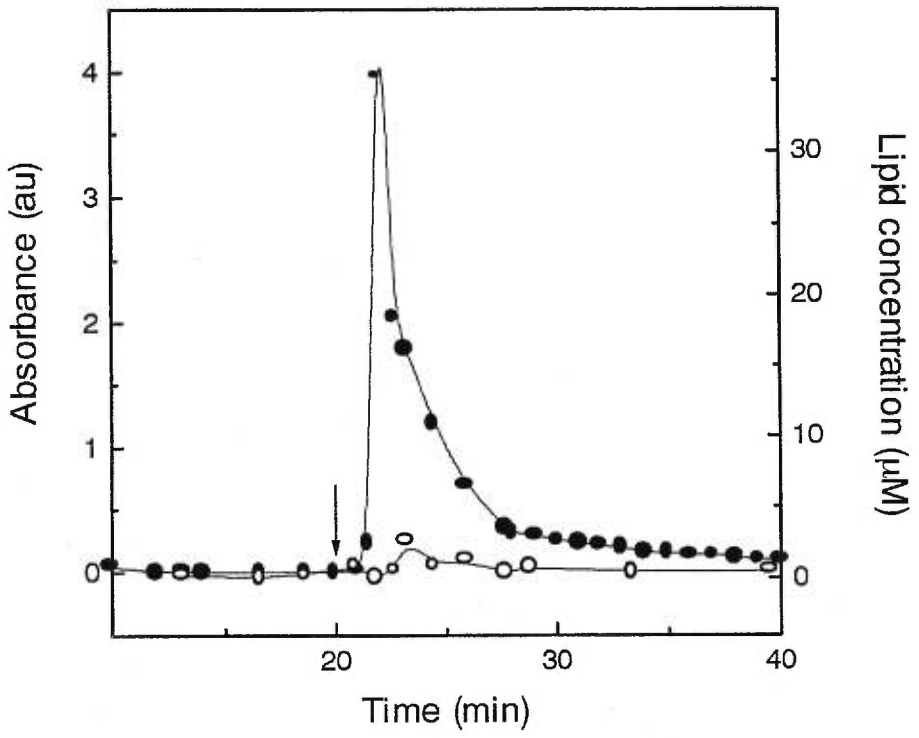

Figure 5.6 Elution profile determined by measuring the SRB absorbance (●) and lipid concentration (○) as a function of time. At an elution time of 20 min (↓), the temperature of the column is raised to 50°C. Both y axes have been normalized so they relate directly the SRB absorbance to the lipid concentration according to measurements on intact vesicles.

5.5 Conclusions

A family of hydrogels based of on polyacrylamide and polylysine were synthesized and characterized to develop a system for the immobilization of lipid vesicles. Among the hydrogels tested, PNIPAS6-PLℓ is the most suitable. PNIPAS6-PLℓ enables the immobilization of a considerable amount of negatively charged vesicles without apparent perturbation of the vesicle permeability. The polylysine content appears to be a crucial factor for the properties of the gel since the charges borne by the polypeptide provide the anchoring sites and allow the gel to display an appropriate swelling to make the charges accessible to lipid vesicles. PNIPAS6-PLℓ has interesting mechanical properties since it is firm enough to be easily ground in small particles that can be used in suspensions or in columns. In addition, the thermosensitivity of the gel can be efficiently used to have a controlled release of the vesicle content.

Acknowledgments

Financial support from the Natural Sciences and Engineering Research Council (NSERC) of Canada and Fonds FCAR from the Province of Quebec is gratefully acknowledged.

5.6 References

[1] Stevenson WTK, Sefton MV. TRIP 1994;2:98-104.

[2] Pidgeon C, Venkataram UV. Anal. Biochem. 1989;176:36-47.

[3] Ong S, Qiu X, Pidgeon C. J. Phys. Chem. 1994;98:10189-10199.

[4] Yang Q, Lundahl P. Anal. Biochem. 1994;218:210-221.

[5] Zhang Y, Xiao Y, Kellar KJ, Wainer IW. Anal. Biochem. 1998;264:22-25.

[6] Gotoh T, Shidara M, Iwanaga T, Kikuchi K-I, Hozawa M. J. Ferment. Bioeng. 1994;77:268-273.

[7] Gotoh T, Kikuchi K-I J. Chem. Eng. Jpn 1998;31:860-863.

[8] Kino Y, Sawa M, Kasai S, Mito M. J. Surg. Res. 1998;79:71-76.

[9] Gennis RB. In: Cantor CR, editor. Biomembranes: Molecular Structure and Function, Springer-Verlag, New York, 1989.

[10] Schild HG. Prog. Polym. Sci. 1992;17:163.

[11] Pollak A, Blumenfeld H, Wax M, Baughn RL, Whitesides GM. J. Am. Chem. Soc. 1980;102:6324-6336.

[12] Wu XS, Hoffman AS, Yager P. Polymer 1992;33:4659-4662.

[13] Hayashi H, Kono K, Takagishi T. Biochim. Biophys. Acta 1996;1280:127-134.

[14] Chen J-P, Chu D-H, Sun Y-M. J. Chem. Tech. Biotechnol. 1997;69:421-428.

[15] Sun Y-M, Chen J-P, Chu D-H. J. Biomed. Mater. Res. 1999;45:125-132.

[16] Elbert DL, Hubbell JA. J. Biomed. Mater. Res. 1998;42:55-65.

[17] Carrier D, Pézolet M. Biochemistry 1986;25:4167-4174.

[18] Walter A, Steer CJ, Blumenthal R. Biochim. Biophys. Acta 1986;861:319-330.

[19] Laroche G, Carrier D, Pézolet M. Biochemistry 1988;27:6220-6228.

[20] Cole C-A, Schreiner SM, Priest JH, Monji N, Hoffman AS. In: Reversible Polymeric Gels and Related Systems (Ed. P. Russo) ACS Symposium Series 350, American Chemical Society, Washington DC, 1987. pp. 245-254.

[21] Ferruti P, Bettelli A, Feré A. Polymer 1972;13:462-464.

[22] Yang HJ, Cole C-A, Monji N, Hoffman AS. J. Polym. Sci. Polym. Chem. Ed. 1990;28:219-226.

[23] Lowry OH, Rosebrough NJ, Farr AL, Randall RJ. J. Biol. Chem. 1951;193:265-275.

[24] Riordan JF, Wacker WEC, Vallee BL. Biochemistry 1965;4:1758-1765.

[25] Brown WD, Green S. Anal. Biochem. 1970;34:595-598.

[26] El-Jastimi R, Lafleur M. Biochim. Biophys. Acta 1997;1324:151-158.

[27] Benachir T, Monette M, Grenier J, Lafleur M. Eur. Biophys. J. 1997;25:201-210.

[28] Fiske CH, SubbaRow Y. J. Biol. Chem. 1925;66:375-400.

[29] El Jastimi R, Lafleur M. Biospectroscopy 1999;5:133-140.

[30] Bellamy LJ. In: The Infrared Spectra of Complex Molecules, Chapman and Hall, London, 1975. pp. 144-146.

[31] Miron T, Wilchek M. Anal. Biochem. 1982;126:433-435.

[32] Chen JP, Yang HJ, Hoffman AS. Biomaterials 1990;11:625-630.

CHAPITRE 6

CONCLUSIONS

Au cours de ce projet, nous avons mis au point deux nouveaux systèmes composites permettant d'immobiliser des vésicules lipidiques par l'intermédiaire d'une ancre peptidique. Ces projets ont été menés de la conceptualisation à l'application.

Lors du développement du premier système, l'étude du design du nouveau peptide amphiphile servant de lien entre le support solide et la vésicule a permis d'améliorer la compréhension des interactions lipides-peptide amphiphile primaire. Tout d'abord, nous avons constaté que le segment hydrophobe doit être suffisamment long pour que les interactions hydrophobes puissent jouer un rôle lors de l'interaction peptide-lipide. Un peptide dont le segment hydrophobe a environ la longueur des chaînes alkyles des lipides est trop court pour interagir avec des vésicules neutres. En revanche, un peptide ayant un segment hydrophobe de 24 acides aminés (environ l'épaisseur du cœur hydrophobe d'une bicouche lipidique) est suffisamment long. Cependant, pour nos peptides qui incluent des lysines à au moins une extrémité, les interactions électrostatiques restent primordiales. En effet, l'interaction avec les vésicules lipidiques croît avec la proportion de lipides chargés négativement présents dans la membrane. Ceci est aussi observé lorsque le peptide le plus performant est greffé sur un support solide puisque dans ce cas, l'interaction avec les vésicules est inexistante si les charges positives des lysines sont neutralisées. On a aussi montré que la présence de charges aux deux extrémités du peptide empêche l'insertion spontanée du peptide dans la membrane lipidique et que le sens du peptide n'a aucune influence sur l'interaction lipide-peptide. Aucune information n'a été obtenue quant à l'orientation des peptides lors de l'interaction avec les membranes lipidiques, confirmant ou non les schémas de la Figure 1.8 (p18). Suite à cette étude, nous avons finalement pu déterminer le peptide le plus performant: $A_2L_3A_{19}WK_6$. Ce peptide a été synthétisé en phase solide sur des billes de PS. On a confirmé que l'interaction support solide-vésicule est de nature électrostatique et ne perturbe pas la perméabilité des membranes. On a pu immobiliser un maximum de 200

µmol de lipides chargés négativement par gramme de résine sèche. Finalement, des vésicules incorporant une enzyme membranaire ont pu être immobilisées sur le support solide développé et ce, de façon suffisamment solide pour permettre une réutilisation de la biomasse. Après 8 cycles de réutilisation, l'enzyme conserve encore 50 % de son activité initiale.

Pour développer le deuxième système, un nouveau type de support solide a été synthétisé au laboratoire. Il s'agit d'un hydrogel résultant de la réticulation d'un copolymère thermosensible, le poly(*N*-isopropylacrylamide-co-*N*-acryloxysuccinimide) par de la polylysine. Au cours de ce projet, nous avons mis au point une nouvelle méthode spectroscopique infrarouge simple qui permet de déterminer de façon claire et rapide la température de transition ainsi que de mieux comprendre les interactions impliquées lors de ce phénomène. La température de transition a pu être déterminée avec succès pour un polymère linéaire, ainsi que pour les hydrogels synthétisés au laboratoire. On a pu montrer que les groupements hydrophobes ainsi que les groupements amides sont impliqués lors de la transition, entraînant une réorganisation de la chaîne principale. De plus, l'analyse des bandes amide montre que 20 % des liaisons hydrogène entre les groupements amide et les molécules d'eau sont remplacées par des liaisons intramoléculaires. On a pu conclure que les chaînes latérales, ainsi que la chaîne principale sont impliqués dans cette transition et que cette transition est de même nature pour les polymères linéaires, ainsi que pour les gels en dérivant.

Ensuite, nous avons synthétisé plusieurs hydrogels à base de poly(*N*-isopropylacrylamide-co-*N*-acryloxysuccinimide) réticulé par de la polylysine. On a tout d'abord développé une nouvelle méthode infrarouge permettant de doser la quantité de comonomère NAS dans les copolymères synthétisés, ainsi que dans les gels synthétisés par la suite. Deux copolymères contenant dans un cas 4 % et dans l'autre 6 % de NAS ont ainsi été synthétisés puis caractérisés. Ces copolymères ont été réticulés avec des polylysines de longueurs différentes. Des hydrogels transparents, avec des propriétés thermosensibles ont été obtenus. La quantité de NAS introduite dans le copolymère a une influence sur la masse molaire du copolymère, et par conséquent sur les propriétés mécaniques du gel. Une masse molaire élevée conduit à un gel ferme facilement broyable. Cette propriété a une forte influence sur l'immobilisation des vésicules puisque

les gels facilement broyables en petites particules offrent une plus grande surface disponible pour l'interaction avec les vésicules. La longueur de la polylysine a une influence sur les propriétés de gonflement du gel ainsi que sur l'immobilisation des vésicules. On a montré que les charges de la polylysine sont responsables du gonflement en étudiant les propriétés d'un gel dont les charges de la polylysine ont été neutralisées par l'acéthylation des lysines. On conclut que l'immobilisation est de nature électrostatique, en neutralisant les charges des lysines et en utilisant des vésicules neutres ou chargées lors des mesures d'affinité. Les meilleurs résultats ont été obtenus avec l'hydrogel contenant 6 % de NAS et réticulé par de la polylysine ayant un DP élevé de 288. Dans ce cas, 1000±100 μmol de lipides ont pu être immobilisées par gramme de gel sec. On a aussi vérifié que les vésicules immobilisées étaient intactes suite à l'immobilisation, sans perturbation de leur perméabilité.

En utilisant l'infrarouge, on a pu déterminer une LCST de l'ordre de 35°C pour un hydrogel réticulé par de la polylysine. On a donc utilisé ce support solide pour une application de libération contrôlée. En élevant la température du gel au-dessus de sa LCST, on a pu induire la libération du contenu des vésicules immobilisées.

Au cours de ce travail, nous avons conçu et développé deux systèmes fonctionnels, cependant, dans le futur, certaines améliorations pourraient être apportées à ces systèmes. Dans le premier système, on pourrait tout d'abord optimiser le support solide utilisé lors de la synthèse du peptide amphiphile. Un polymère plus hydrophile permettrait au support de gonfler dans l'eau et d'augmenter ainsi la proportion de peptides accessibles aux vésicules. De plus, la nature hydrophobe du PS ainsi que les résultats obtenus montrent que le peptide n'a pas le même comportement lorsqu'il est greffé sur la bille de polymère et lorsqu'il est solubilisé. Afin de donner un peu plus de liberté au peptide greffé, on pourrait ajouter un espaceur entre le support et le peptide. Cet espaceur pourrait être un segment d'éthylèneglycol ou un segment de lysine plus long, ce qui en plus, augmenterait les interactions électrostatiques potentielles. En ce qui concerne l'hydrogel thermosensible, le broyage du gel en petites particules semble être le paramètre limitant l'immobilisation des vésicules. Afin d'obtenir des particules de gel d'une géométrie contrôlée, on pourrait effectuer une réticulation en suspension, ce qui permettrait d'obtenir des billes de gel et éviterait l'étape de broyage. De plus, les

particules ainsi obtenues seraient sphériques et de taille homogène. On pourrait aussi moduler la température de transition de l'hydrogel thermosensible en vue d'applications spécifiques, en variant les monomères utilisés, ainsi que leur proportion. D'autres types d'ancre pourraient aussi être greffés sur l'hydrogel réticulé par du MBA (ancre de nature lipidique ou peptide d'adhésion en vue de l'immobilisation de cellules).

Finalement, on pourrait développer d'autres applications. Au cours de ce travail, une seule application a été mise au point pour chaque système. Dans les deux cas, seules des vésicules modèles ont été immobilisées sur les supports conçus. La nature électrostatique de l'interaction permet d'envisager l'immobilisation de différents types de membranes incluant celles d'origine biologique. De tels supports pourraient être utilisés pour immobiliser des cellules vivantes. En ce qui concerne le premier système, celui comportant une ancre peptide amphiphile, il pourrait être utilisé comme support pour séparer des populations de vésicules en fonction de leur charge, les vésicules zwitterioniques n'étant pas retenues par les billes. D'autres applications peuvent être envisagées en utilisant les billes de polymère sur lesquelles auront été préalablement immobilisées des membranes. Ce support pourra alors être utilisé pour séparer des molécules en fonction de leur affinité pour les lipides. Ce système a aussi été utilisé pour immobiliser une enzyme membranaire modèle. Le système pourrait être utilisé pour immobiliser des enzymes plus spécifiques, inactives en solution aqueuse. Dans le cas du deuxième système, la propriété de libération contrôlée en fonction de la température permet d'envisager diverses applications telles que la libération contrôlée de médicament, d'engrais... On pourrait aussi envisager des applications de libération contrôlée en fonction du pH en exploitant le changement de conformation de la PL en fonction du pH.